

7th International Conference on Holography, String Theory in Da Nang

Exploring hot and dense QCD by holography

Li Li (李理)

**Institute of Theoretical Physics,
Chinese Academy of Sciences**

Da Nang, Vietnam

22 August 2024



References:

Rong-Gen Cai, Song He, **Li Li** and Yuan-Xu Wang,
Probing QCD critical point and induced gravitational wave by black hole physics,
Phys. Rev. D 106 no.12, L121902 (2022)

Zhibin Li, Jinmin Liang, Song He and **Li Li**,
Holographic study of higher-order baryon number susceptibilities at finite temperature and density,
Phys. Rev. D 108, no.4, 046008 (2023)

Song He, **Li Li**, Sai Wang and Shao-Jiang Wang,
Constraints on holographic QCD phase transitions from PTA observations,
[arXiv:2308.07257 [hep-ph]]. (to appear in Sci.China Phys.Mech.Astron.)

Yan-Qing Zhao, Song He, Defu Hou, **Li Li** and Zhibin Li,
Phase structure and critical phenomena in 2-flavor QCD by holography,
Phys.Rev.D 109 (2024) 8, 086015

Rong-Gen Cai, Song He, **Li Li** and Hong-An Zeng,
QCD Phase Diagram at finite Magnetic Field and Chemical Potential: A Holographic Approach
Using Machine Learning, [arXiv:2406.12772 [hep-th]].

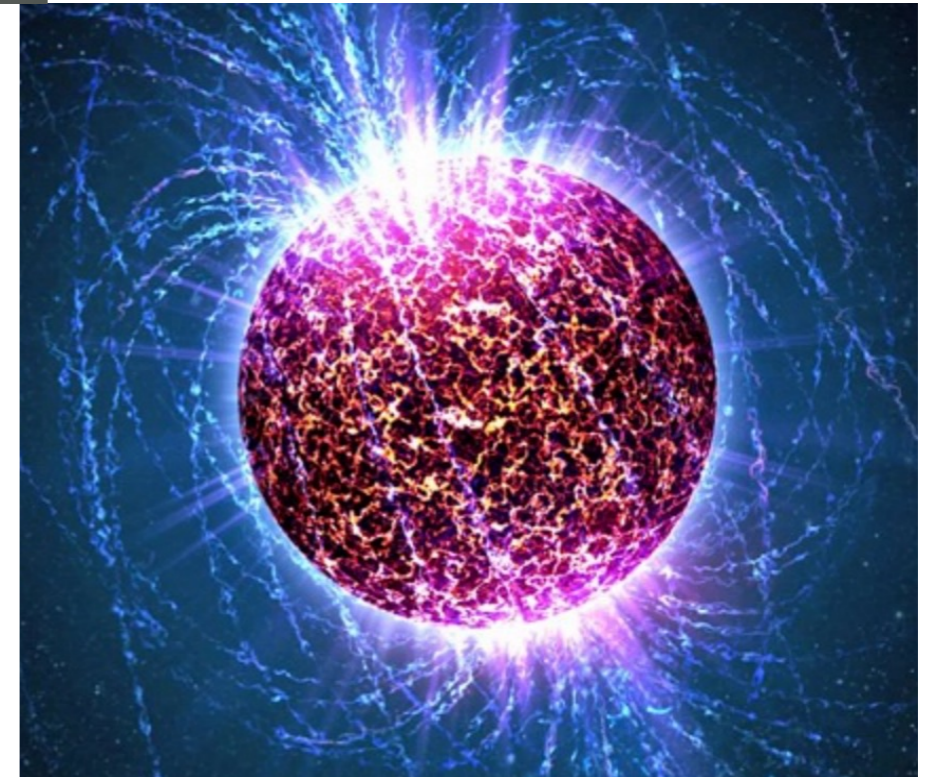
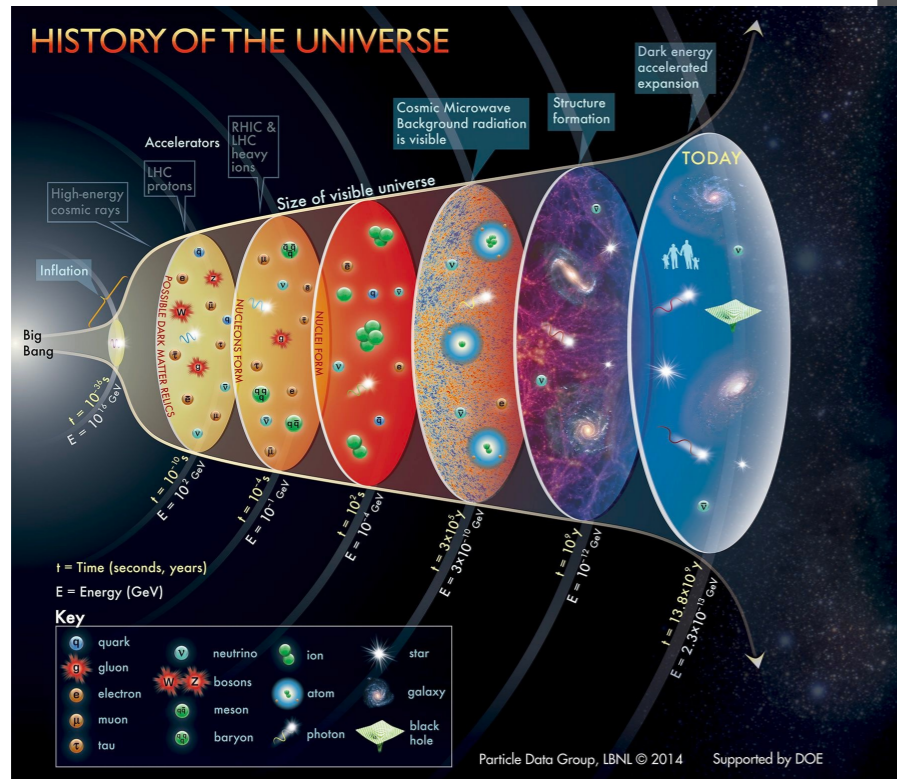
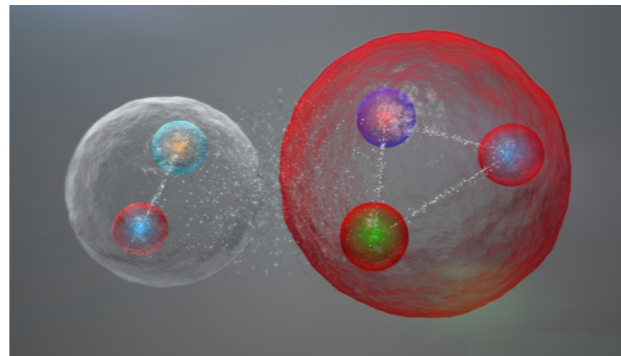
Outline

1. Introduction
2. Holographic QCD model
3. Phase diagram and GWs
4. Summary and discussion

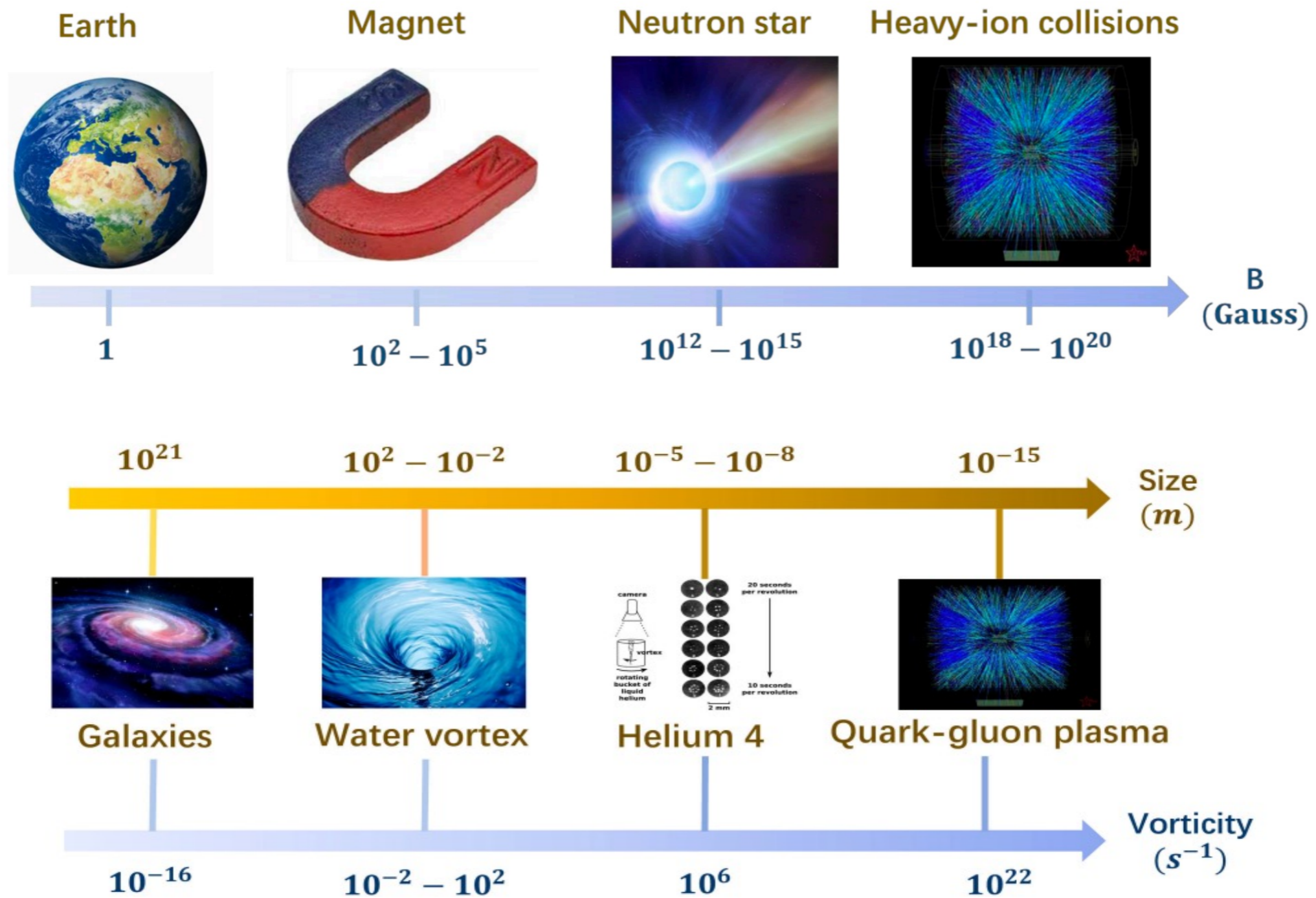
1. Introduction

QCD phase diagram:

One of the most interesting and fundamental challenges of high energy physics!



It involves strongly interacting matter under extreme conditions.



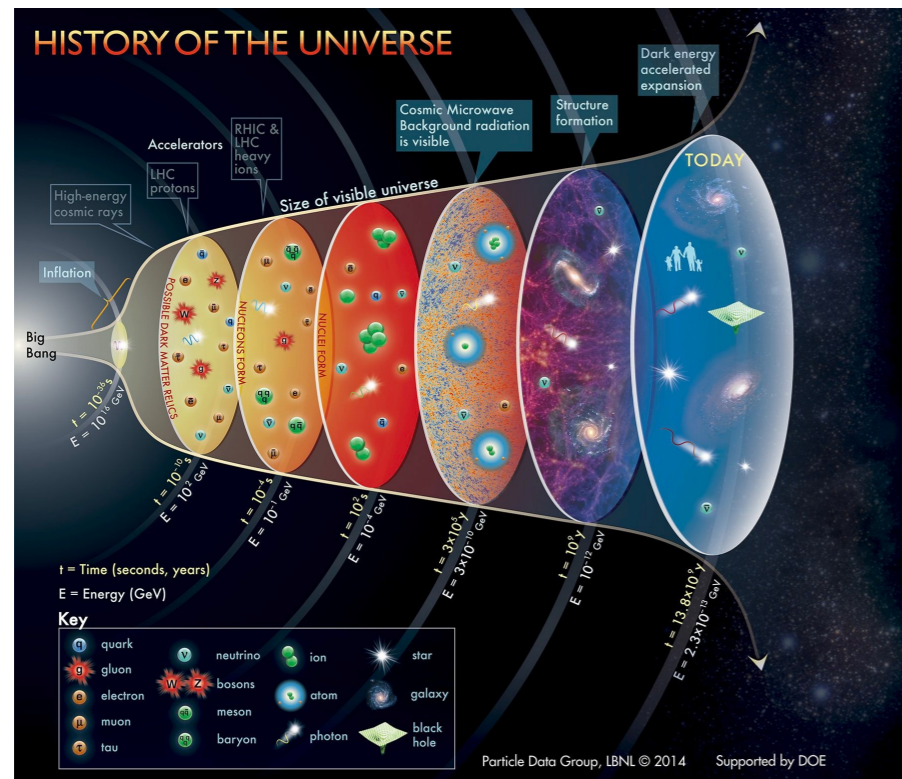
1. Introduction

QCD phase diagram:

One of the most interesting and fundamental challenges of high energy physics!

It involves strongly interacting matter under extreme conditions.

Only little is known about the phase structures in low- T and high- μ_B regions.



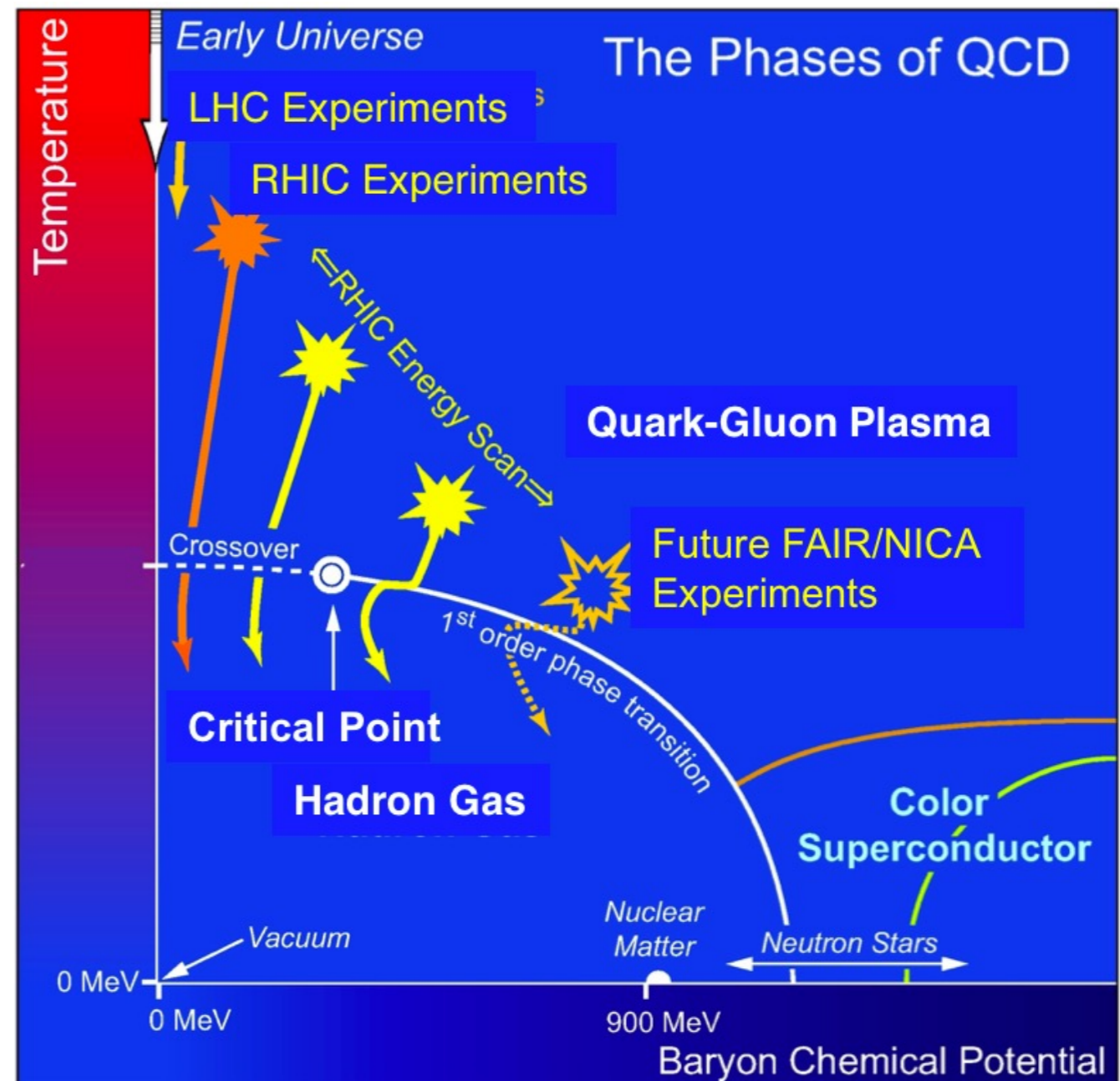
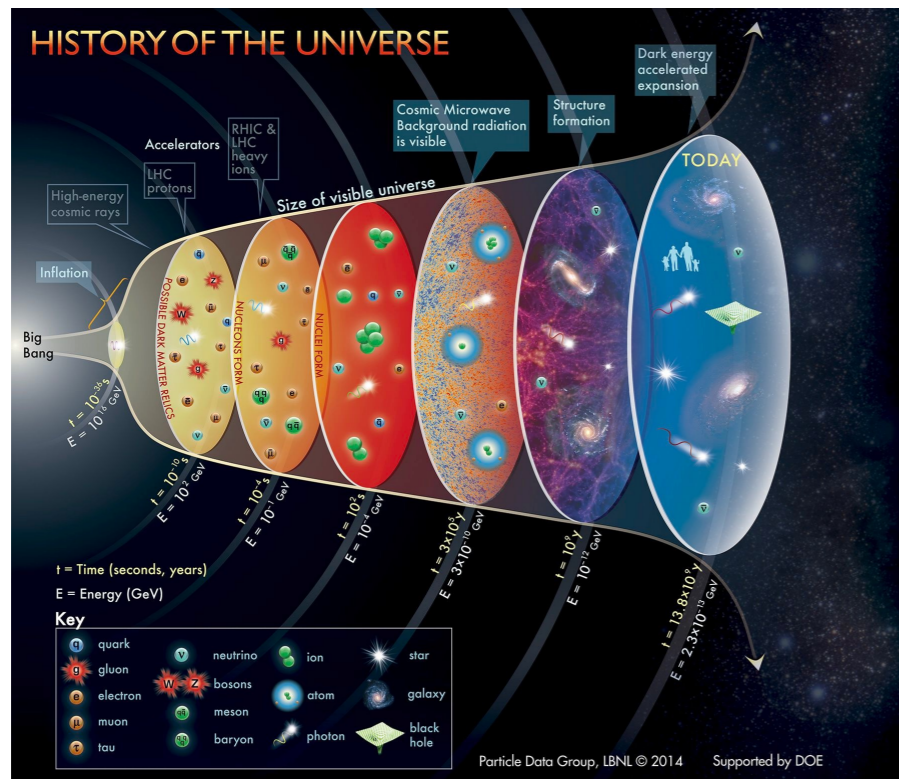
1. Introduction

QCD phase diagram:

One of the most interesting and fundamental challenges of high energy physics!

It involves strongly interacting matter under extreme conditions.

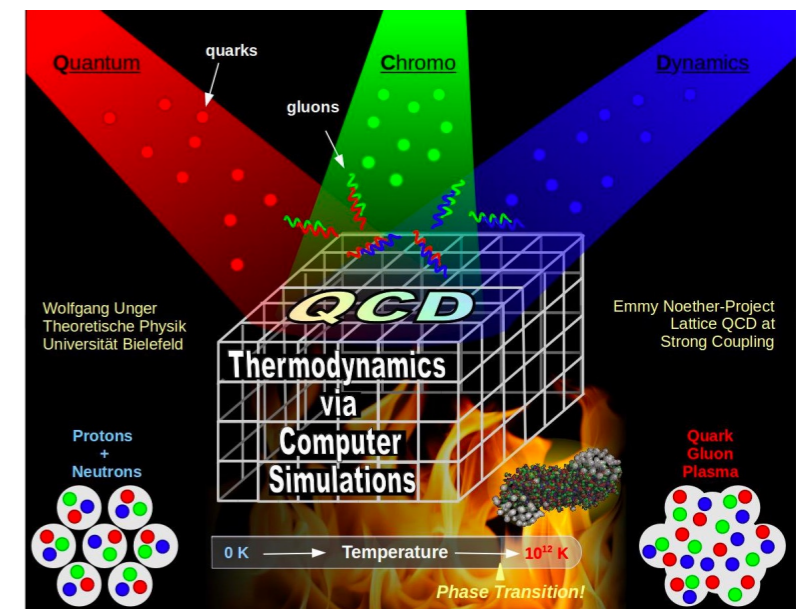
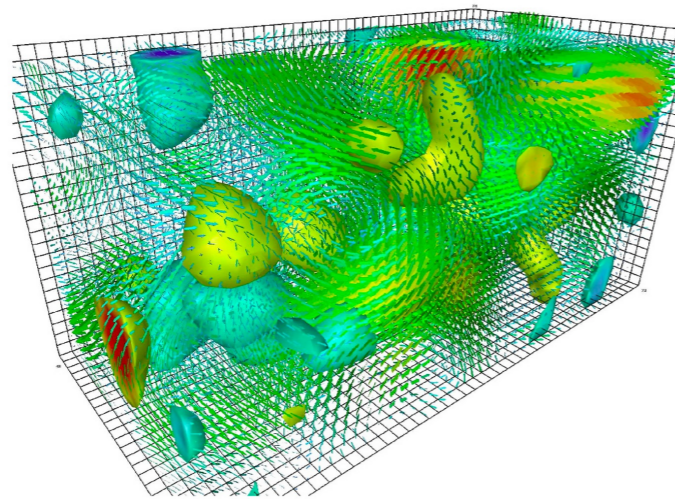
Only little is known about the phase structures in low-T and high- μ_B regions.



It has not been possible to obtain QCD phase diagram directly from QCD!

Lattice QCD: the update algorithm solves the path integral of discretized QCD.

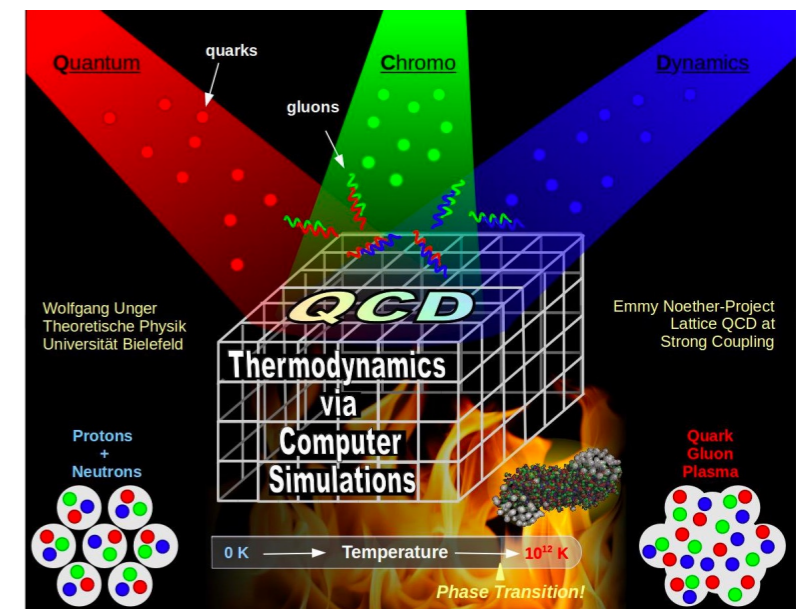
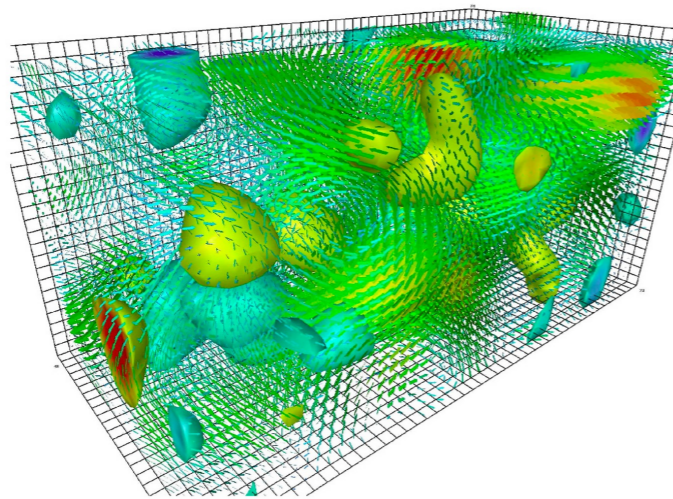
It can give reliable information from the first principle at **zero density**,
but fails at finite density due to the famous **sign problem**



It has not been possible to obtain QCD phase diagram directly from QCD!

Lattice QCD: the update algorithm solves the path integral of discretized QCD.

It can give reliable information from the first principle at **zero density**, but fails at finite density due to the famous **sign problem**



Challenges of lattice QCD – costs

Today, 1000 configurations on a $64^3 \times 16$ lattice cost about 1 million core hours.

Traditional supercomputer: 1 million core hours = cca 30 k€, 15 tons CO₂

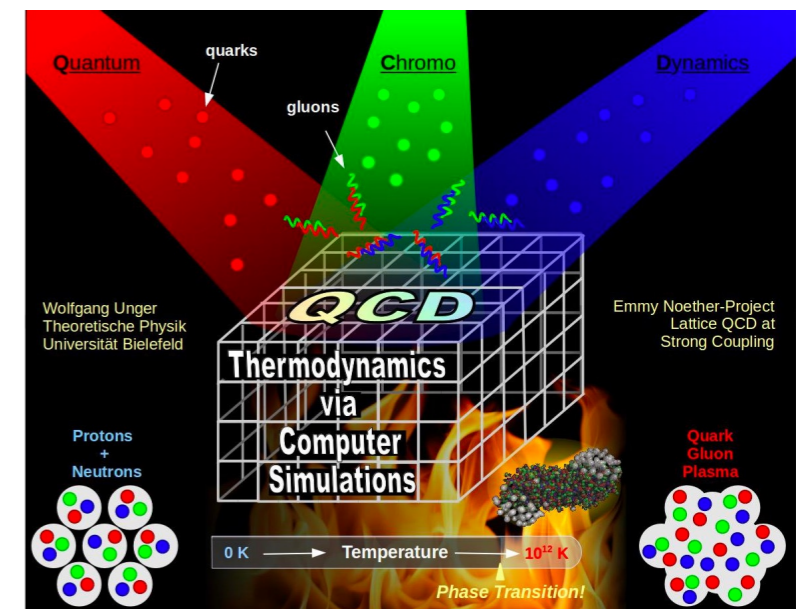
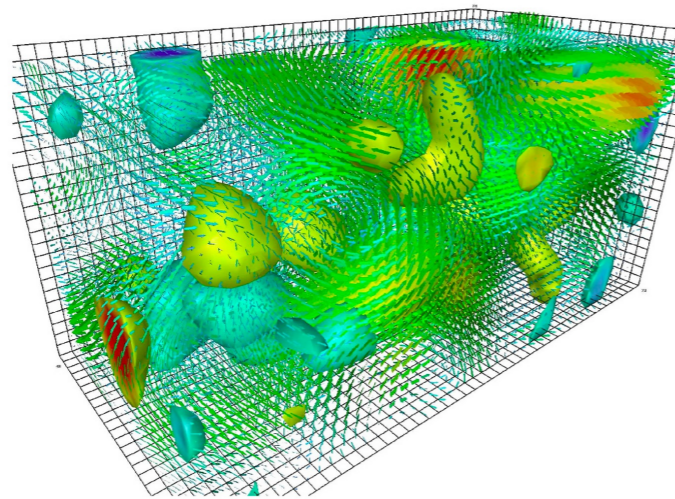
GPU based supercomputer: 1 million core hours = cca 10 k€, 6 tons CO₂

[S. Borsanyi, 2018]

It has not been possible to obtain QCD phase diagram directly from QCD!

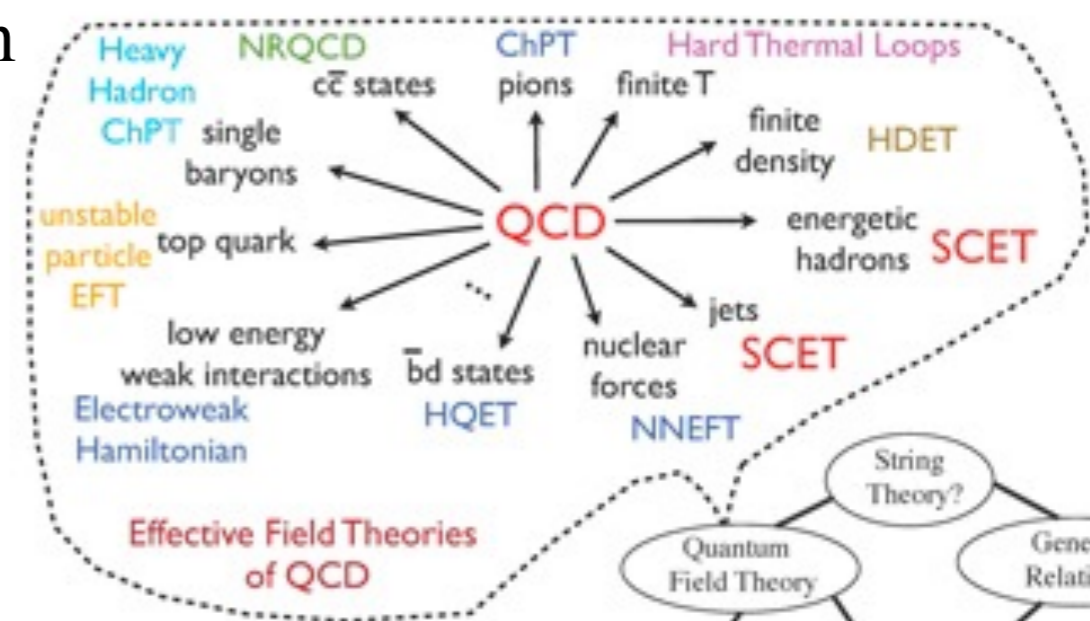
Lattice QCD: the update algorithm solves the path integral of discretized QCD.

It can give reliable information from the first principle at **zero density**, but fails at finite density due to the famous **sign problem**



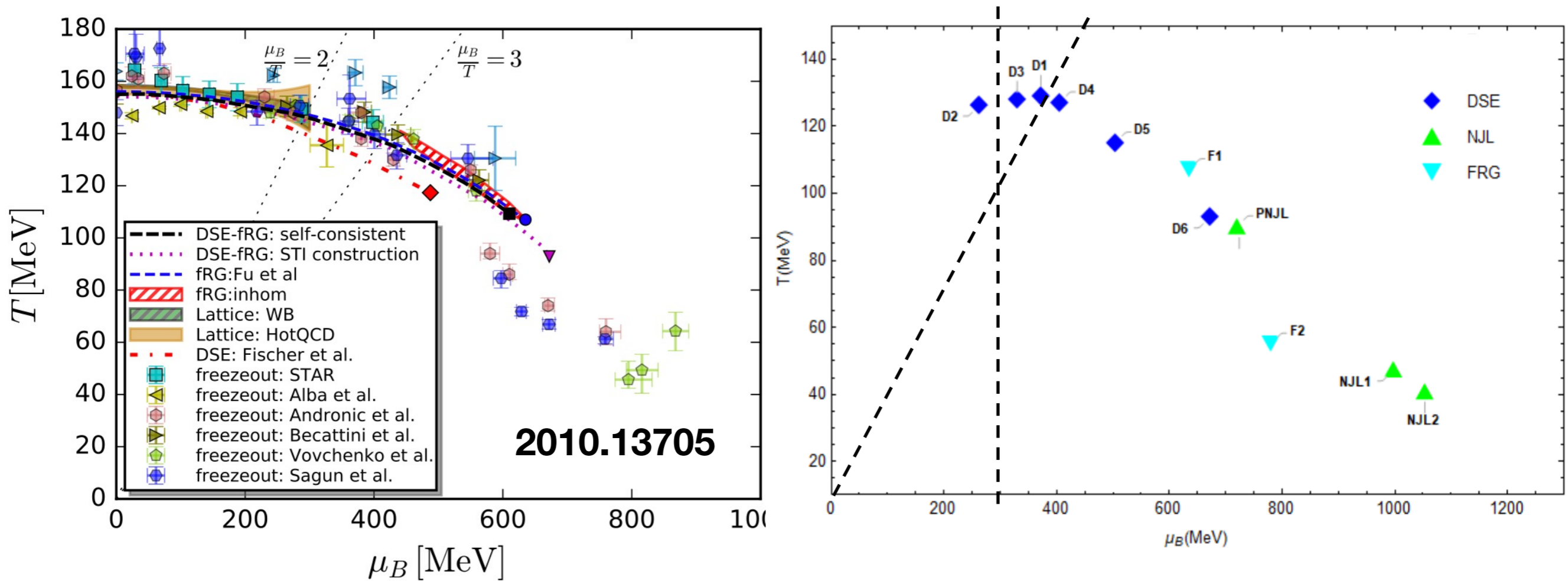
EFT: many low energy **effective models** have been proposed to study QCD in certain conditions.

Match lattice QCD data quantitatively?



Searching CEP from EFT

The exact location of CEP is still under dispute, and the lattice-QCD results disfavors the existence of the QCD Critical Point for $\mu_B / T \leq 3, \mu_B < 300\text{MeV}$.



Schwinger–Dyson equation (DSE): 2109.09935, 1607.01675, 1405.4762, 2002.07500.

Nambu–Jona-Lasinio models (NJL, PNJL): 1801.09215, Nucl. Phys. A 504 (1989), 668-684

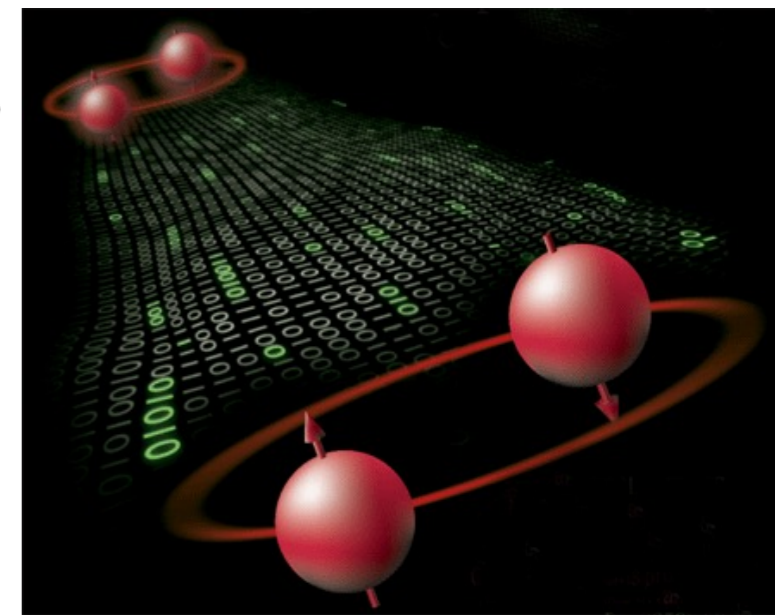
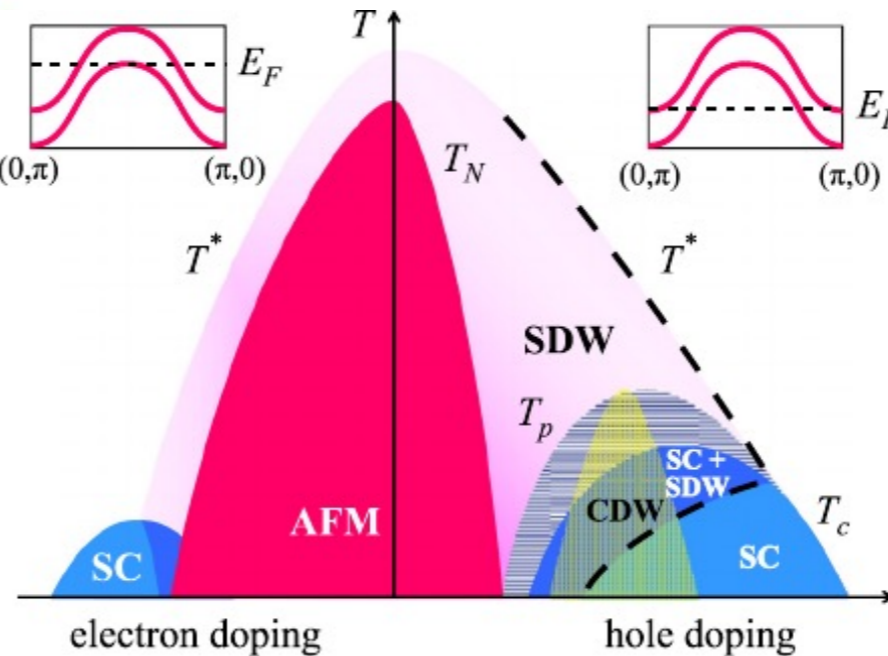
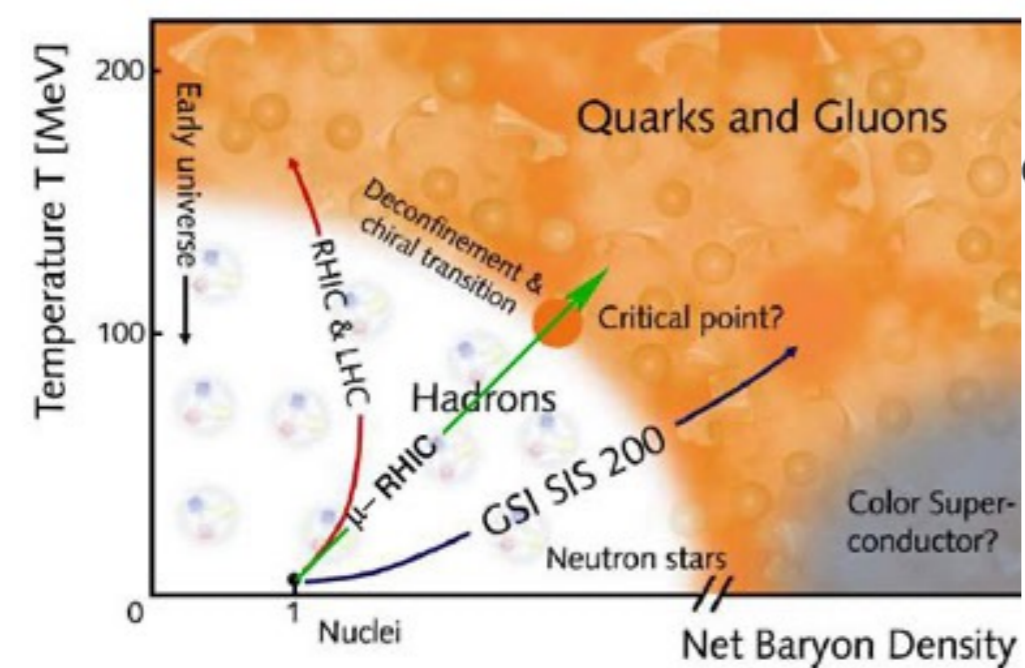
Functional renormalization group (FRG): 1909.02991, 1709.05654...

Holography as a Theoretical Laboratory

Non gravitational system
at strong coupling



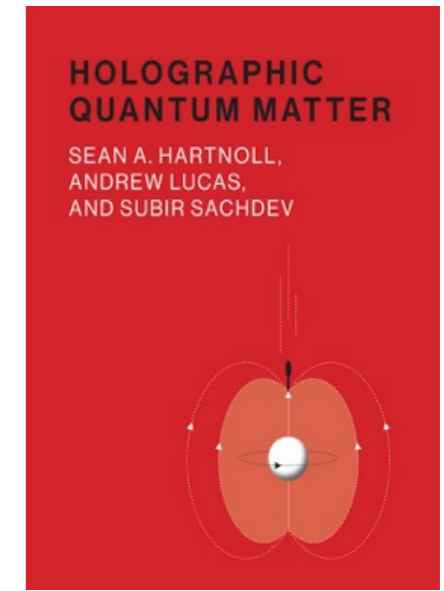
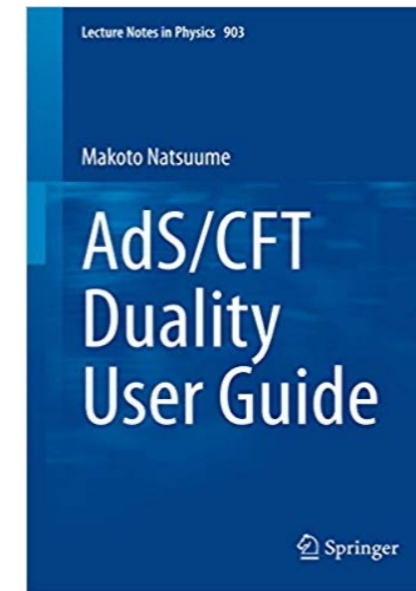
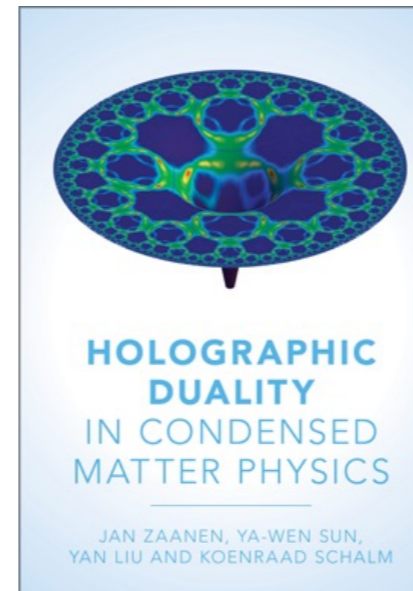
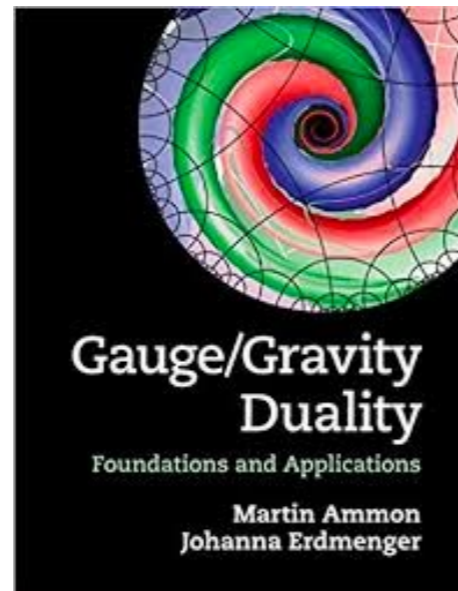
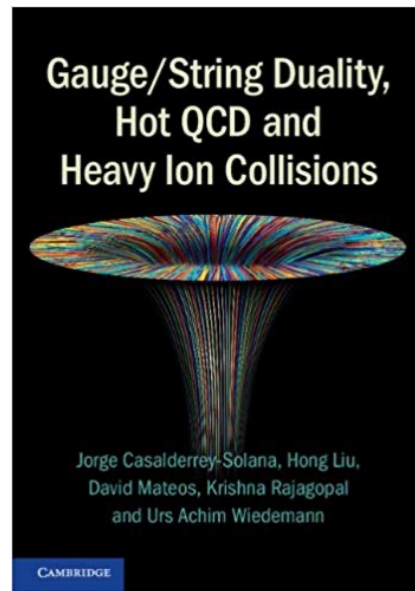
Gravitational theory
at weak coupling



Applied holography:

QGP and QCD (drag force, jet quenching, confinement/deconfinement,...),
Condensed matter (quantum criticality, strange metal, superconductivity,...),
Quantum Entanglement, Non-equilibrium dynamics...

References



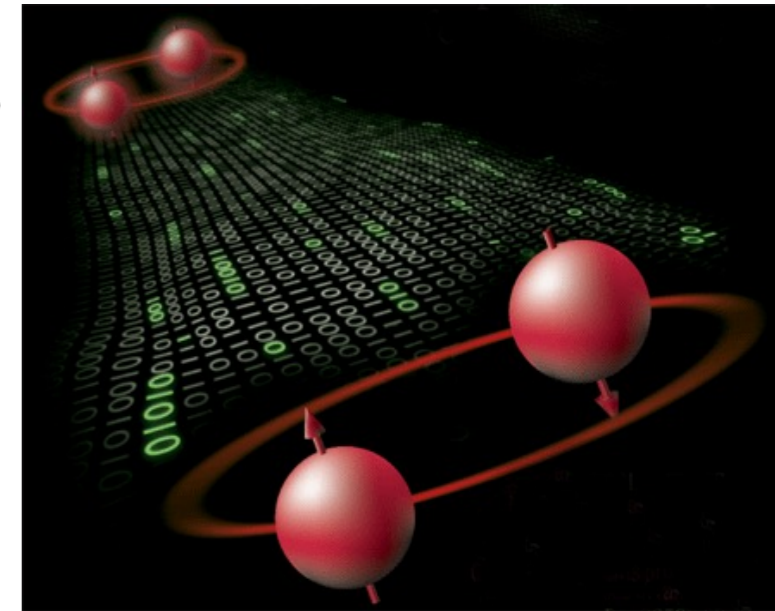
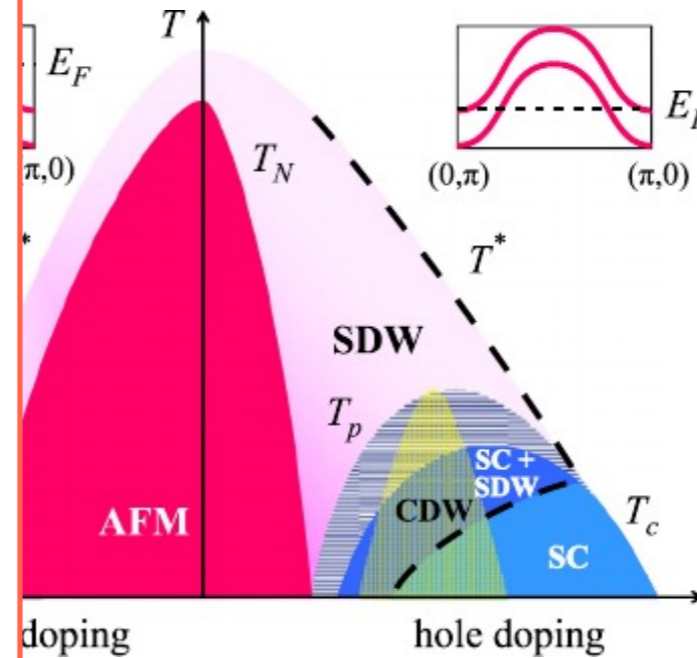
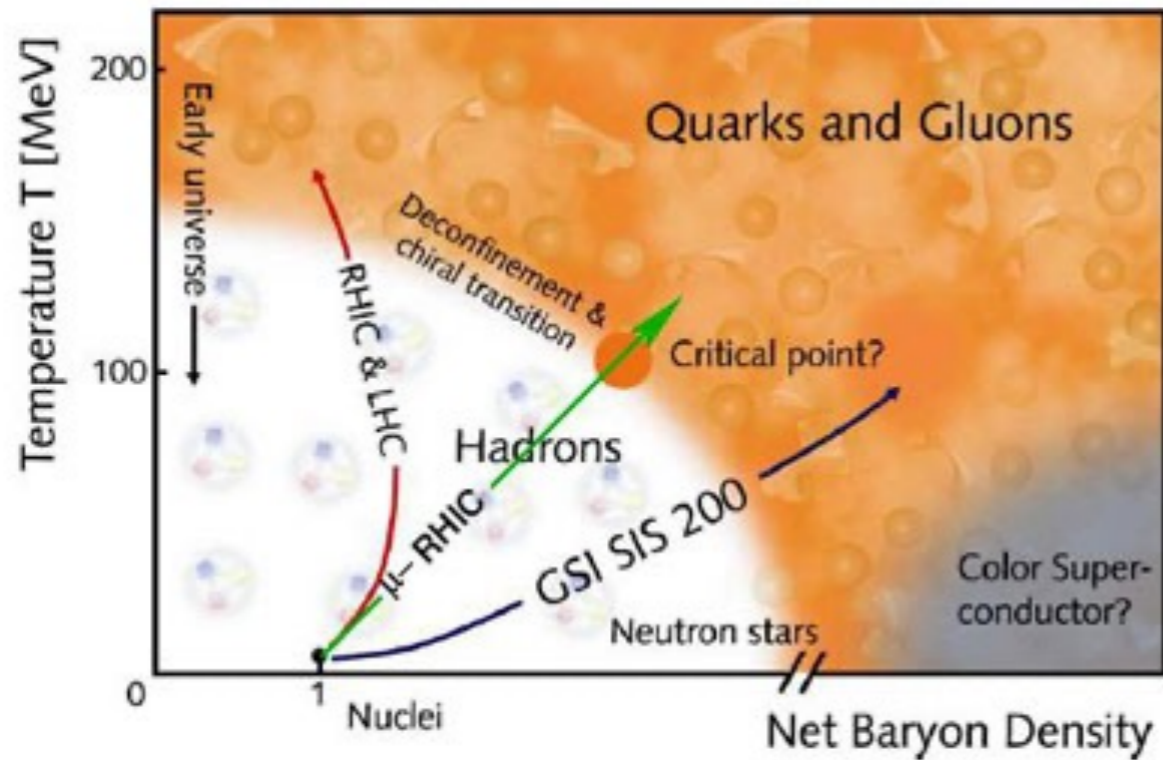
**Hartnoll, 0903.3246; Herzog, 0904.1975; Mcgreevy, 0909.0518;
Hubeny et al, 1006.3675; Takayanagi, 1204.2450; Cai et al, 1502.00437;
Landsteiner et al, 1911.07978; Baggioli et al, 2101.01892.....**

Holography as a Theoretical Laboratory

Non gravitational system
at strong coupling



Gravitational theory
at weak coupling



Holographic QCD:

Using holography to tackle non-perturbative QCD problems

❖ **Top-Down approach: D-brane construction, from superstring**

Witten-Sakai Sugimoto model [hep-th/0412141, hep-th/0507073]

D3-D7 model [hep-th/0306018]

D4-D6 model [hep-th/0311270]

Limited ability to characterize QCD properties as its rigidity

Far from real QCD

❖ **Top-Down approach: D-brane construction, from superstring**

Witten-Sakai Sugimoto model [hep-th/0412141, hep-th/0507073]

D3-D7 model [hep-th/0306018]

D4-D6 model [hep-th/0311270]

Limited ability to characterize QCD properties as its rigidity

Far from real QCD

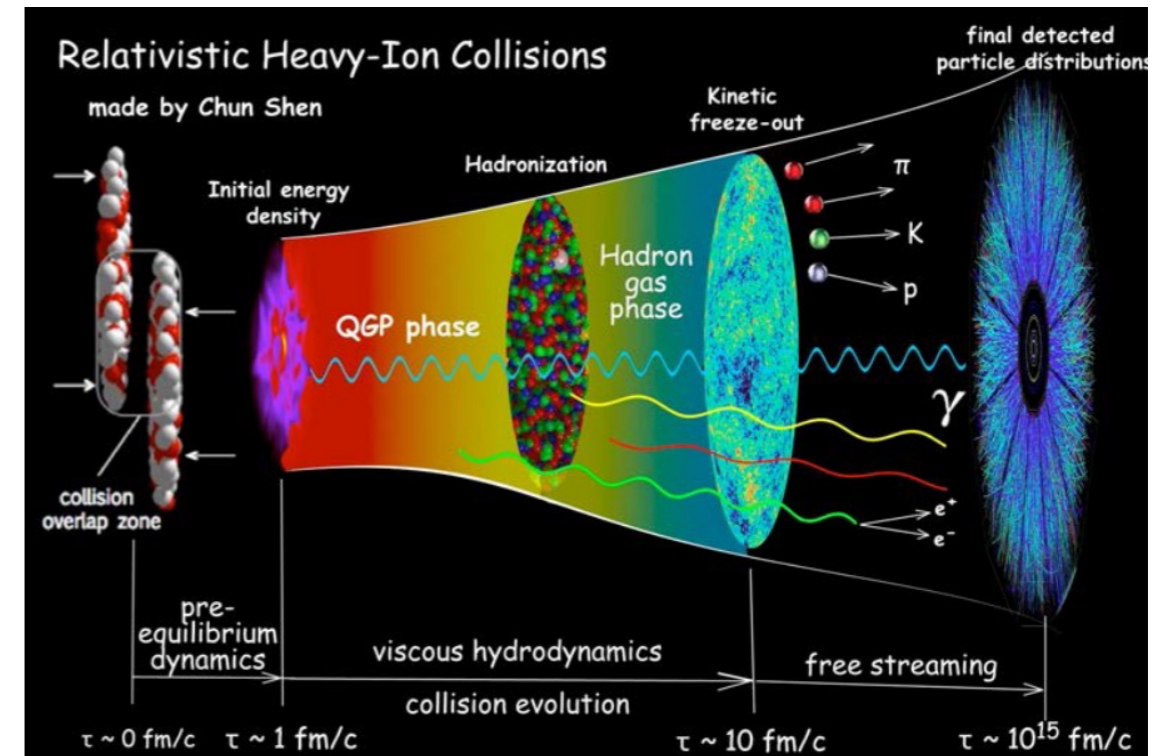
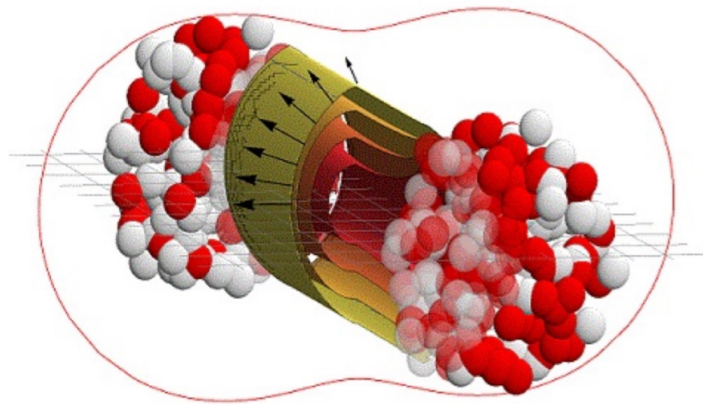
❖ **Bottom-up approach: phenomenology**

Effective models (more freedom), no clear string origin

However, low energy QCD properties are easier to incorporate

Remarkably, these models yield consistent results of low energy hadron physics with experiments.

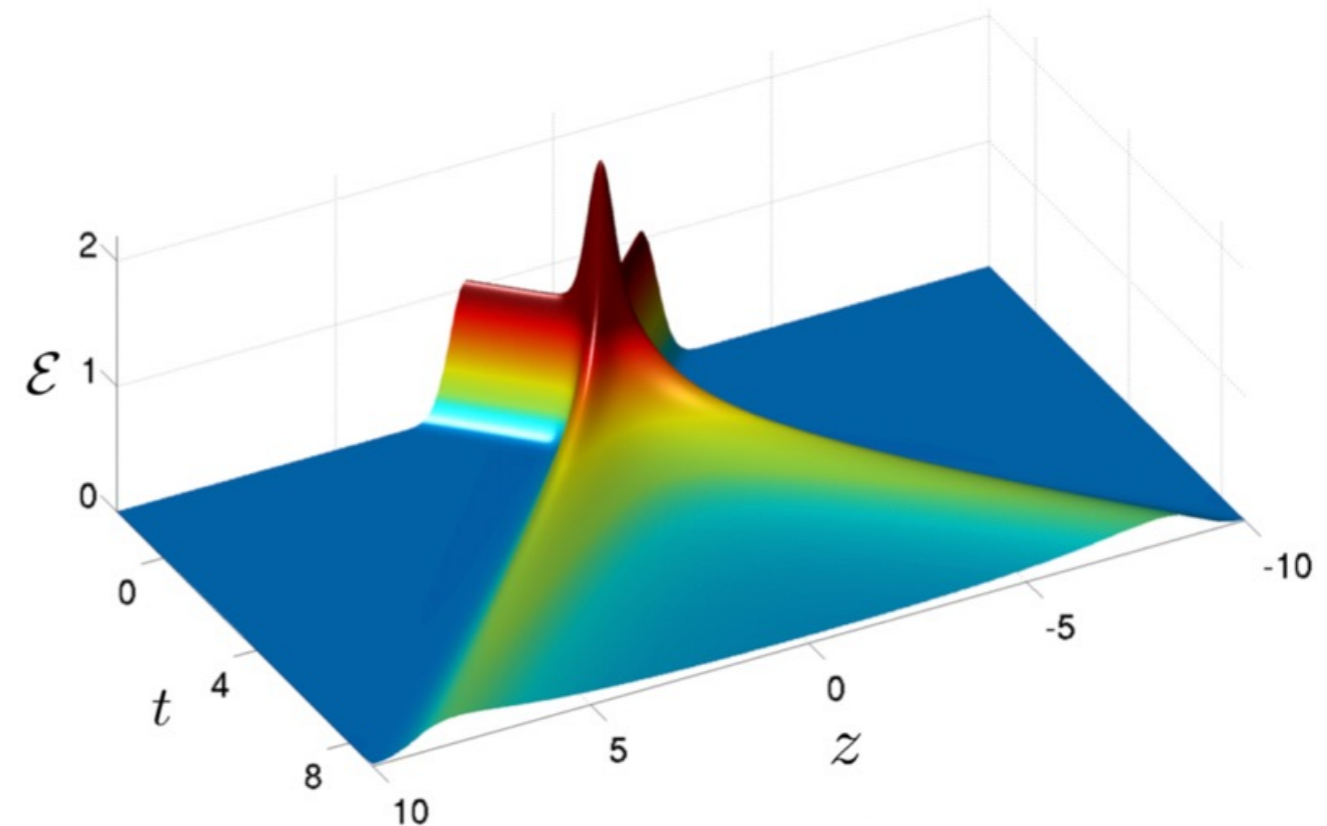
Holographic QGP



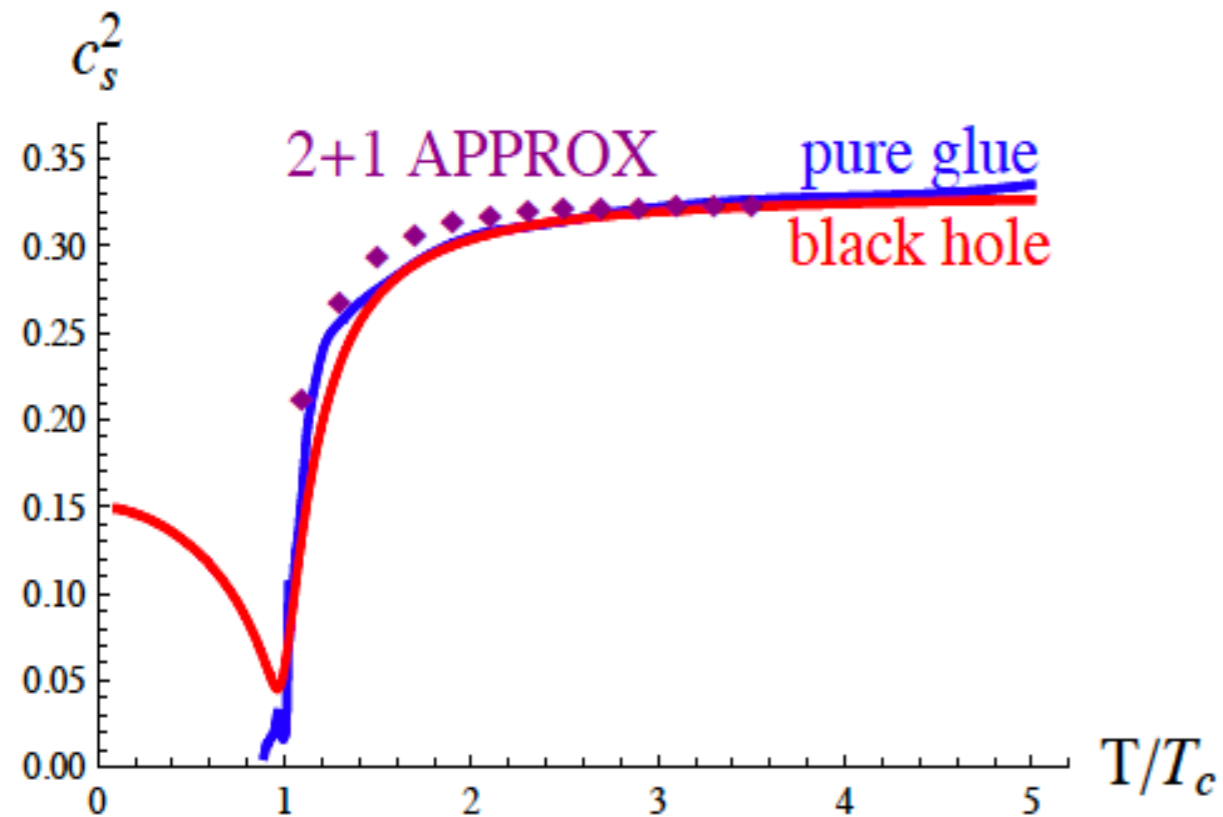
A fully dynamical simulation:

from far-from-equilibrium to viscous hydrodynamics, to a hadronic gas cascade, to the final (measured) particle spectra.

good agreement with head-on collisions performed at the LHC accelerator.

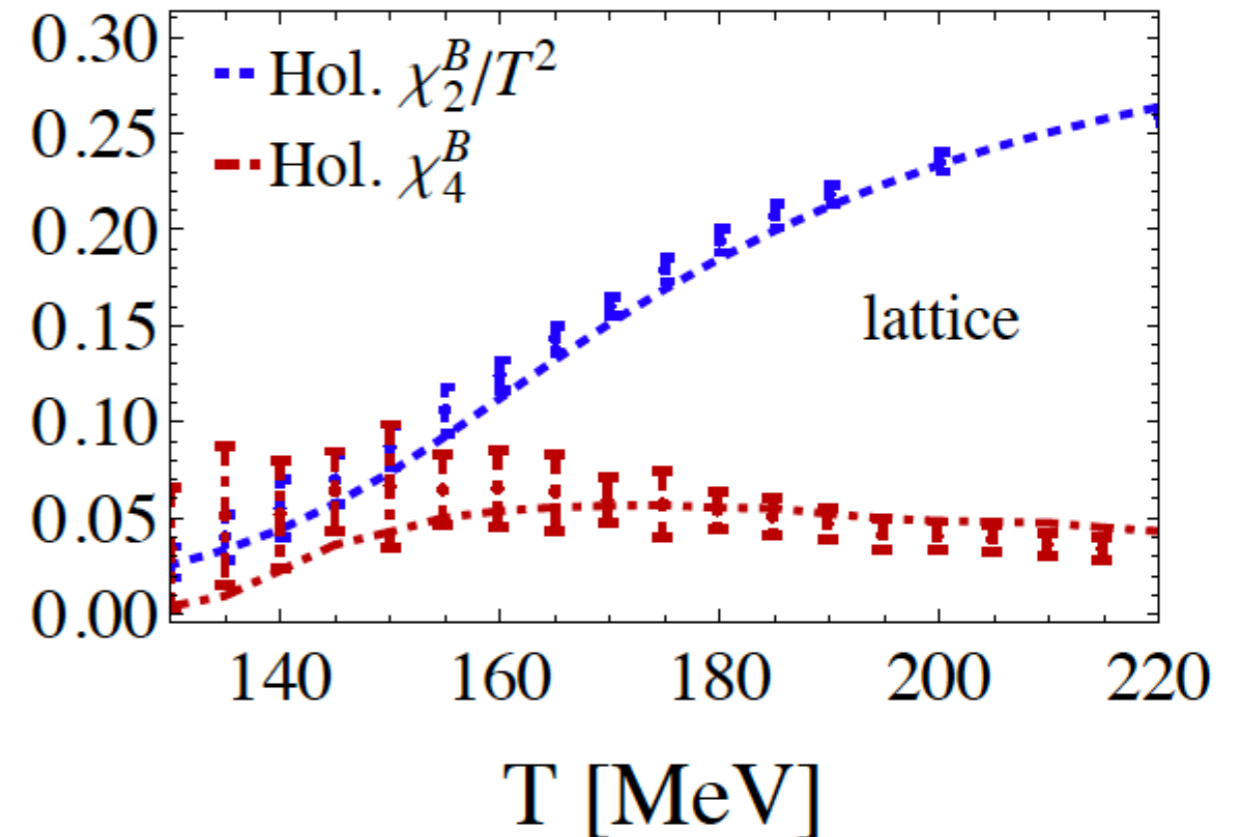


QCD equation of state at zero μ_B



Speed of sound,

Phys.Rev.Lett. 101 (2008) 131601



Baryon susceptibility,

Phys.Rev.Lett. 115 (2015) 20, 202301

A strong indication that holography can make **quantitative predictions** for the properties of QCD in **non-perturbative** regime.

Two recent reviews:

Bottom-up approach

The dynamical holographic QCD method for hadron physics and QCD matter

[Yidian Chen](#) (Beijing, GUCAS), [Danning Li](#) (Jinan U.), [Mei Huang](#) (Beijing, GUCAS) (Jun 2, 2022)

Published in: *Commun.Theor.Phys.* 74 (2022) 9, 097201 • e-Print: [2206.00917](#) [hep-ph]



pdf



DOI



cite



claim



reference search

Hot QCD Phase Diagram From Holographic Einstein-Maxwell-Dilaton Models

[Romulo Rougemont](#) (Goias U.), [Joaquin Grefa](#) (Houston U.), [Mauricio Hippert](#) (Illinois U., Urbana), [Jorge Noronha](#) (Illinois U., Urbana), [Jacquelyn Noronha-Hostler](#) (Illinois U., Urbana) et al. (Jul 7, 2023)

e-Print: [2307.03885](#) [nucl-th]



pdf



cite



claim



reference search

Outline

1. Introduction

2. Holographic QCD model

3. Phase diagram and GWs

4. Summary and discussion

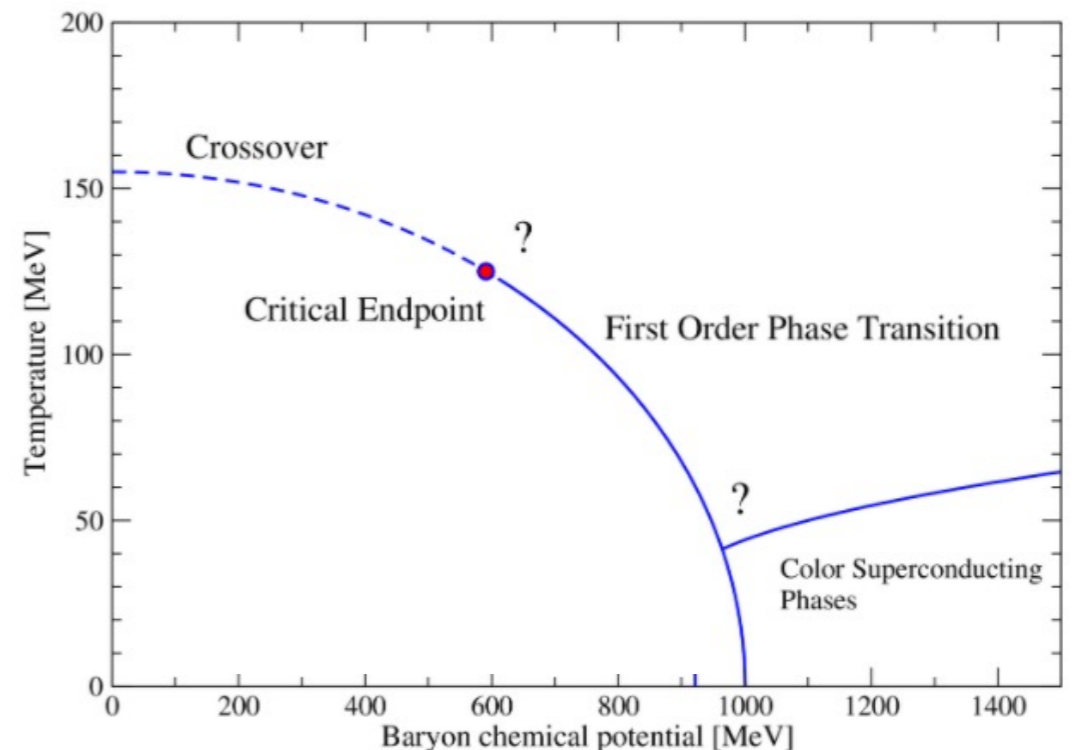
2. Holographic QCD Model

Einstein-Maxwell-Dilaton theory:

Rong-Gen Cai, Song He, **Li Li**, Yuan-Xu Wang,
Phys. Rev. D 106 no.12, L121902 (2022)

$$S = \frac{1}{2\kappa_N^2} \int d^5x \sqrt{-g} \left[\mathcal{R} - \frac{1}{2} \nabla_\mu \phi \nabla^\mu \phi - \frac{Z(\phi)}{4} F_{\mu\nu} F^{\mu\nu} - V(\phi) \right],$$

To match the degrees of freedom
in QCD phase Diagram: ϕ , A_μ



2. Holographic QCD Model

Einstein-Maxwell-Dilaton theory:

Rong-Gen Cai, Song He, **Li Li**, Yuan-Xu Wang,
Phys. Rev. D 106 no.12, L121902 (2022)

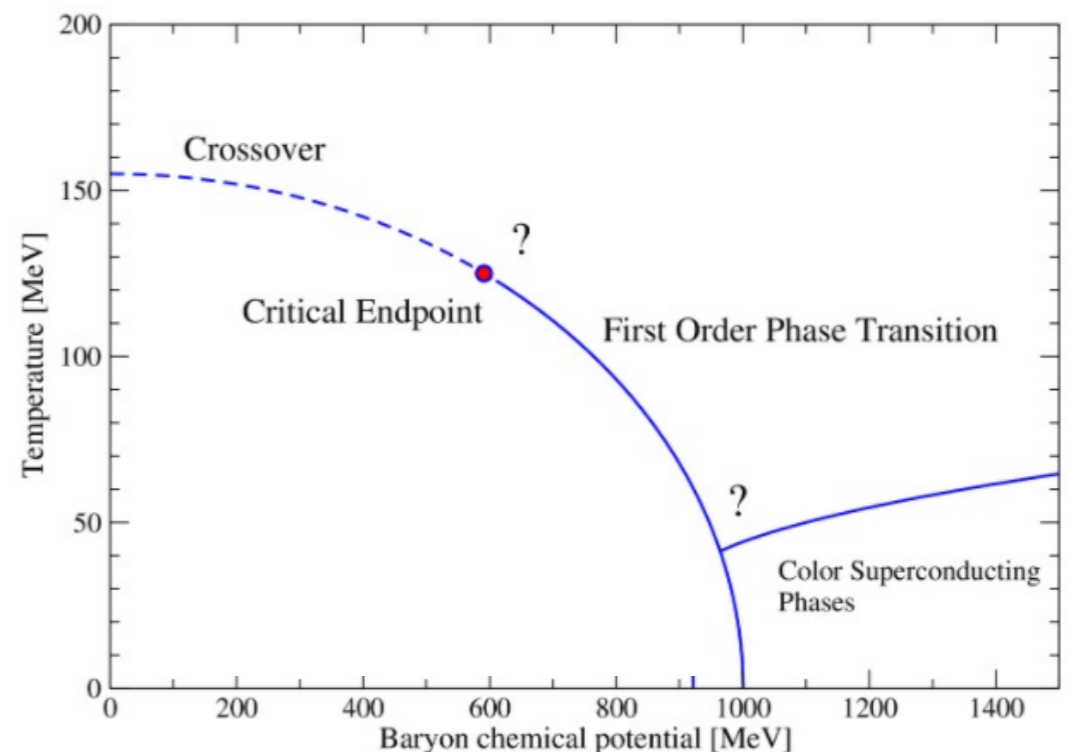
$$S = \frac{1}{2\kappa_N^2} \int d^5x \sqrt{-g} \left[\mathcal{R} - \frac{1}{2} \nabla_\mu \phi \nabla^\mu \phi - \frac{Z(\phi)}{4} F_{\mu\nu} F^{\mu\nu} - V(\phi) \right],$$

Break conformal symmetry

Baryon chemical potential

To match the degrees of freedom
in QCD phase Diagram: ϕ , A_μ

To match lattice QCD simulation
at $\mu_B = 0$: $Z(\phi)$, $V(\phi)$



2. Holographic QCD Model

Einstein-Maxwell-Dilaton theory:

Rong-Gen Cai, Song He, **Li Li**, Yuan-Xu Wang,
Phys. Rev. D 106 no.12, L121902 (2022)

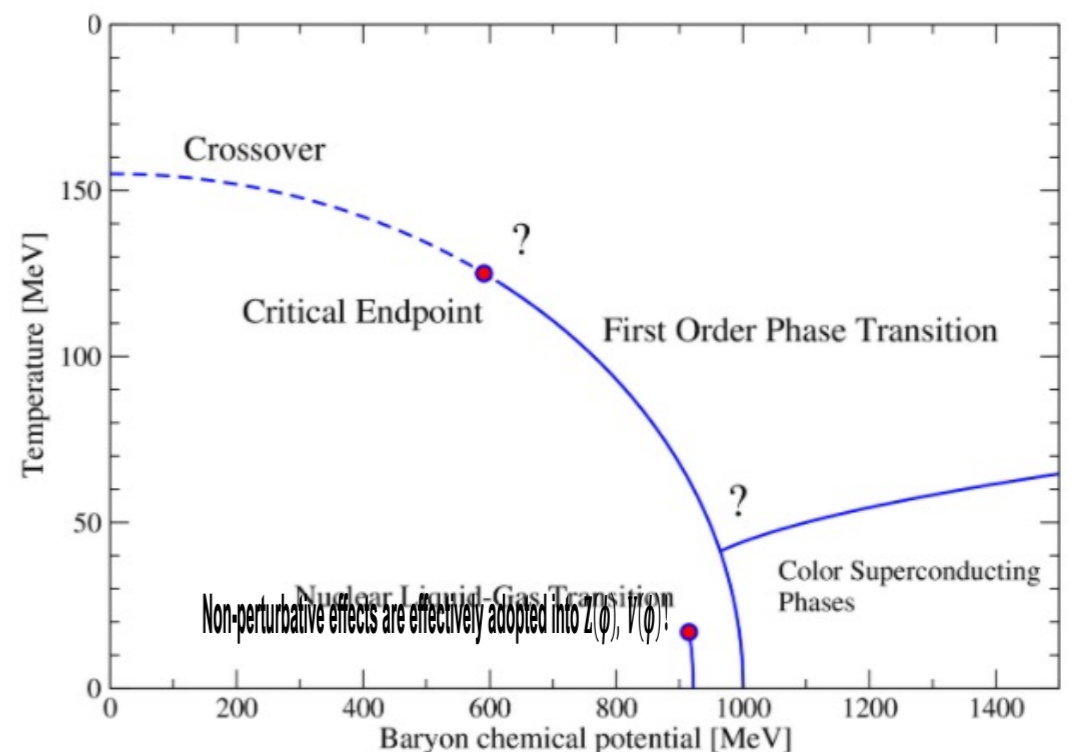
$$S = \frac{1}{2\kappa_N^2} \int d^5x \sqrt{-g} \left[\mathcal{R} - \frac{1}{2} \nabla_\mu \phi \nabla^\mu \phi - \frac{Z(\phi)}{4} F_{\mu\nu} F^{\mu\nu} - V(\phi) \right],$$

Break conformal symmetry

Baryon chemical potential

To match the degrees of freedom
in QCD phase Diagram: ϕ , A_μ

To match lattice QCD simulation
at $\mu_B = 0$: $Z(\phi)$, $V(\phi)$



Non-perturbative effects are effectively adopted into $Z(\phi)$, $V(\phi)$!

2. Holographic QCD Model

To fix $Z(\phi)$ and $V(\phi)$ is very challenging !

$$S = \frac{1}{2\kappa_N^2} \int d^5x \sqrt{-g} \left[\mathcal{R} - \frac{1}{2} \nabla_\mu \phi \nabla^\mu \phi - \frac{Z(\phi)}{4} F_{\mu\nu} F^{\mu\nu} - V(\phi) \right],$$

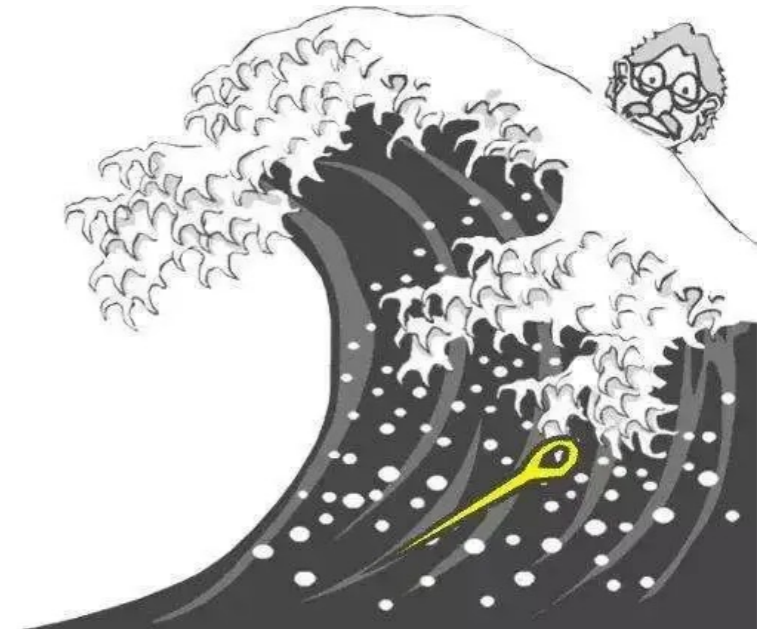
$$V(\phi) = -12 \cosh[c_1 \phi] + \left(6c_1^2 - \frac{3}{2}\right) \phi^2 + c_2 \phi^6,$$

$$Z(\phi) = \frac{1}{1+c_3} \operatorname{sech}[c_4 \phi^3] + \frac{c_3}{1+c_3} e^{-c_5 \phi},$$

Free model parameters

c_1, c_2, c_3, c_4, c_5

κ_N^2



All parameters are fixed using state-of-the-art lattice QCD data

Equation of state in (2 + 1)-flavor QCD

A. Bazavov, Tanmoy Bhattacharya, C. DeTar, H.-T. Ding, Steven Gottlieb, Rajan Gupta, P. Hegde, U. M. Heller, F. Karsch, E. Laermann, L. Levkova, Swagato Mukherjee, P. Petreczky, C. Schmidt, C. Schroeder, R. A. Soltz, W. Soeldner, R. Sugar, M. Wagner, and P. Vranas (HotQCD Collaboration)
Phys. Rev. D **90**, 094503 – Published 4 November 2014

Black hole thermodynamics

Black hole ansatz:

$$ds^2 = -f(r)e^{-\eta(r)} dt^2 + \frac{dr^2}{f(r)} + r^2 d\mathbf{x}_3^2$$

$$\phi = \phi(r), \quad A_t = A_t(r)$$

To solve equations of motion:

$$\phi'' + \left(\frac{f'}{f} - \frac{\eta'}{2} + \frac{3}{r} \right) \phi' + \frac{\partial_\phi Z}{2f} e^\eta A_t'^2 - \frac{1}{f} \partial_\phi V = 0$$

$$\partial_r (e^{\eta/2} r^3 Z A_t') = 0$$

$$\frac{\eta'}{r} + \frac{1}{3} \phi'^2 = 0$$

$$\frac{2f'}{r} - \frac{\eta'}{r} + \frac{Z}{3f} e^\eta A_t'^2 + \frac{2}{3f} V + \frac{4}{r^2} = 0$$

$$V(\phi) = -12 \cosh[c_1 \phi] + \left(6c_1^2 - \frac{3}{2}\right) \phi^2 + c_2 \phi^6$$

$$Z(\phi) = \frac{1}{1+c_3} \operatorname{sech}[c_4 \phi^3] + \frac{c_3}{1+c_3} e^{-c_5 \phi},$$

asymptotic expansion at boundary:

$$\phi(r) = \frac{\phi_s}{r} + \frac{\phi_v}{r^3} - \frac{\ln(r)}{6r^3} (1 - 6c_1^4) \phi_s^3 + \mathcal{O}\left(\frac{\ln(r)}{r^5}\right).$$

$$A_t(r) = \mu_B - \frac{2\kappa_N^2 \rho_B}{2r^2} - \frac{2\kappa_N^2 \rho_B c_3 c_5 \phi_s}{3(1+c_3)r^3} + \frac{2\kappa_N^2 \rho_B \phi_s^2 ((1+c_3)^2 - 6(-1+c_3)c_3 c_5^2)}{48(1+c_3)^2 r^4} + \frac{2\kappa_N^2 \rho_B c_3 c_5 (-10c_5^2(1+(-4+c_3)c_3)) \phi_s^3}{300(1+c_3)^3 r^5} + \frac{2\kappa_N^2 \rho_B c_3 c_5 ((7-12c_1^4) \phi_s^3 - 60\phi_v)}{300(1+c_3)r^5} - \frac{2\kappa_N^2 \rho_B c_3 c_5 \phi_s^3 (-1+6c_1^4) \ln(r)}{30(1+c_3)r^5} + \mathcal{O}\left(\frac{\ln(r)}{r^6}\right).$$

$$\eta(r) = 0 + \frac{\phi_s^2}{6r^2} + \frac{(1-6c_1^4)\phi_s^4 + 72\phi_s\phi_v}{144r^4}$$

$$- \frac{\ln(r)}{12r^4} (1-6c_1^4)\phi_s^4 + \mathcal{O}\left(\frac{\ln(r)^2}{r^6}\right).$$

$$f(r) = r^2 \left[1 + \frac{\phi_s^2}{6r^2} + \frac{f_v}{r^4} - \frac{\ln(r)}{12r^4} (1-6c_1^4)\phi_s^4 + \mathcal{O}\left(\frac{\ln(r)^2}{r^6}\right) \right].$$

Black hole thermodynamics

Black hole ansatz:

$$ds^2 = -f(r)e^{-\eta(r)} dt^2 + \frac{dr^2}{f(r)} + r^2 d\mathbf{x}_3^2$$

$$\phi = \phi(r), \quad A_t = A_t(r)$$

Temperature and entropy

$$T = \frac{1}{4\pi} f'(r_h) e^{-\eta(r_h)/2}, \quad s = \frac{2\pi}{\kappa_N^2} r_h^3$$

Free energy

$$\Omega = \frac{1}{2\kappa_N^2} \left(f_v - \phi_s \phi_v - \frac{3 - 48b - 8c_1^4}{48} \phi_s^4 \right)$$

Energy and pressure

$$\epsilon := T_{tt} = \frac{1}{2\kappa_N^2} \left(-3f_v + \phi_s \phi_v + \frac{1 + 48b}{48} \phi_s^4 \right),$$

$$P := T_{xx} = T_{yy} = T_{zz}$$

$$= \frac{1}{2\kappa_N^2} \left(-f_v + \phi_s \phi_v + \frac{3 - 48b - 8c_1^4}{48} \phi_s^4 \right),$$

asymptotic expansion at boundary:

$$\begin{aligned} \phi(r) &= \frac{\phi_s}{r} + \frac{\phi_v}{r^3} - \frac{\ln(r)}{6r^3} (1 - 6c_1^4) \phi_s^3 + \mathcal{O}\left(\frac{\ln(r)}{r^5}\right). \\ A_t(r) &= \mu_B - \frac{2\kappa_N^2 \rho_B}{2r^2} - \frac{2\kappa_N^2 \rho_B c_3 c_5 \phi_s}{3(1 + c_3) r^3} \\ &\quad + \frac{2\kappa_N^2 \rho_B \phi_s^2 ((1 + c_3)^2 - 6(-1 + c_3) c_3 c_5^2)}{48(1 + c_3)^2 r^4} \\ &\quad + \frac{2\kappa_N^2 \rho_B c_3 c_5 (-10 c_5^2 (1 + (-4 + c_3) c_3)) \phi_s^3}{300(1 + c_3)^3 r^5} \\ &\quad + \frac{2\kappa_N^2 \rho_B c_3 c_5 ((7 - 12 c_1^4) \phi_s^3 - 60 \phi_v)}{300(1 + c_3) r^5} \\ &\quad - \frac{2\kappa_N^2 \rho_B c_3 c_5 \phi_s^3 (-1 + 6 c_1^4) \ln(r)}{30(1 + c_3) r^5} + \mathcal{O}\left(\frac{\ln(r)}{r^6}\right). \\ \eta(r) &= 0 + \frac{\phi_s^2}{6r^2} + \frac{(1 - 6c_1^4) \phi_s^4 + 72 \phi_s \phi_v}{144r^4} \\ &\quad - \frac{\ln(r)}{12r^4} (1 - 6c_1^4) \phi_s^4 + \mathcal{O}\left(\frac{\ln(r)^2}{r^6}\right). \\ f(r) &= r^2 \left[1 + \frac{\phi_s^2}{6r^2} + \frac{f_v}{r^4} - \frac{\ln(r)}{12r^4} (1 - 6c_1^4) \phi_s^4 \right. \\ &\quad \left. + \mathcal{O}\left(\frac{\ln(r)^2}{r^6}\right) \right]. \end{aligned}$$

Black hole thermodynamics

Black hole ansatz:

$$ds^2 = -f(r)e^{-\eta(r)}dt^2 + \frac{dr^2}{f(r)} + r^2 d\mathbf{x}_3^2$$

$$\phi = \phi(r), \quad A_t = A_t(r)$$

Temperature and entropy

$$T = \frac{1}{4\pi} f'(r_h) e^{-\eta(r_h)/2}, \quad s = \frac{2\pi}{\kappa_N^2} r_h^3$$

Free energy

$$\Omega = \frac{1}{2\kappa_N^2} \left(f_v - \phi_s \phi_v - \frac{3 - 48b - 8c_1^4}{48} \phi_s^4 \right)$$

Energy and pressure

$$\epsilon := T_{tt} = \frac{1}{2\kappa_N^2} \left(-3f_v + \phi_s \phi_v + \frac{1 + 48b}{48} \phi_s^4 \right),$$

$$P := T_{xx} = T_{yy} = T_{zz}$$

$$= \frac{1}{2\kappa_N^2} \left(-f_v + \phi_s \phi_v + \frac{3 - 48b - 8c_1^4}{48} \phi_s^4 \right),$$

◆ Thermodynamic relation

$$\Omega = \epsilon - Ts - \mu_B \rho_B = -P$$

$$Q = \frac{1}{2\kappa_N^2} r^3 e^{\eta/2} \left[r^2 \left(\frac{f}{r^2} e^{-\eta} \right)' - Z A_t A_t' \right]$$

◆ First law of thermodynamics

$$d\epsilon = T ds + \mu_B d\rho_B - Q d\phi_s$$

Scalar source ϕ_s will be fixed

Thermodynamics of AdS Black Holes with Scalar Hair

$$S = \frac{1}{2\kappa_N^2} \int d^{d+1}x \sqrt{-g} \left[\mathcal{R} - \frac{1}{2} \nabla_\mu \phi \nabla^\mu \phi - V(\phi) \right]$$

$$ds^2 = -f(r)e^{-\eta(r)} dt^2 + \frac{dr^2}{f(r)} + r^2 d\vec{x}_{d-1}^2, \quad \phi = \phi(r)$$

Naively-expected 1st law of thermodynamics does not hold [1408.0010,1408.1514]

$$dE = TdS + XdY = TdS - (c_1 \phi_v d\phi_s - c_2 \phi_s d\phi_v)$$

Thermodynamics of AdS Black Holes with Scalar Hair

$$S = \frac{1}{2\kappa_N^2} \int d^{d+1}x \sqrt{-g} \left[\mathcal{R} - \frac{1}{2} \nabla_\mu \phi \nabla^\mu \phi - V(\phi) \right]$$

$$ds^2 = -f(r)e^{-\eta(r)} dt^2 + \frac{dr^2}{f(r)} + r^2 d\vec{x}_{d-1}^2, \quad \phi = \phi(r)$$

Naively-expected 1st law of thermodynamics does not hold [1408.0010,1408.1514]

$$dE = TdS + XdY = TdS - (c_1\phi_v d\phi_s - c_2\phi_s d\phi_v)$$

Wald formula

holographic renormalization

$$\delta H = -\frac{\Sigma}{2\kappa_N^2} r^{d-1} e^{-\eta/2} \left[\frac{d-1}{r} \delta f + f \phi' \delta \phi \right]$$



$$\langle O \rangle = \frac{\delta}{\delta \phi_s} (S + S_\partial)_{on-shell}$$

$$\frac{\delta H_h}{\Sigma} = \frac{1}{2\kappa_N^2} e^{-\eta(r_h)/2} f'(r_h) (d-1) r_h^{d-2} \delta r_h = T \delta s$$

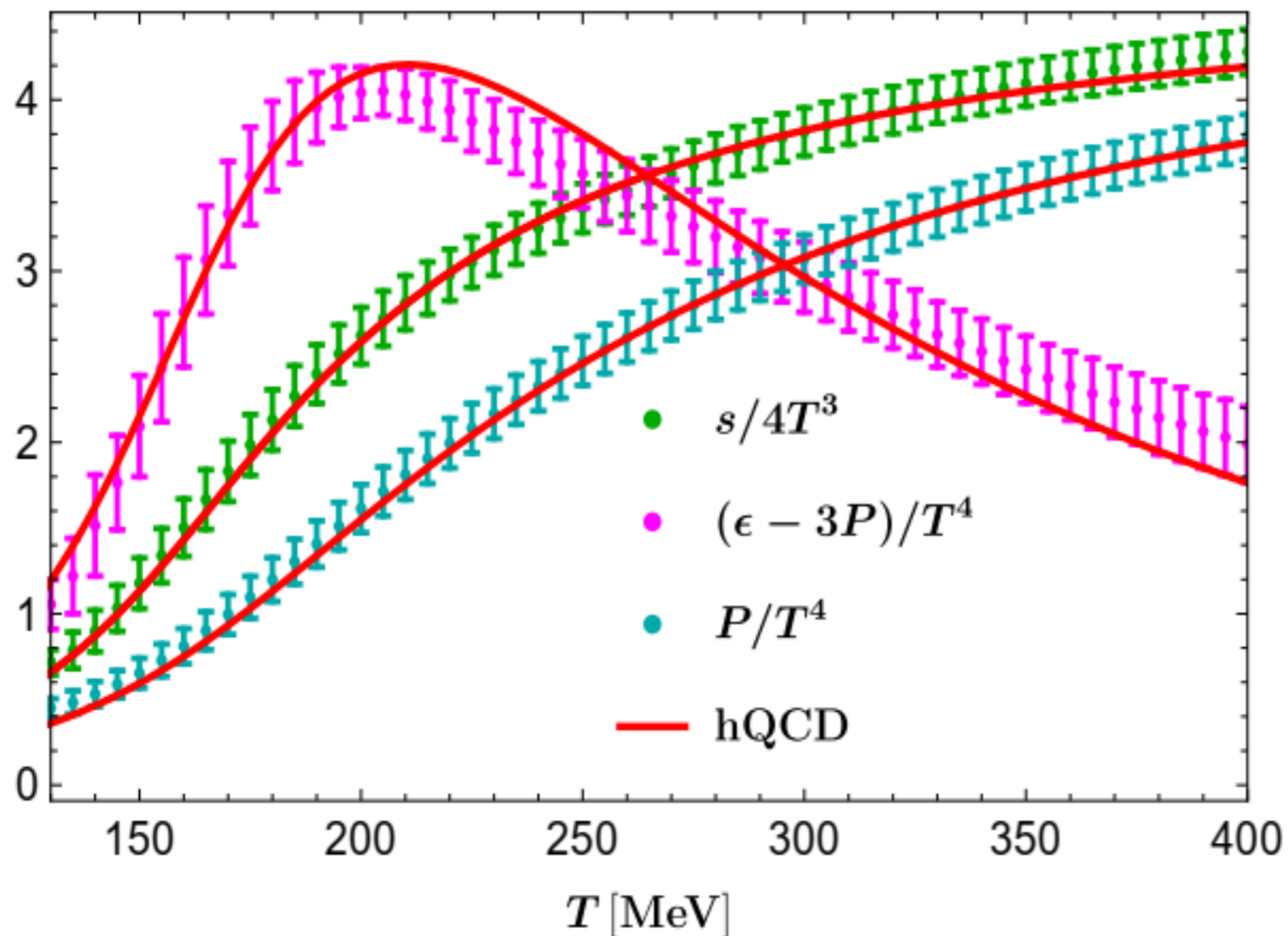
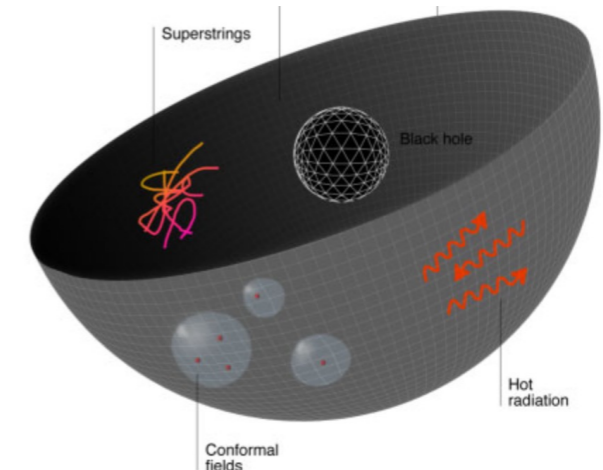
$$\frac{\delta H_\infty}{\Sigma} = \delta \mathcal{E} + \langle O \rangle \delta \phi_s$$

$$d\mathcal{E} = Tds - \langle O \rangle d\phi_s$$

Fix model parameters by thermodynamics

Equations of state at $\mu_B = 0$:

entropy, trace anomaly, pressure



$$T = \frac{1}{4\pi} f'(r_h) e^{-\eta(r_h)/2}$$

$$s = \frac{2\pi}{\kappa_N^2} r_h^3$$

$$\epsilon := T_{tt}$$

$$P := T_{xx}$$

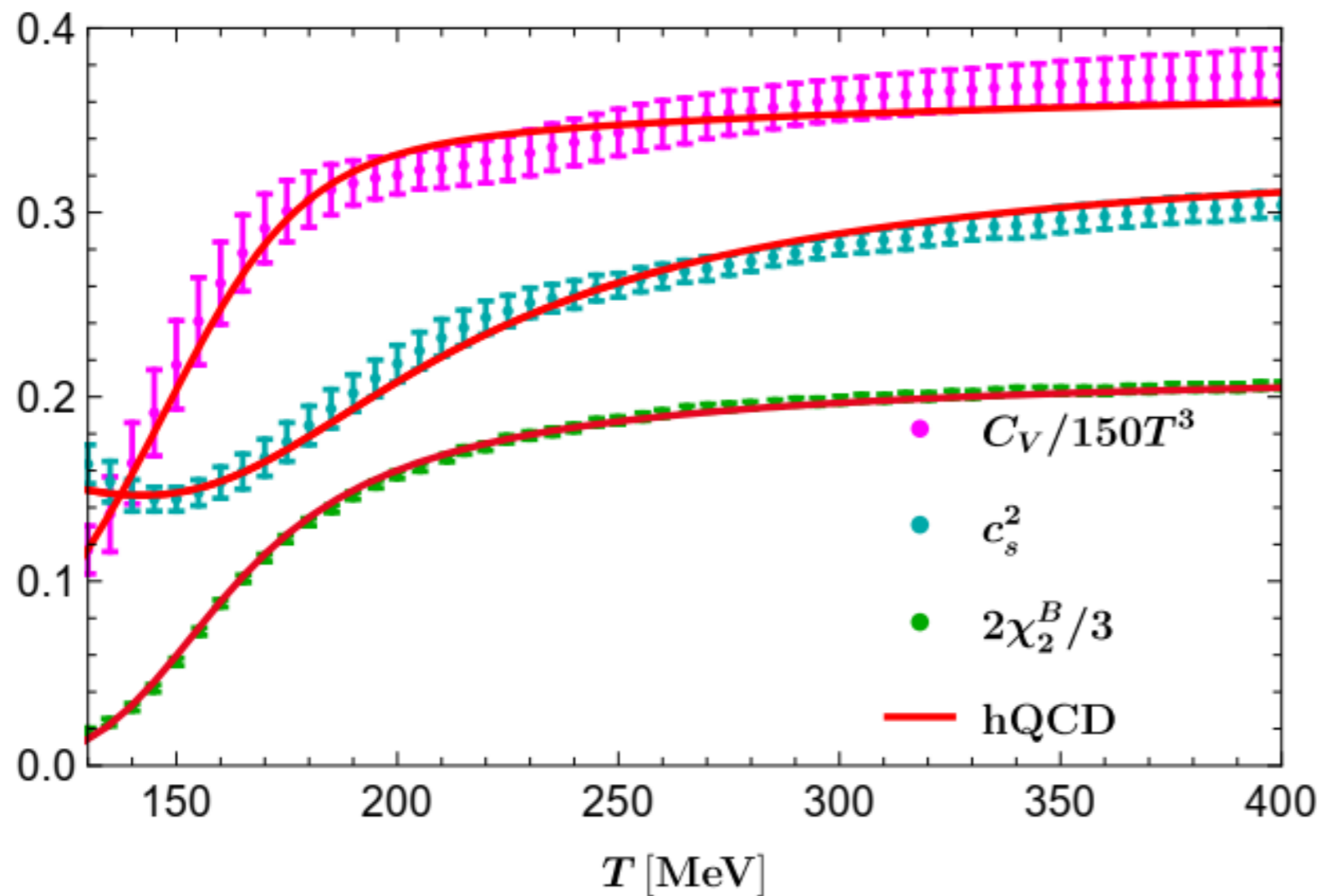
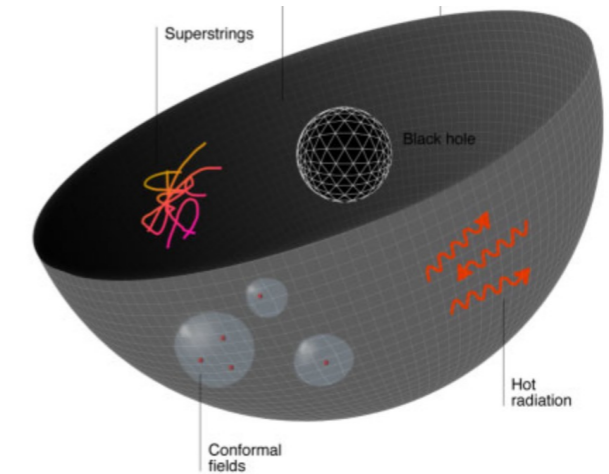
Lattice data for (2+1)-flavor QCD

A. Bazavov *et al.* [HotQCD], Phys. Rev. D 90 (2014), 094503

Fix model parameters by thermodynamics

Transport coefficients at $\mu_B = 0$:

specific heat, sound speed, baryon susceptibility



$$c_s = \sqrt{(dP/d\epsilon)_{\mu_B}}$$
$$C_V = (d\epsilon/dT)_{\mu_B}$$
$$\chi_2^B = (d\rho_B/d\mu_B)_T$$

Lattice data for (2+1)-flavor QCD

A. Bazavov *et al.* [HotQCD], Phys. Rev. D 90 (2014), 094503

Outline

1. Introduction

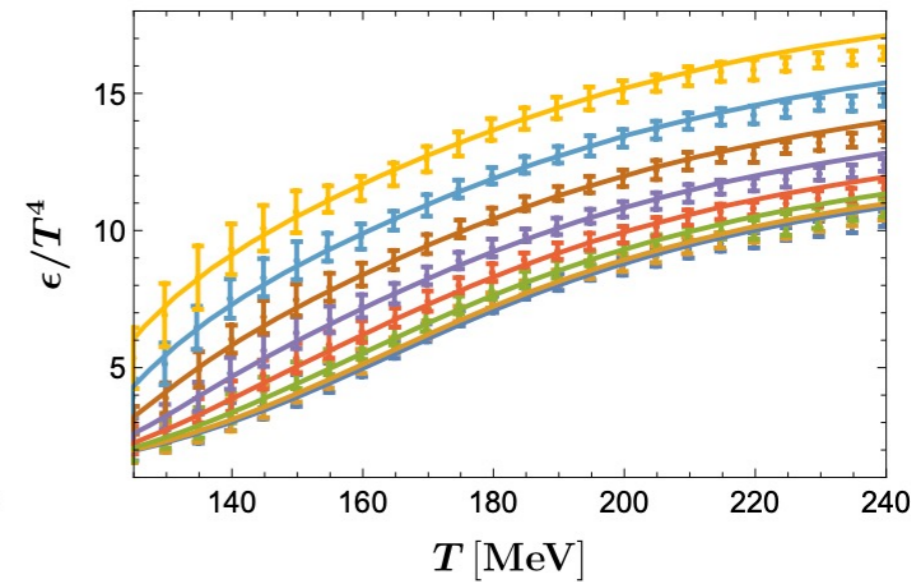
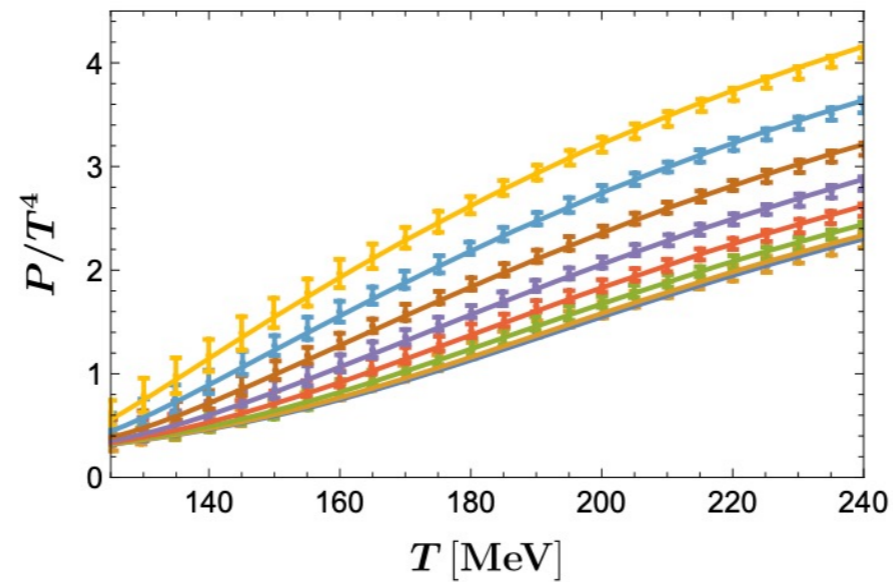
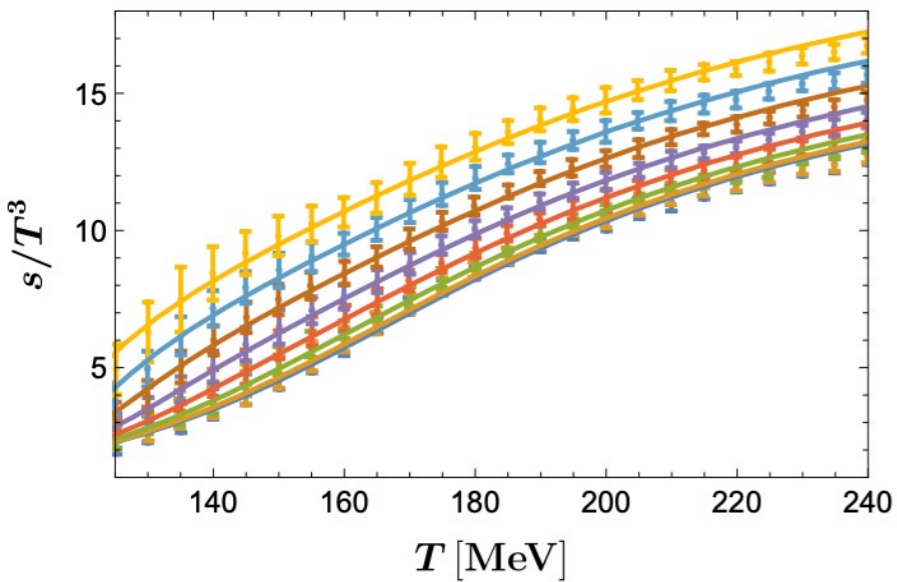
2. Holographic QCD model

3. Phase diagram and GWs

4. Summary and discussion

3. QCD Phase diagram and GWs

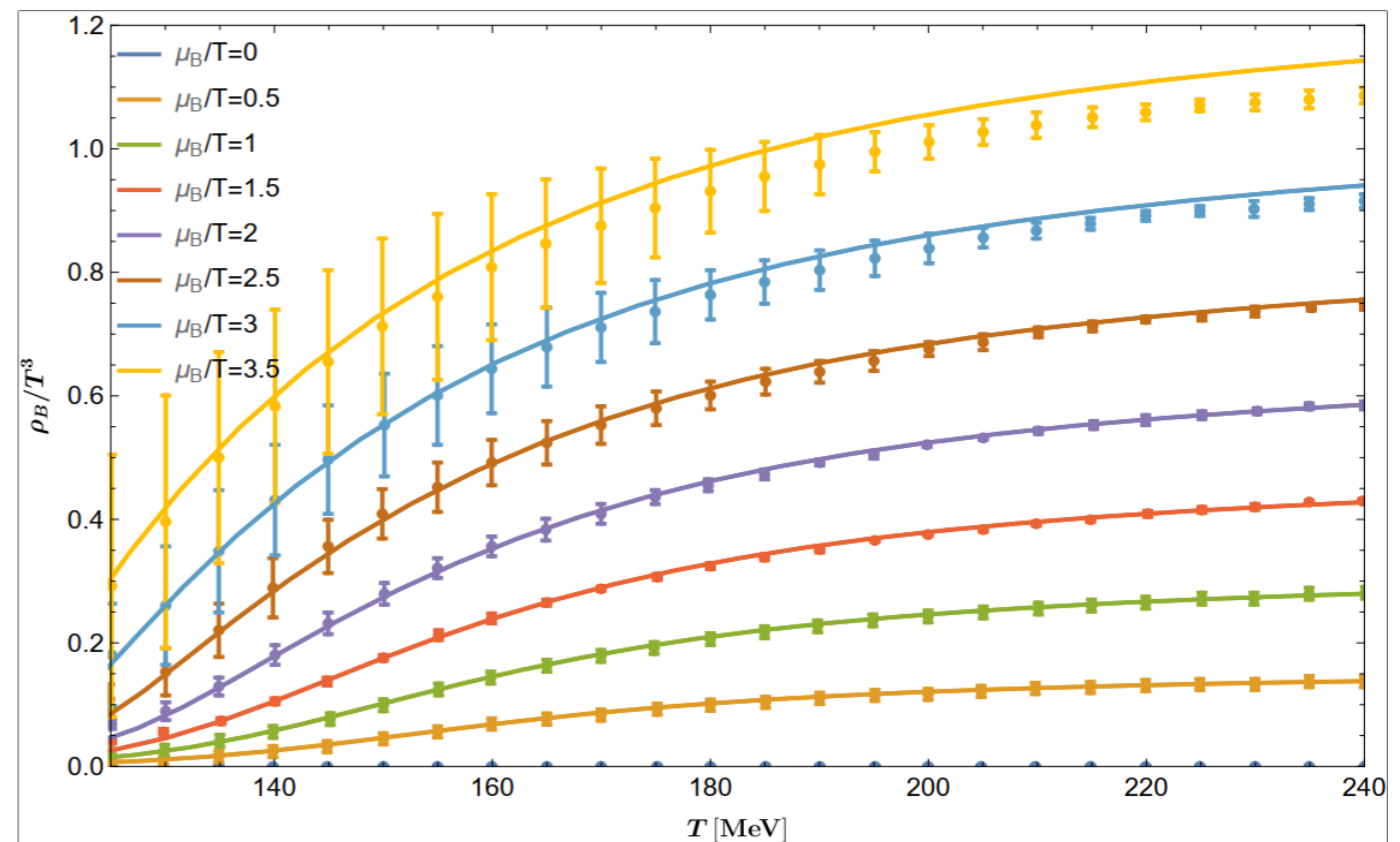
Predictions at finite chemical potential



More challenging to fit ρ_B

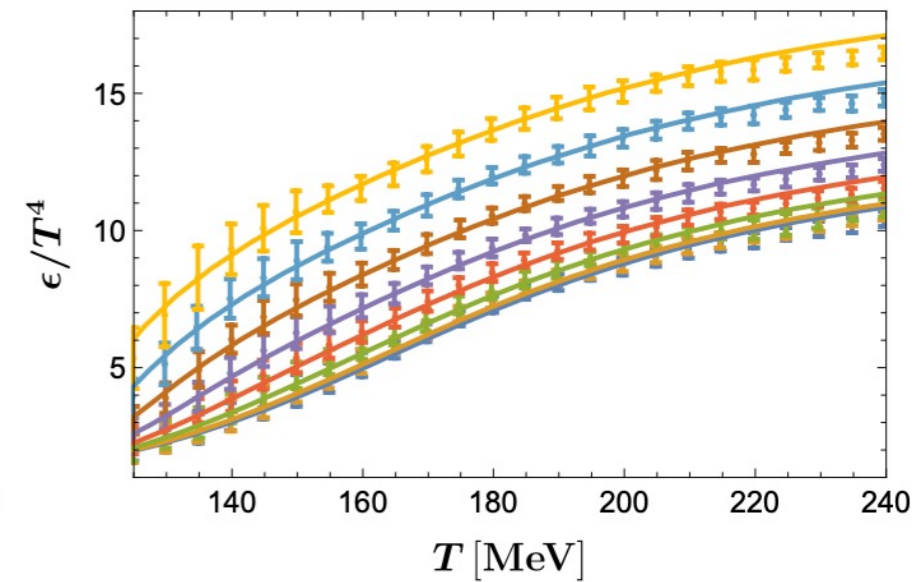
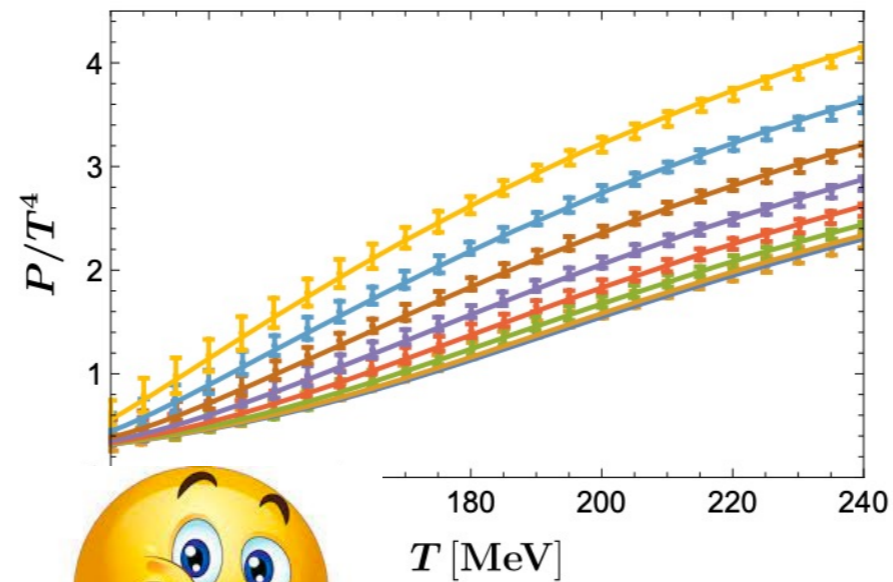
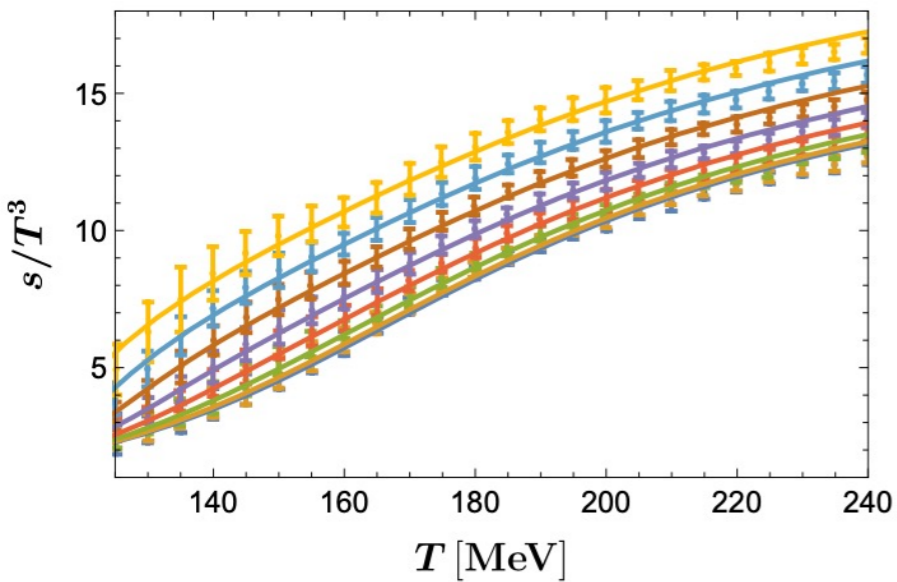
S. Borsanyi, et al., Phys. Rev. Lett. 126
(2021) no.23, 232001

extrapolate lattice QCD data to finite μ_B



3. QCD Phase diagram and GWs

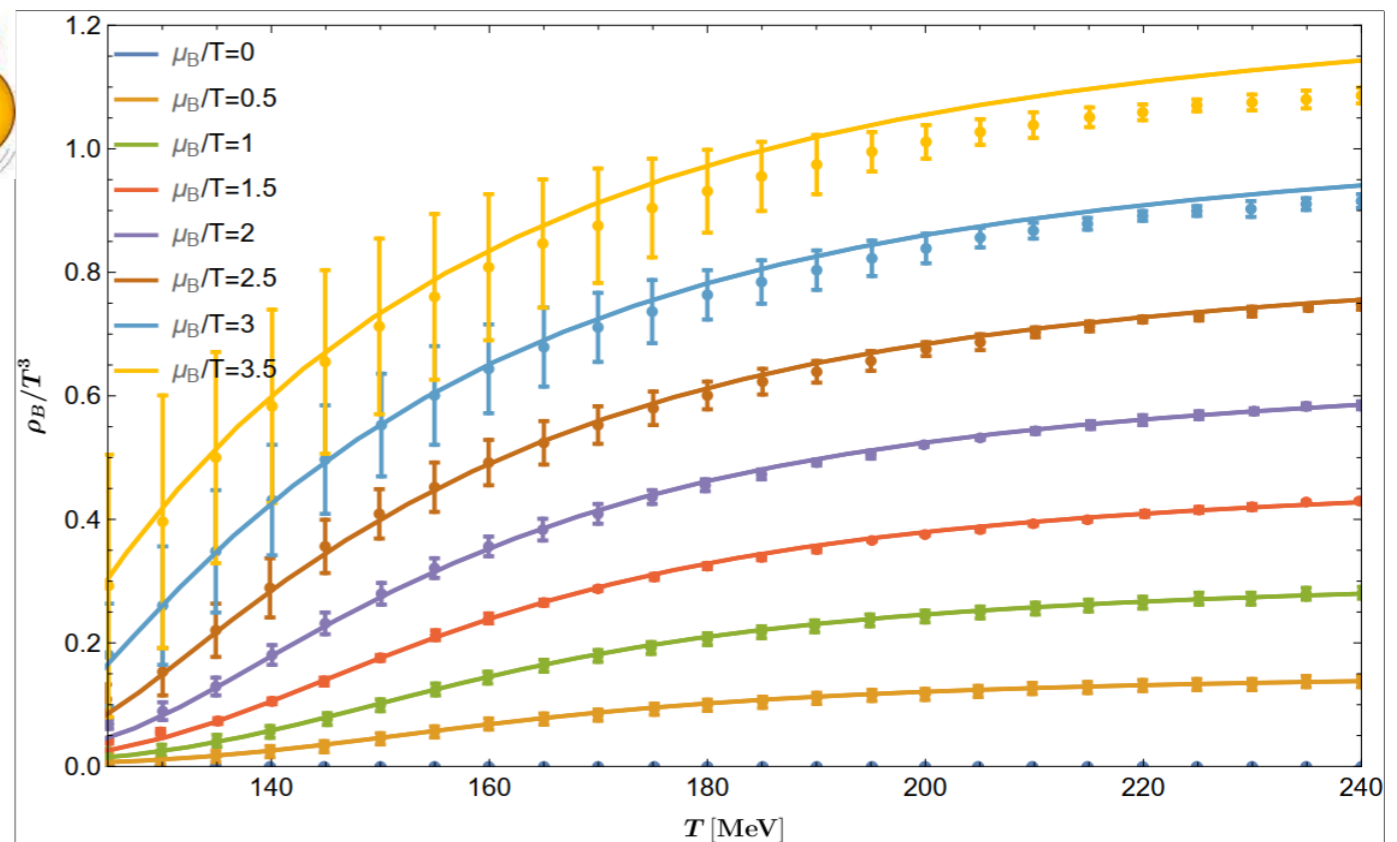
Predictions at finite chemical potential



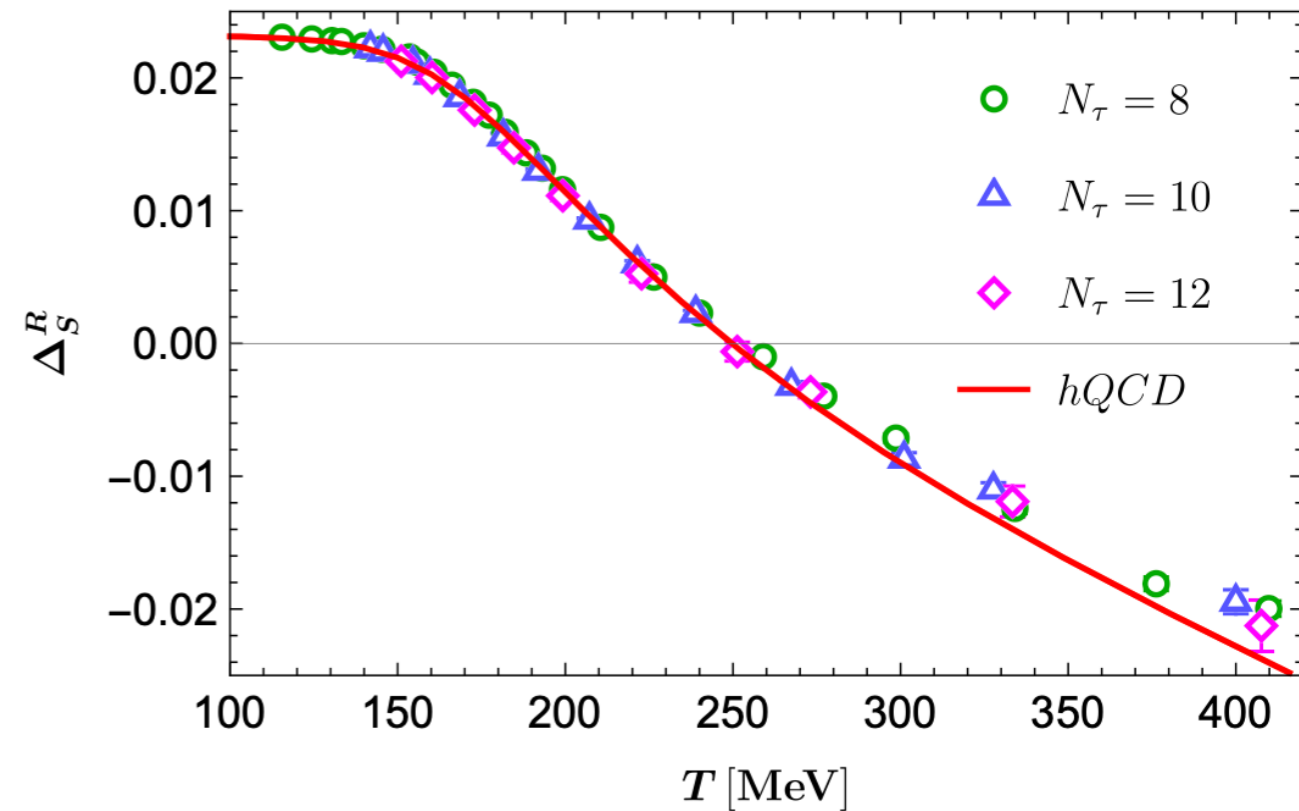
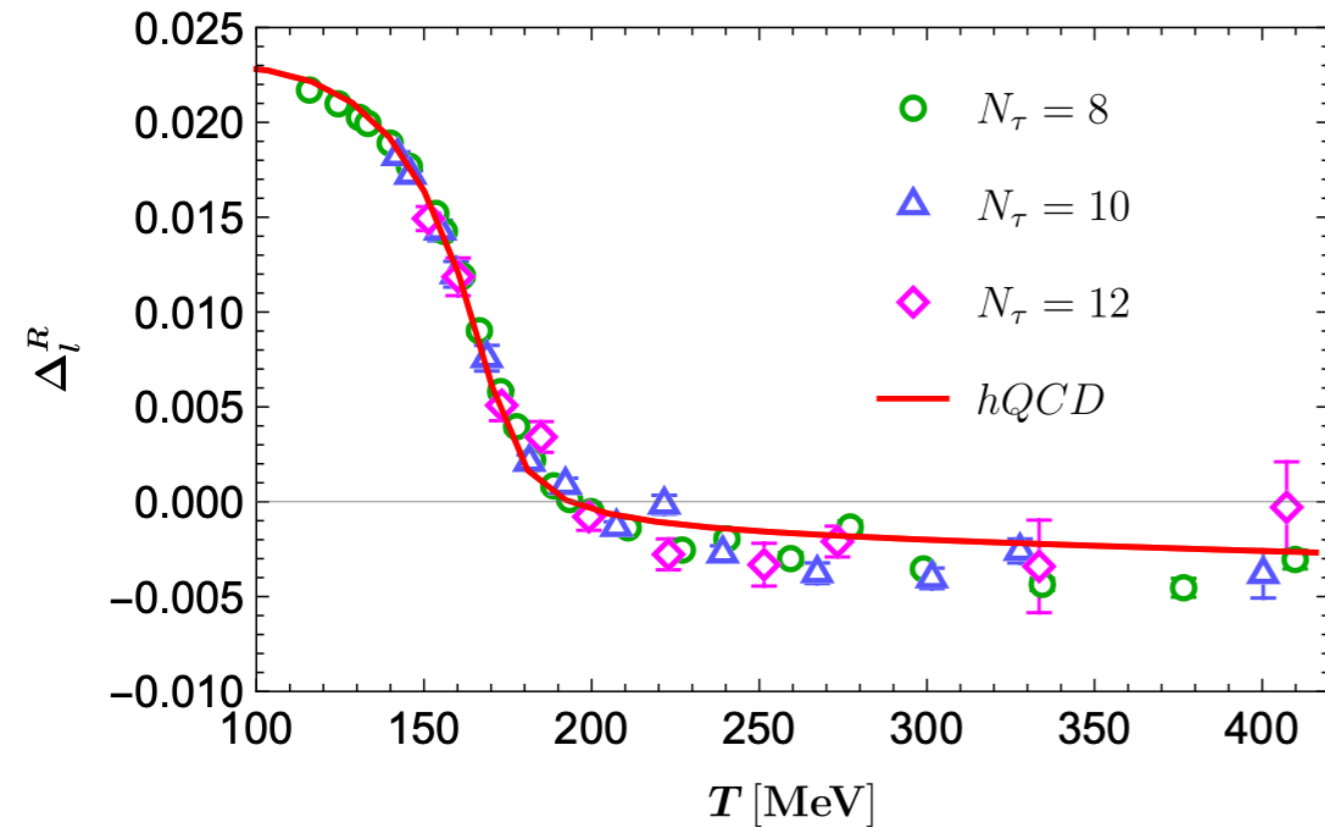
More challenging to fit ρ_B

S. Borsanyi, et al., Phys. Rev. Lett. 126 (2021) no.23, 232001

extrapolate lattice QCD data to finite μ_B



The chiral condensation:



Left panel: u, d quarks

Right panel: s quark

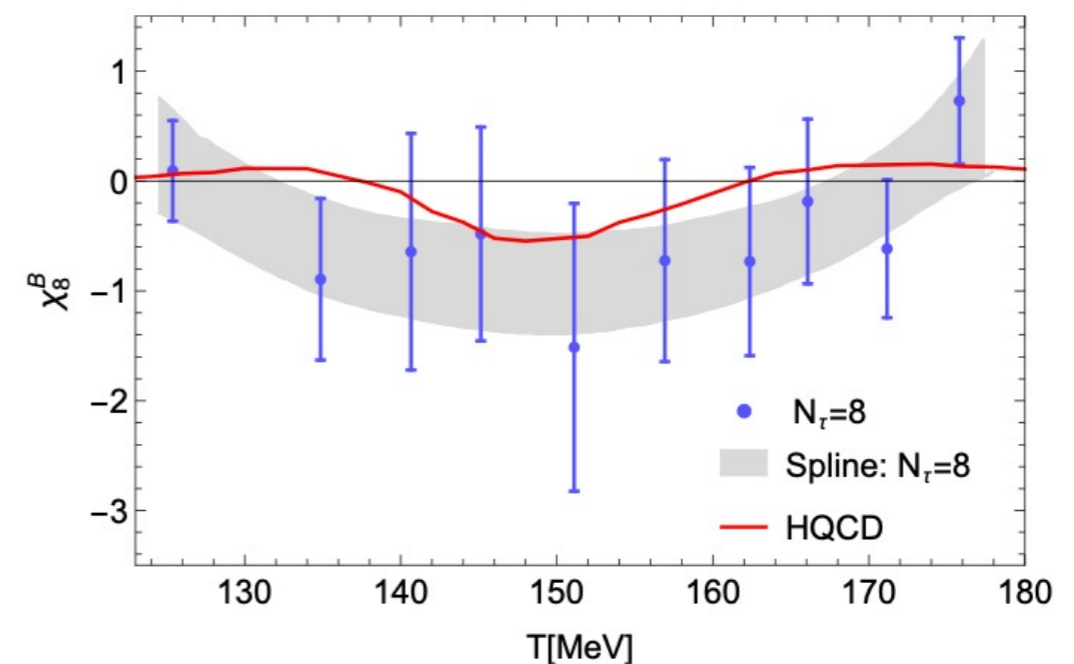
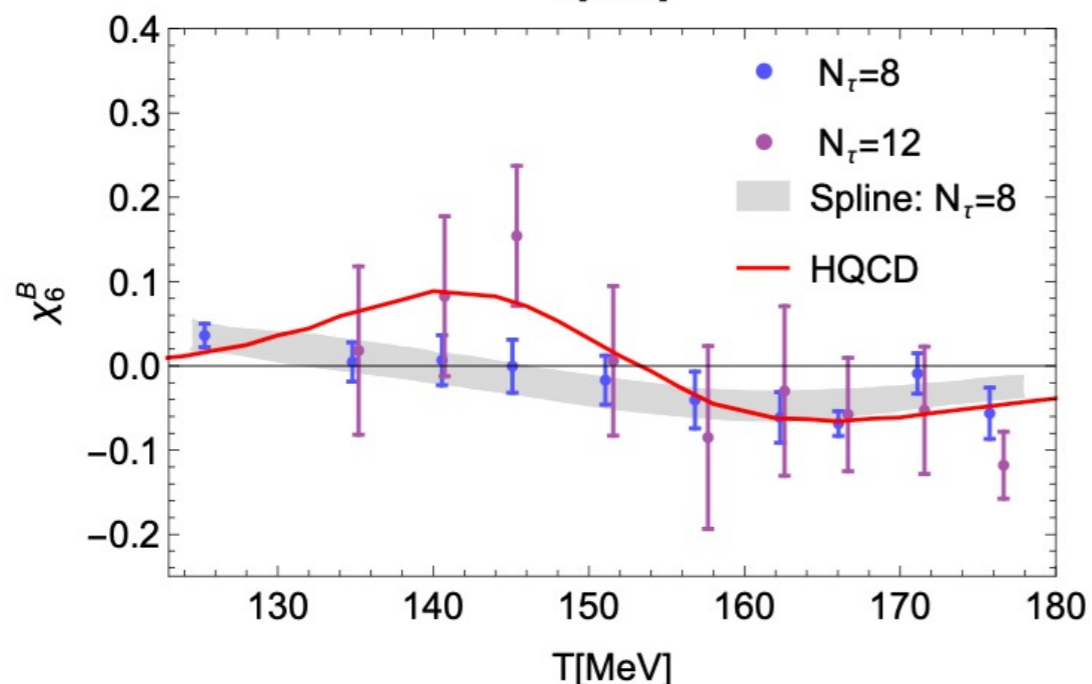
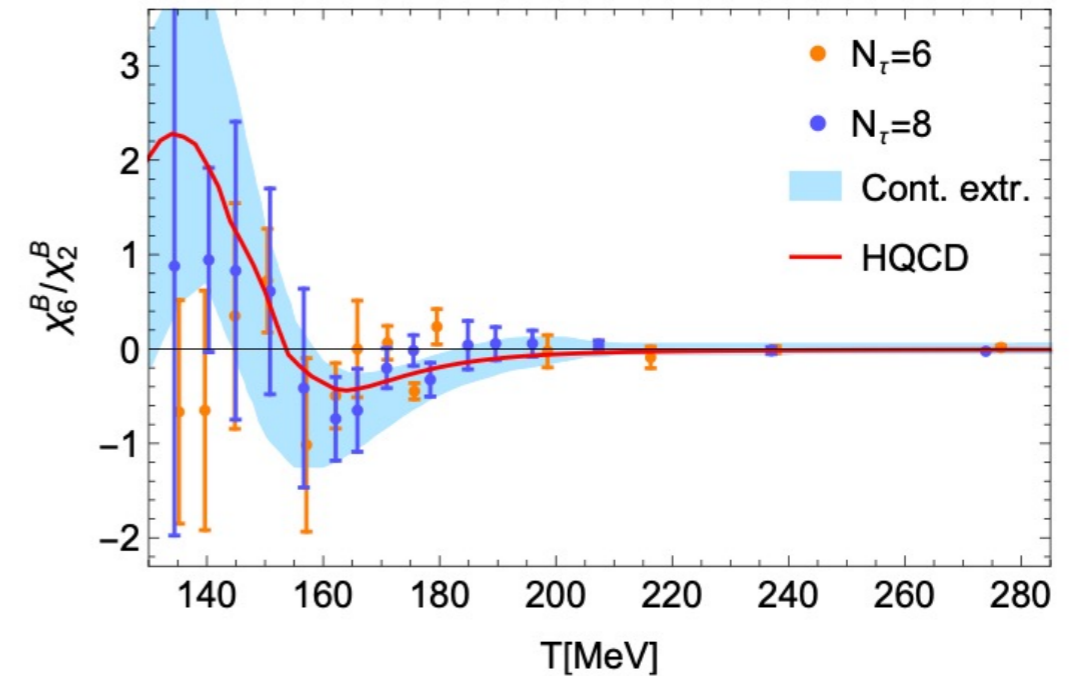
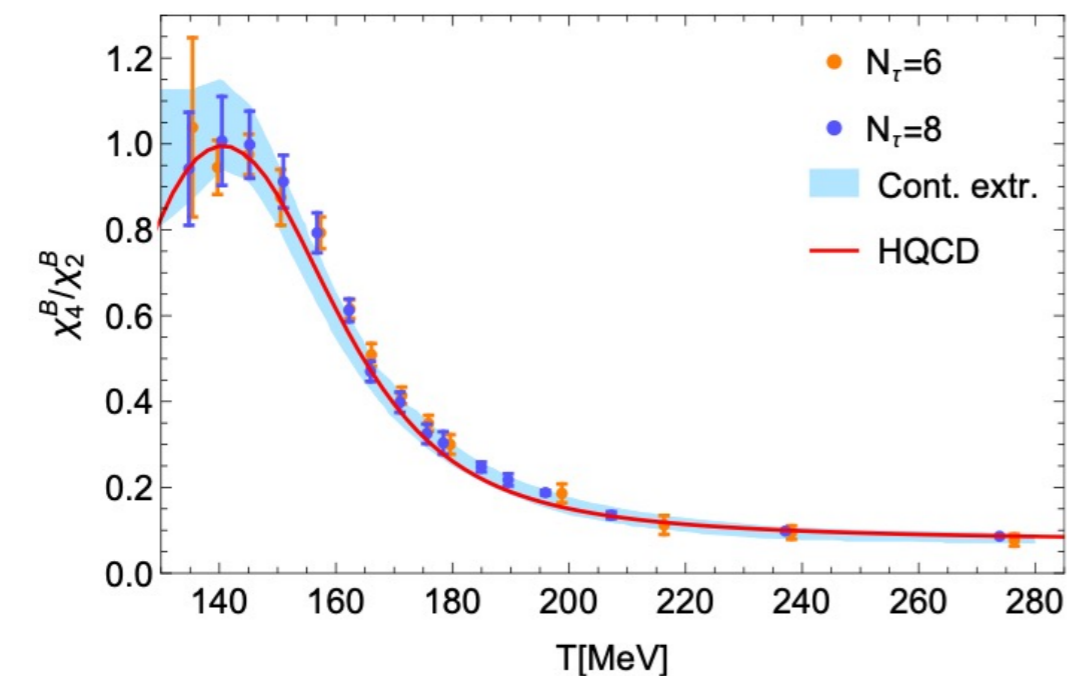
N_τ : the number of lattice sites in the imaginary time direction

$$\Delta_q^R = \hat{d} + 2m_s r_1^4 \left[\langle \bar{\psi}\psi \rangle_{q,T} - \langle \bar{\psi}\psi \rangle_{q,0} \right], \quad q = l, s$$

Generalized susceptibilities

$$\chi_n^B(T, \mu_B) = \frac{\partial^n P}{\partial(\mu_B/T)^n T^4}$$

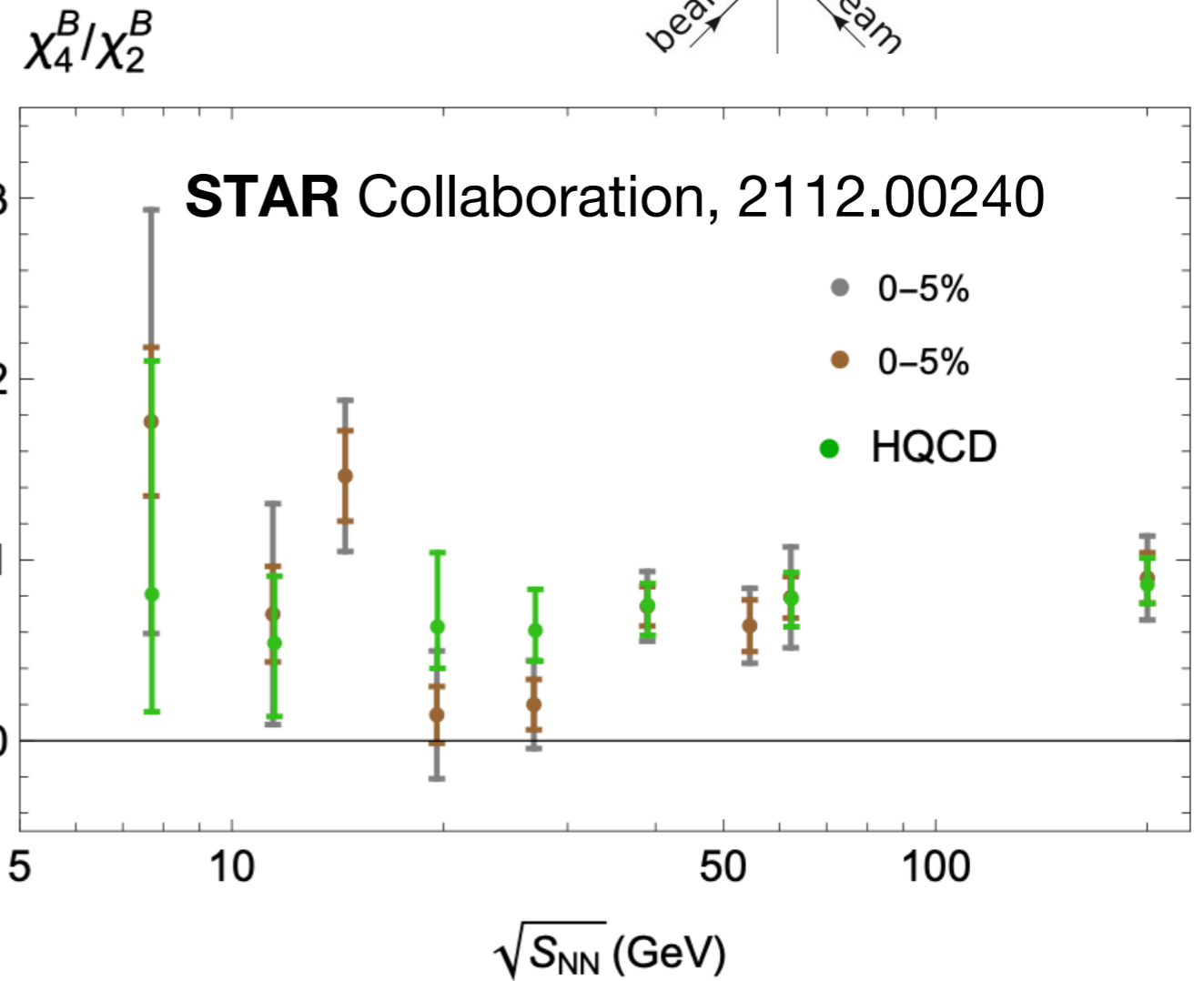
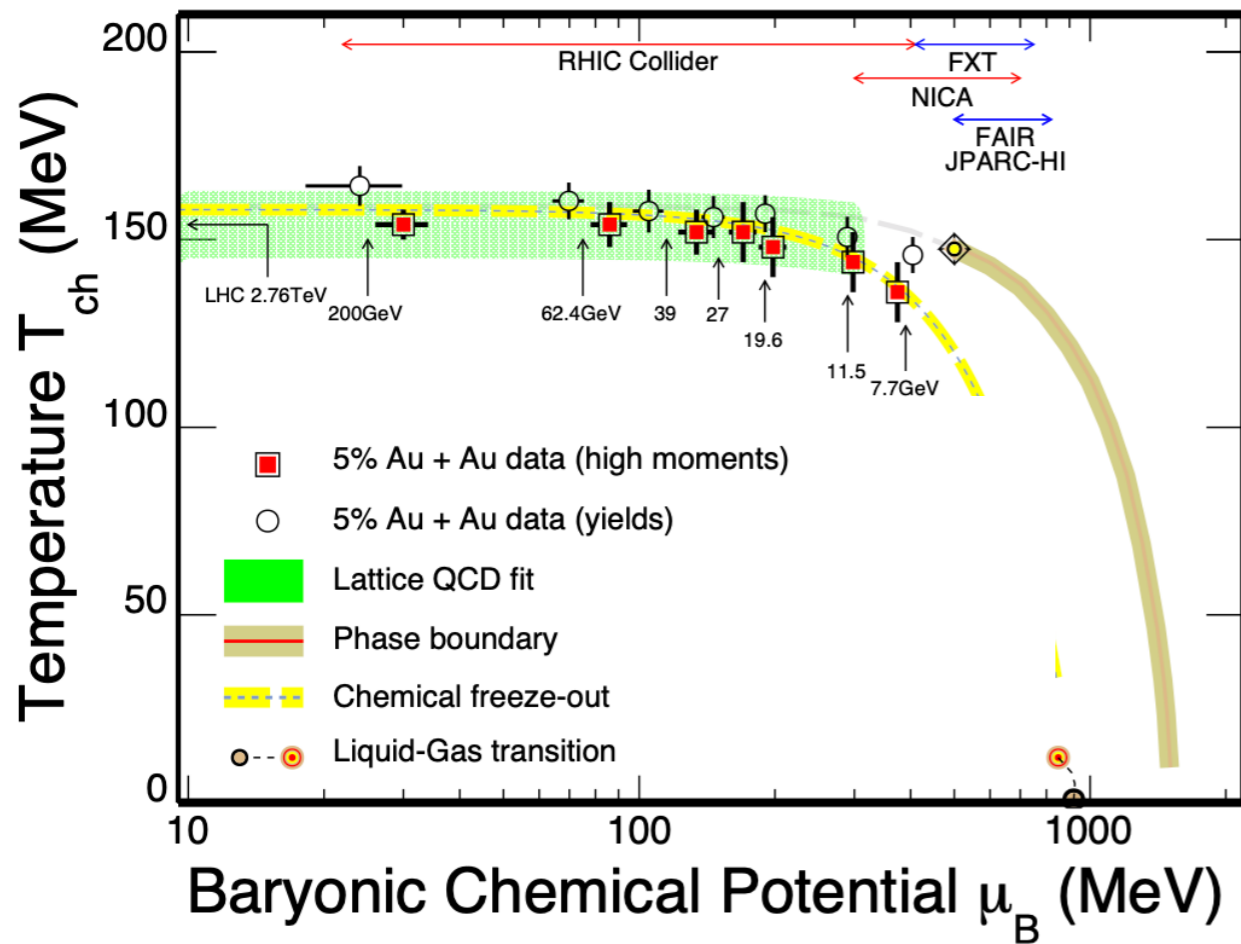
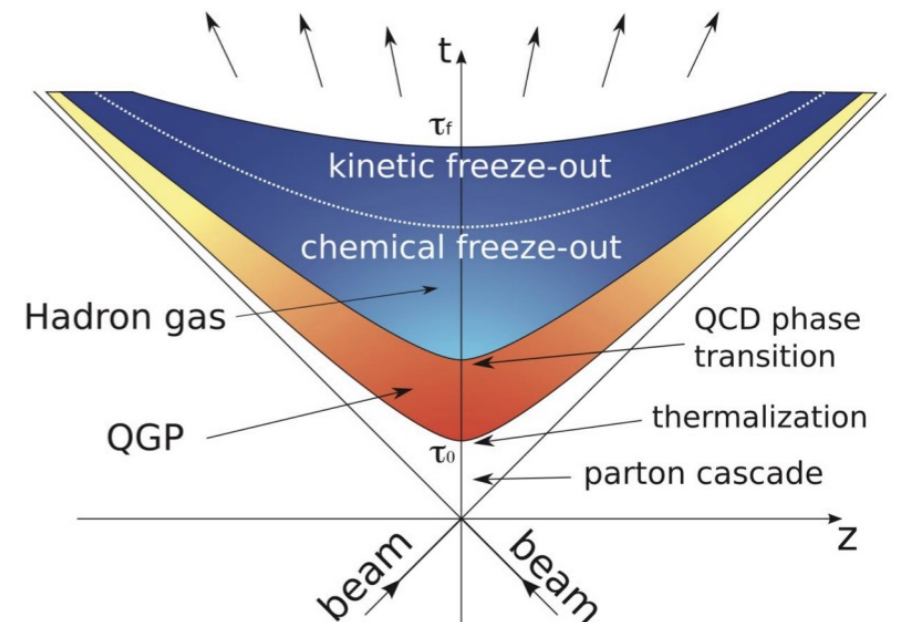
closely related to various cumulants of the baryon number distribution measured in **heavy-ion collision experiments**

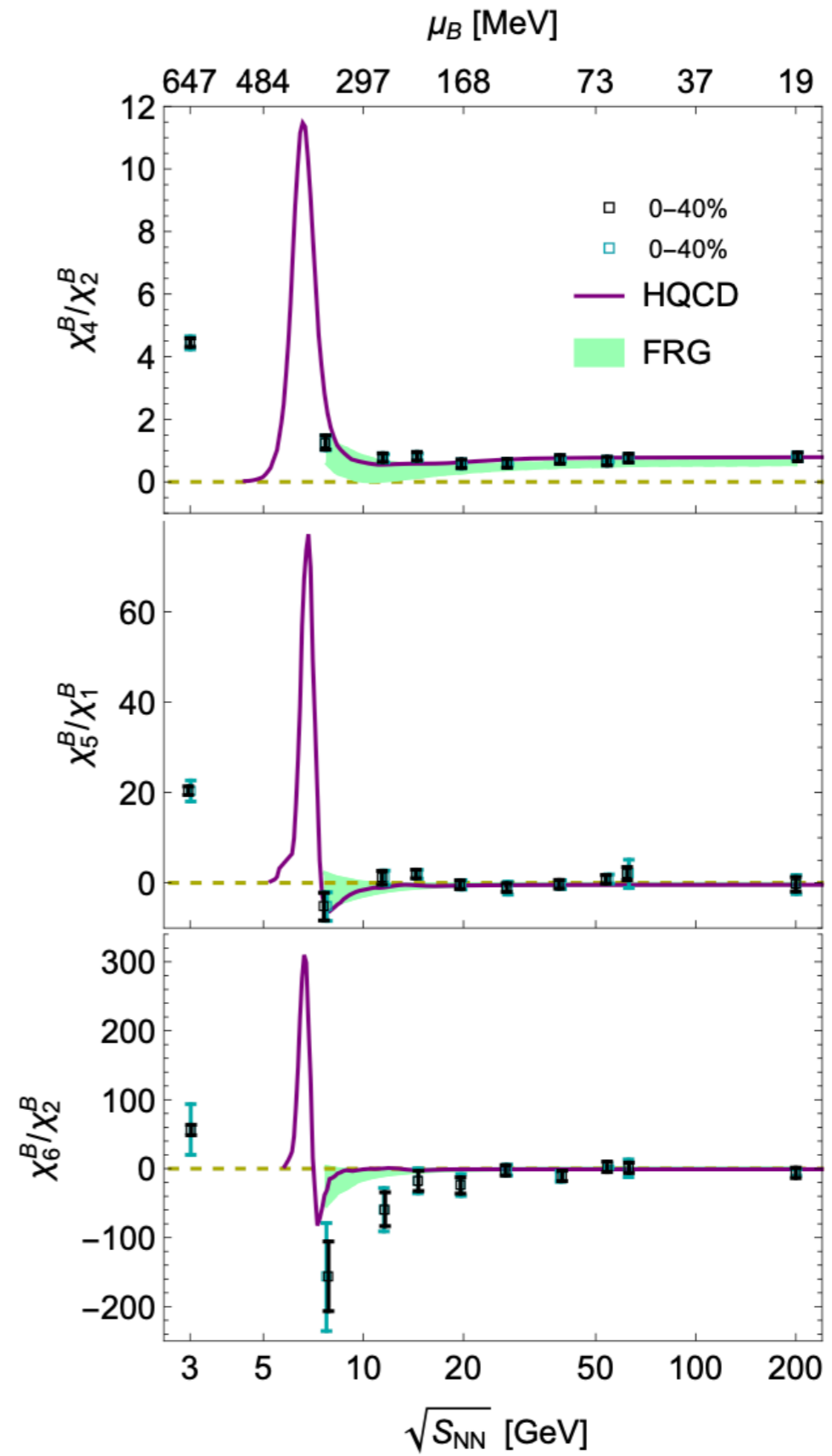
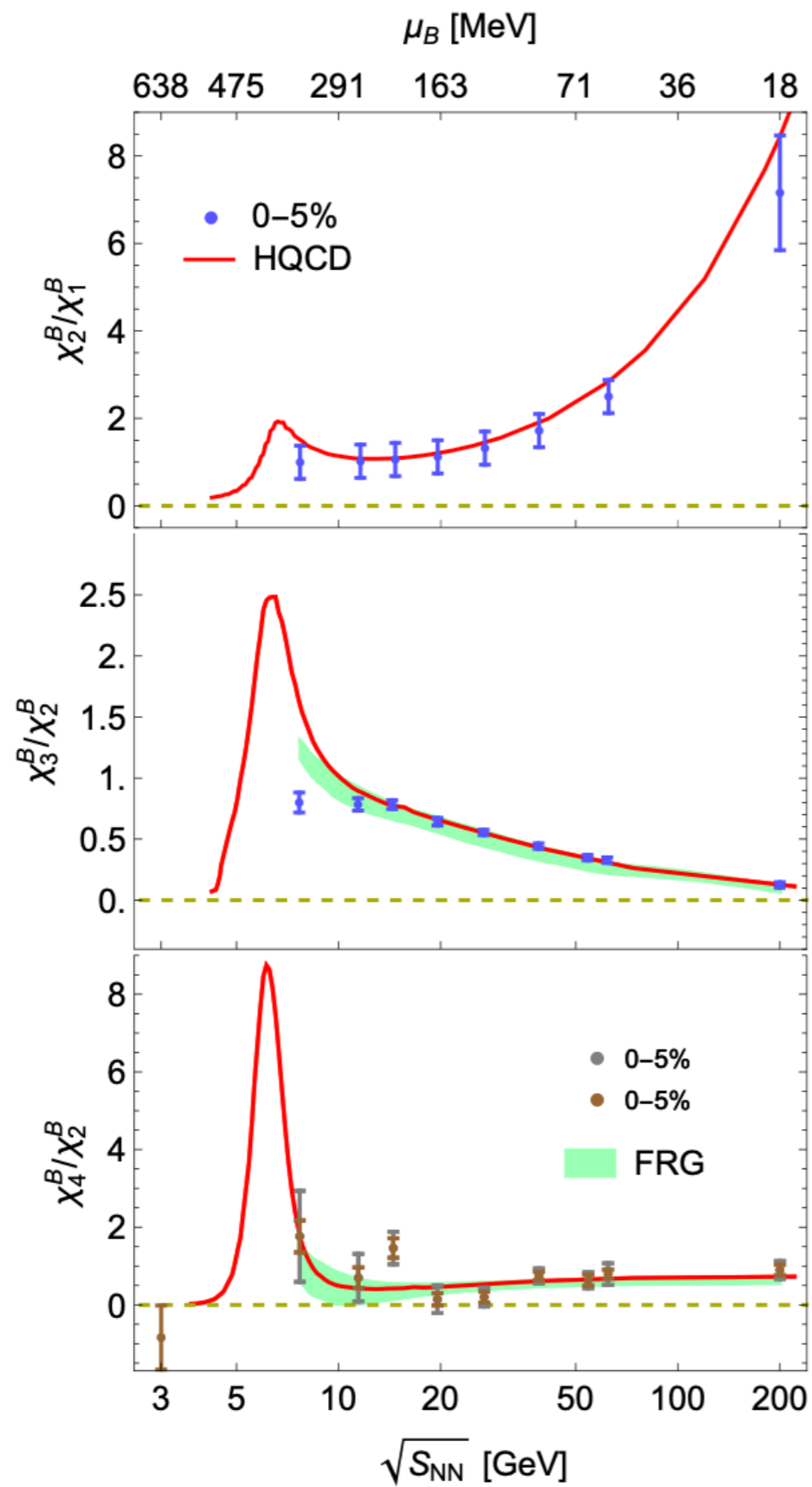


A. Bazavov *et al.* [HotQCD],
Phys. Rev. D 95 (2017) 5, 05404

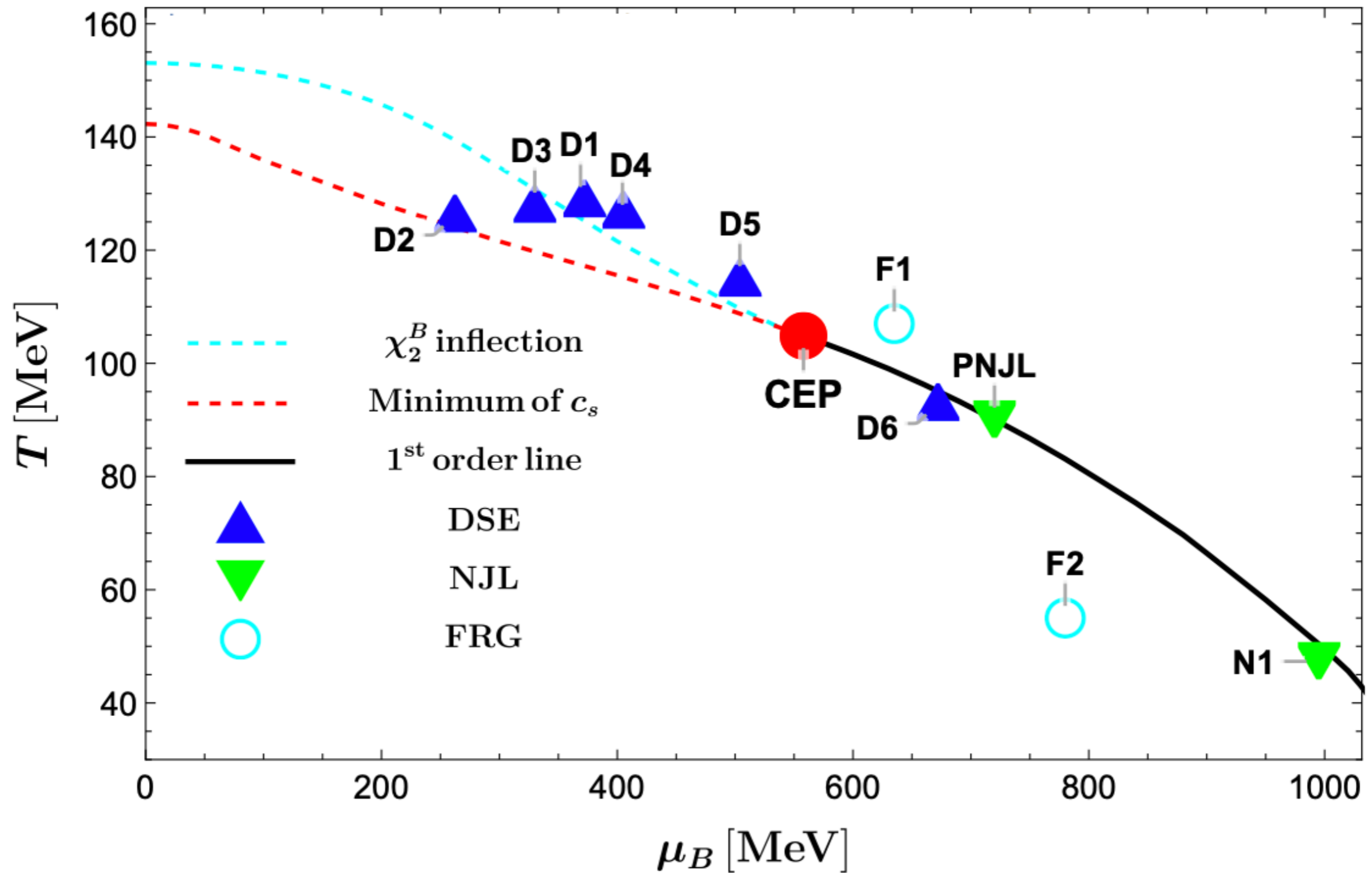
Z. Li, J. Liang, S. He and **Li Li**, Phys. Rev. D 108, no.4, 046008 (2023)

Compare with **STAR** data of net-proton distributions in 0 – 5% centrality (0% being head-on collisions) Au-Au collisions along the chemical freeze-out line

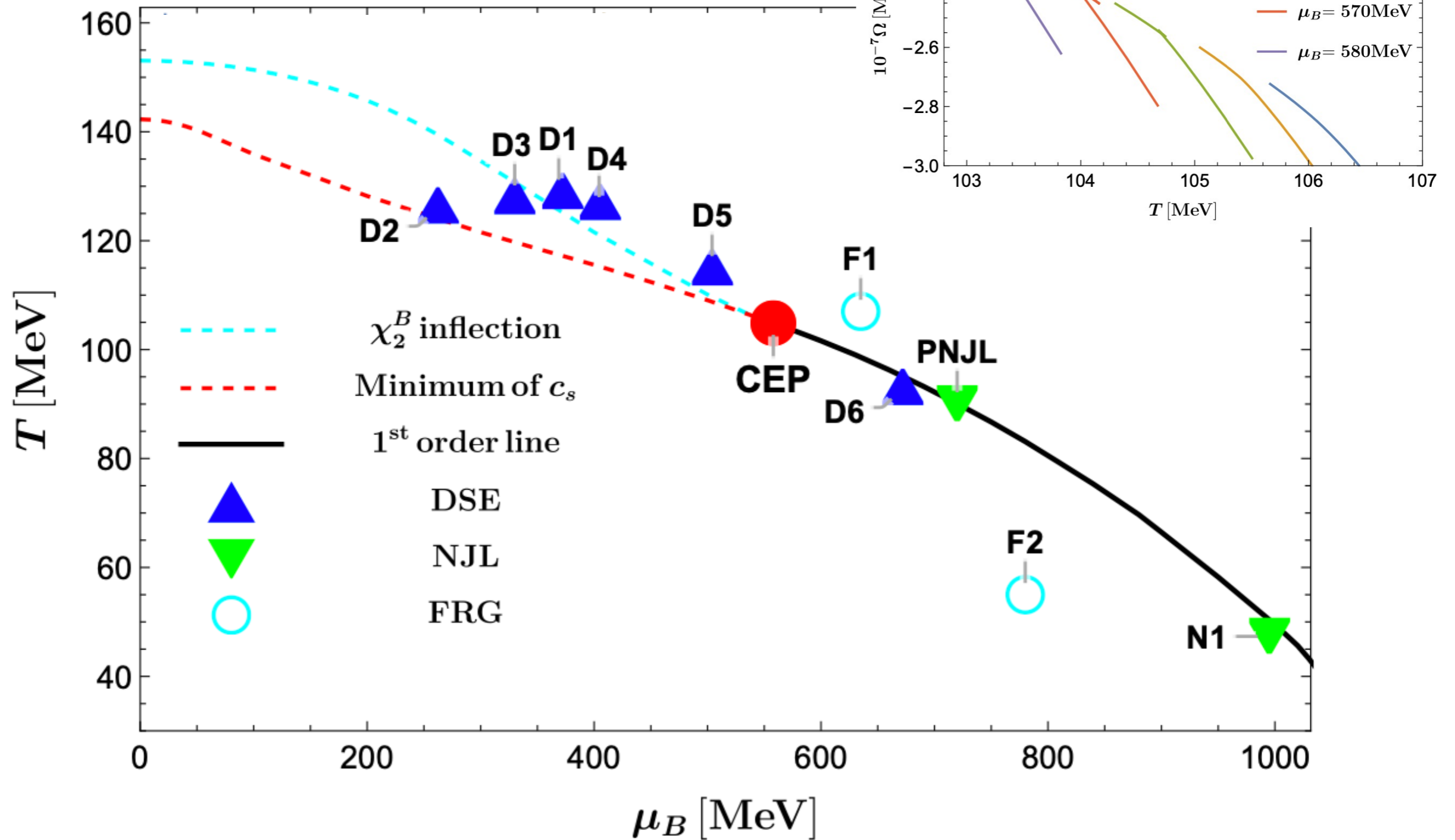




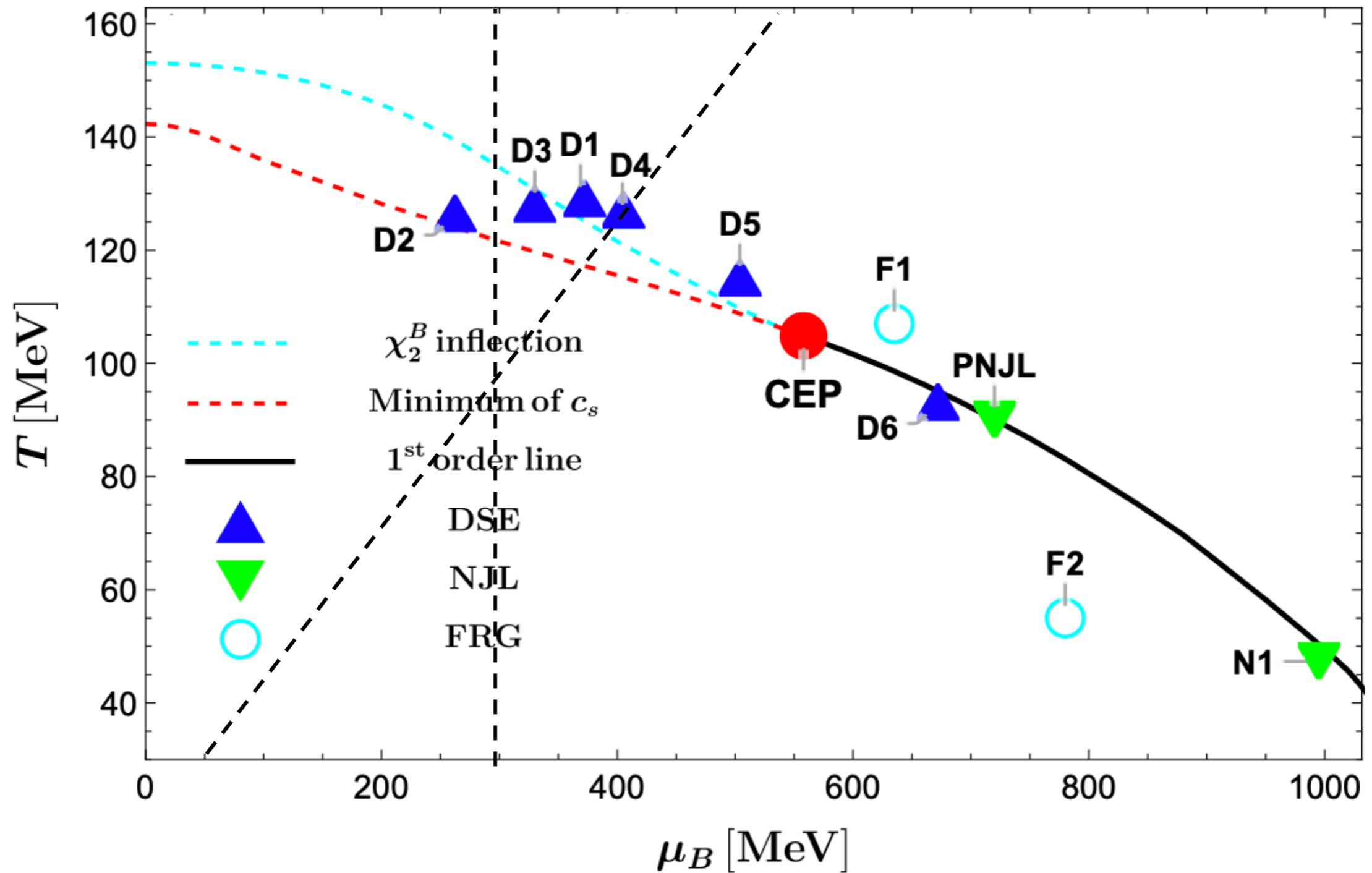
QCD phase diagram from our holographic model



QCD phase diagram from our holographic model

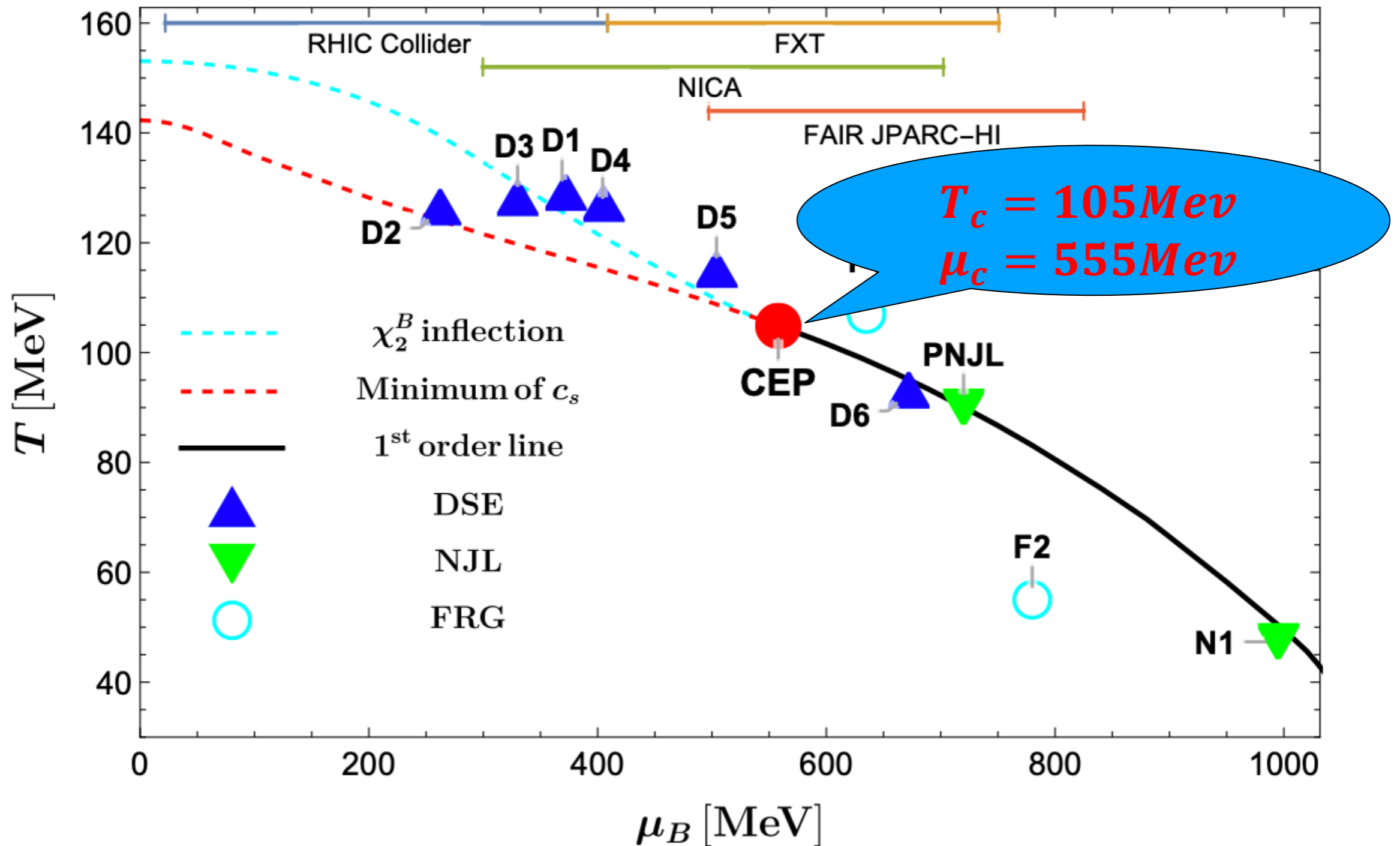


QCD phase diagram from our holographic model



$\mu_B / T \leq 3, \mu_B < 300\text{MeV}$ was excluded by lattice simulation

QCD phase diagram from our holographic model



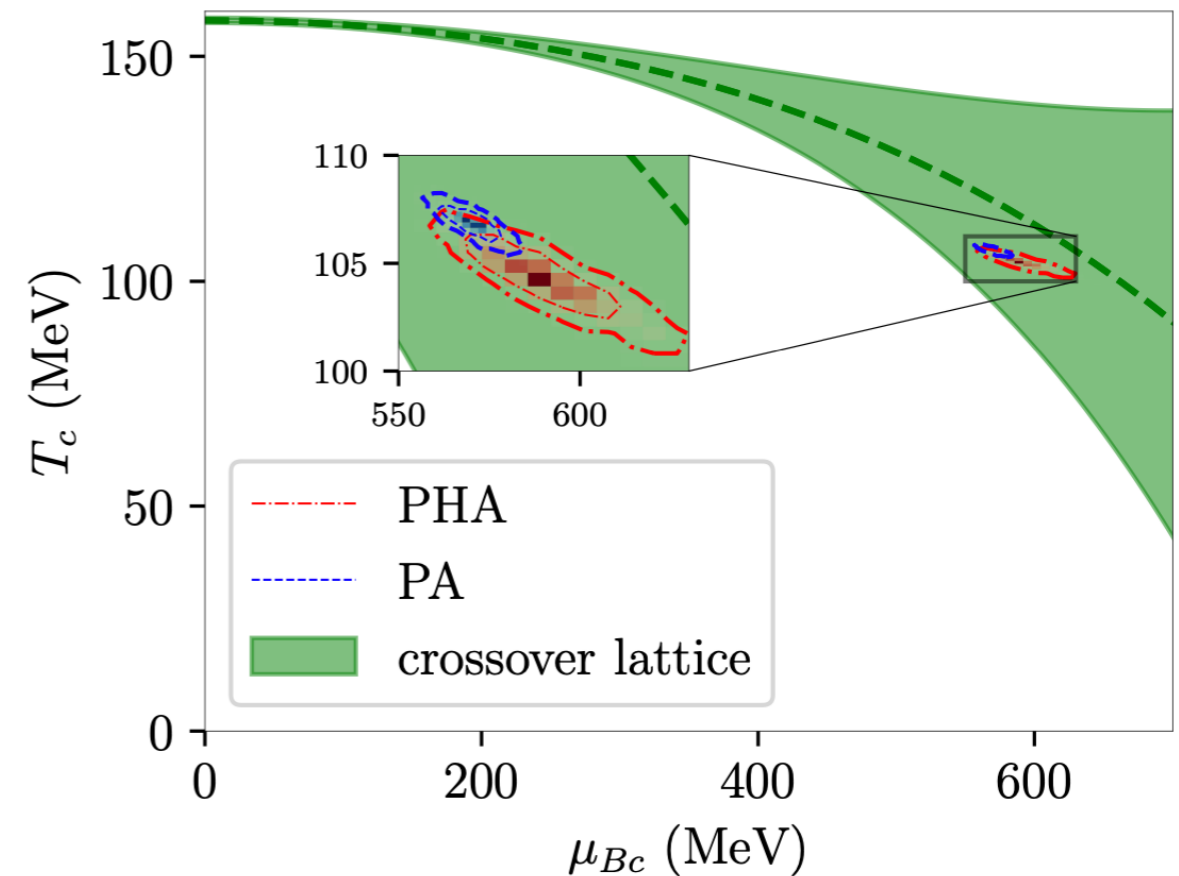
The predicted location of CEP is **within the coverage** of future (FAIR, JPARC-HI, and NICA) experimental facilities.

Our location of CEP $(T_c, \mu_c) = (105, 555)$ MeV has been supported by recent studies.

M. Hippert, et al, **Bayesian location** of the QCD critical point from a holographic perspective, [arXiv:2309.00579 [nucl-th]].

$$(T_c, \mu_{Bc})_{PHA} = (104 \pm 3, 589^{+36}_{-26}) \text{ MeV}$$

$$(T_c, \mu_{Bc})_{PA} = (107 \pm 1, 571 \pm 11) \text{ MeV}$$

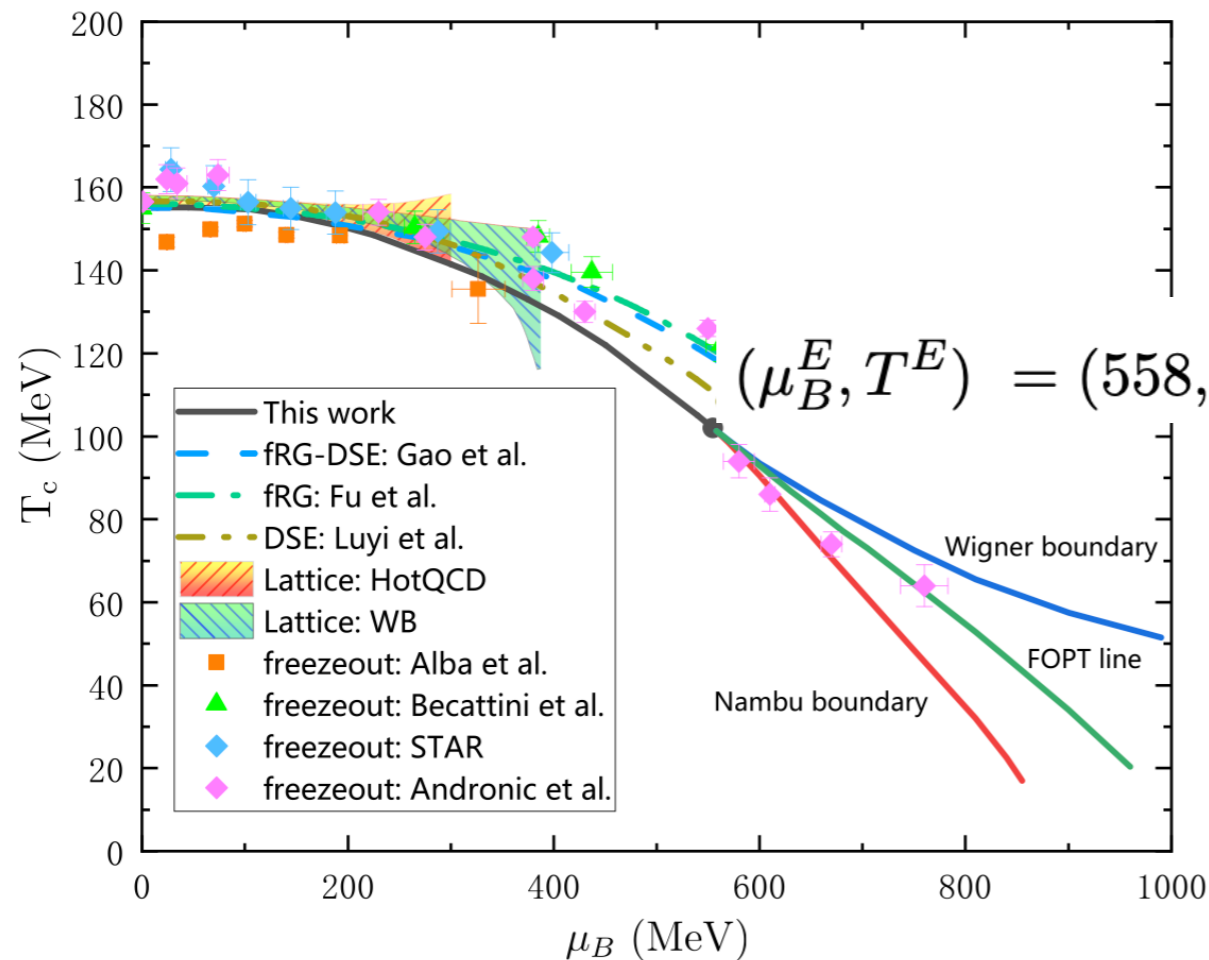
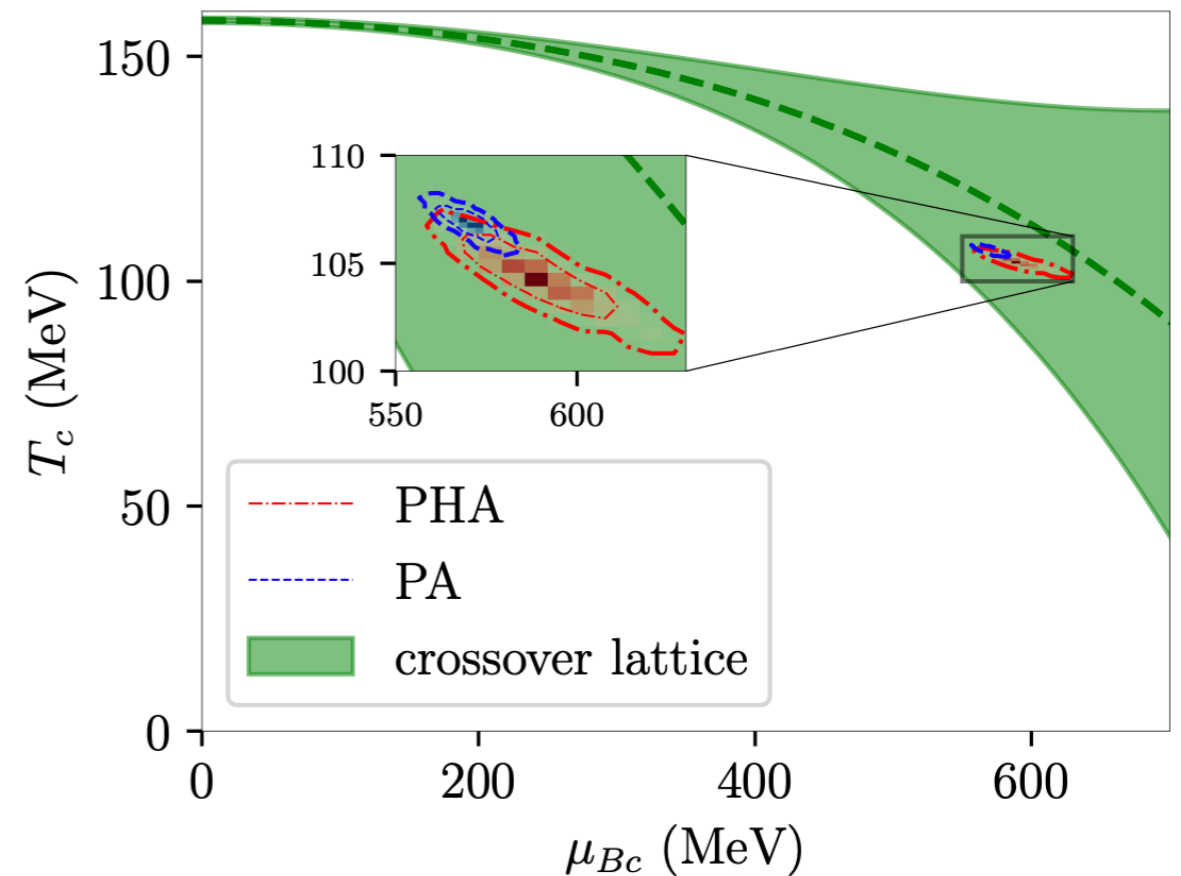


Our location of CEP $(T_c, \mu_c) = (105, 555)$ MeV has been supported by recent studies.

M. Hippert, et al, **Bayesian location** of the QCD critical point from a holographic perspective, [arXiv:2309.00579 [nucl-th]].

$$(T_c, \mu_{Bc})_{PHA} = (104 \pm 3, 589^{+36}_{-26}) \text{ MeV}$$

$$(T_c, \mu_{Bc})_{PA} = (107 \pm 1, 571 \pm 11) \text{ MeV}$$

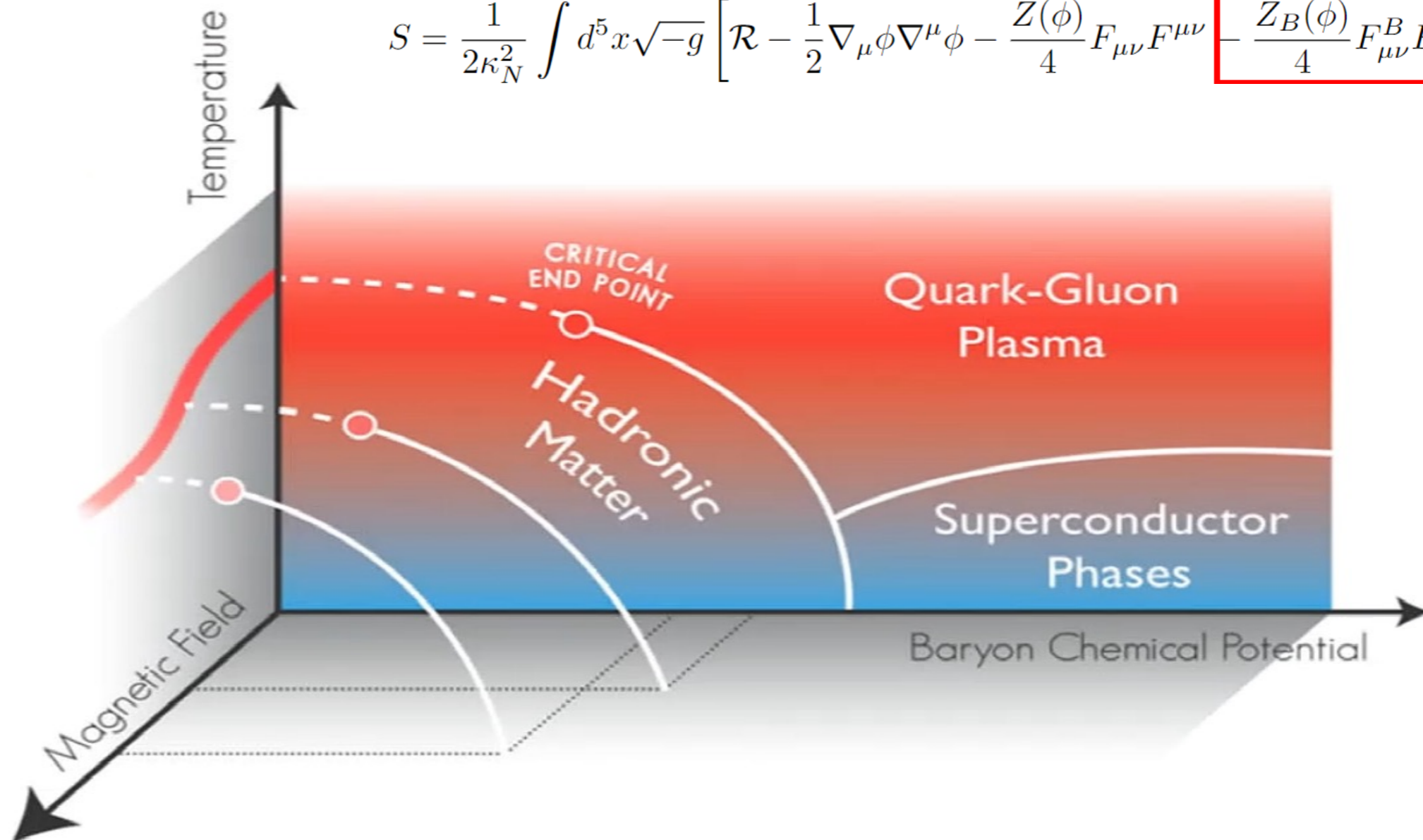


H. w. Zheng, et al, The **effective potential of composite operator** in the first order region of QCD phase transition, [arXiv:2312.00382 [hep-ph]].

hQCD model for 2+1 flavors with B field

Rong-Gen Cai, Song He, **Li Li**, Hong-An Zeng, 2406.12772

$$S = \frac{1}{2\kappa_N^2} \int d^5x \sqrt{-g} \left[\mathcal{R} - \frac{1}{2} \nabla_\mu \phi \nabla^\mu \phi - \frac{Z(\phi)}{4} F_{\mu\nu} F^{\mu\nu} - \frac{Z_B(\phi)}{4} F_{\mu\nu}^B F^{B\mu\nu} - V(\phi) \right]$$

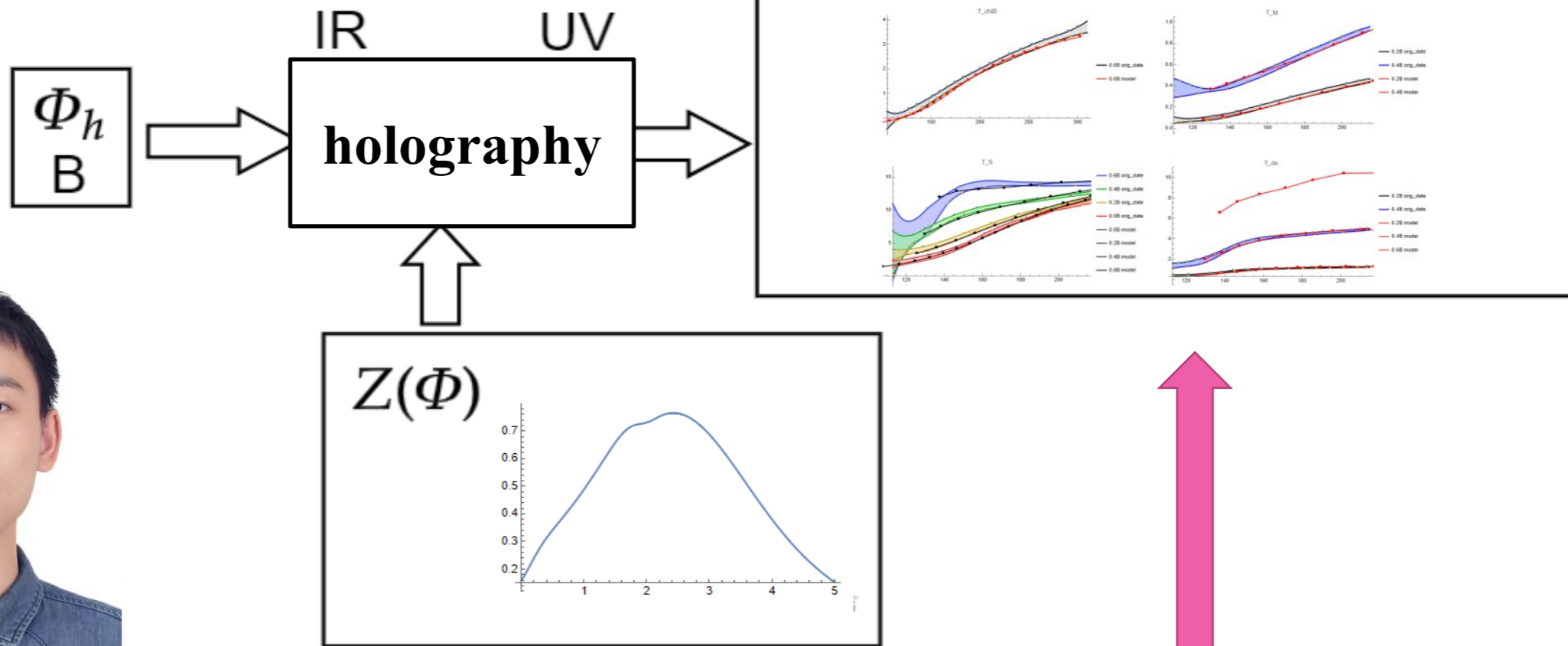


A. N. Tawfik and A. M. Diab, arXiv:2106.04576 [hep-ph]

Neural Network

$$S = \frac{1}{2\kappa_N^2} \int d^5x \sqrt{-g} \left[\mathcal{R} - \frac{1}{2} \nabla_\mu \phi \nabla^\mu \phi - \frac{Z(\phi)}{4} F_{\mu\nu} F^{\mu\nu} - V(\phi) - \frac{Z_B(\phi)}{4} F_{\mu\nu}^B F^{B\mu\nu} \right]$$

Our model algorithm



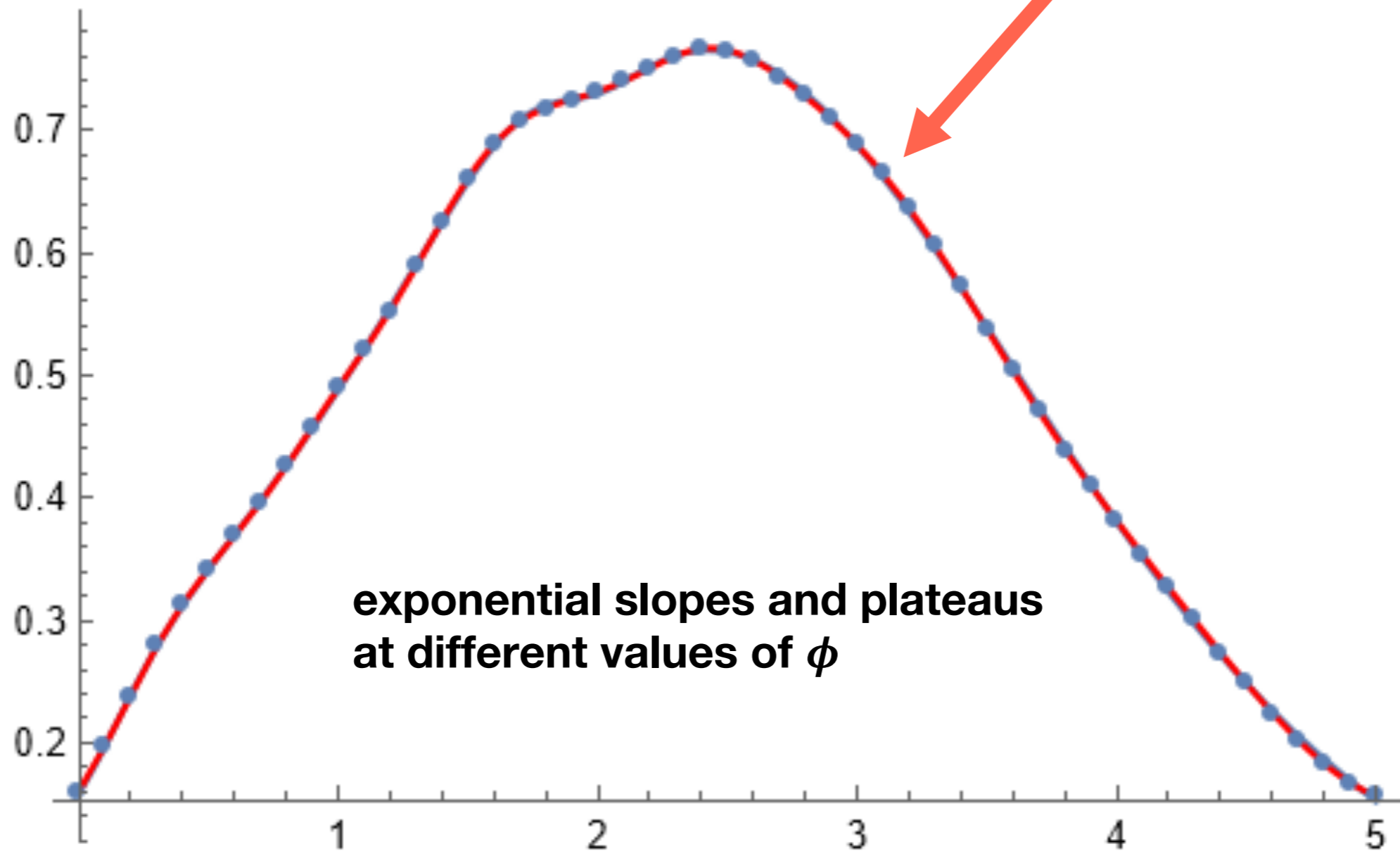
Hong-An Zeng

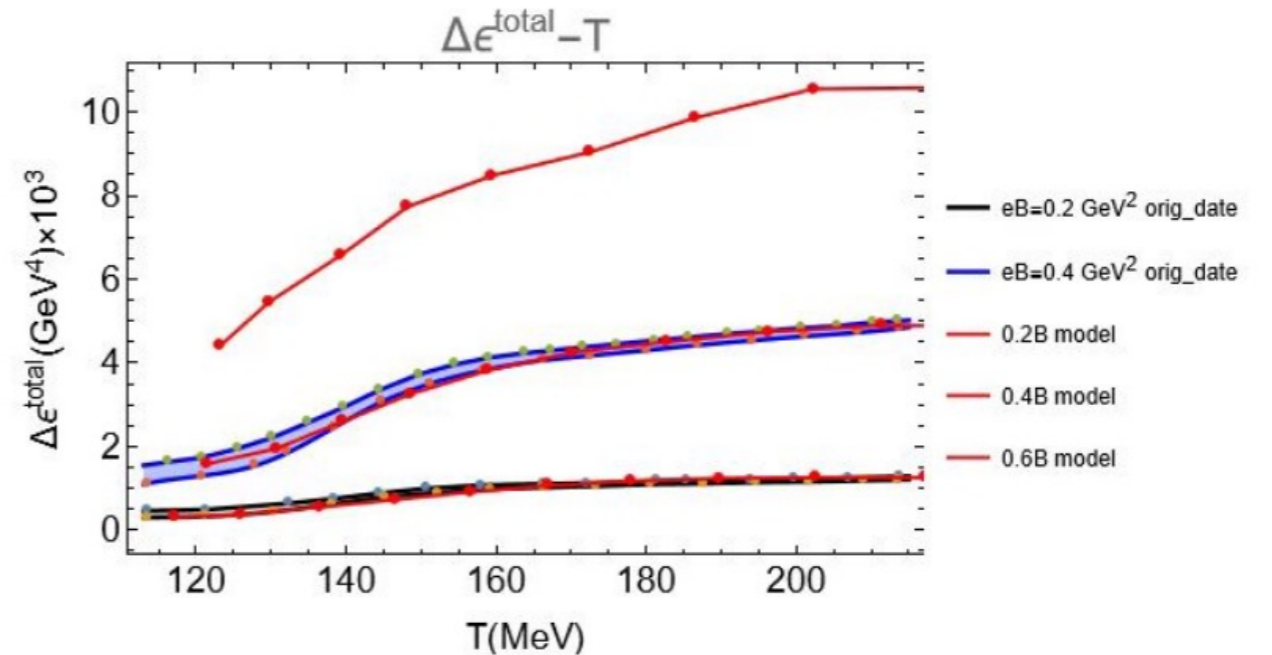
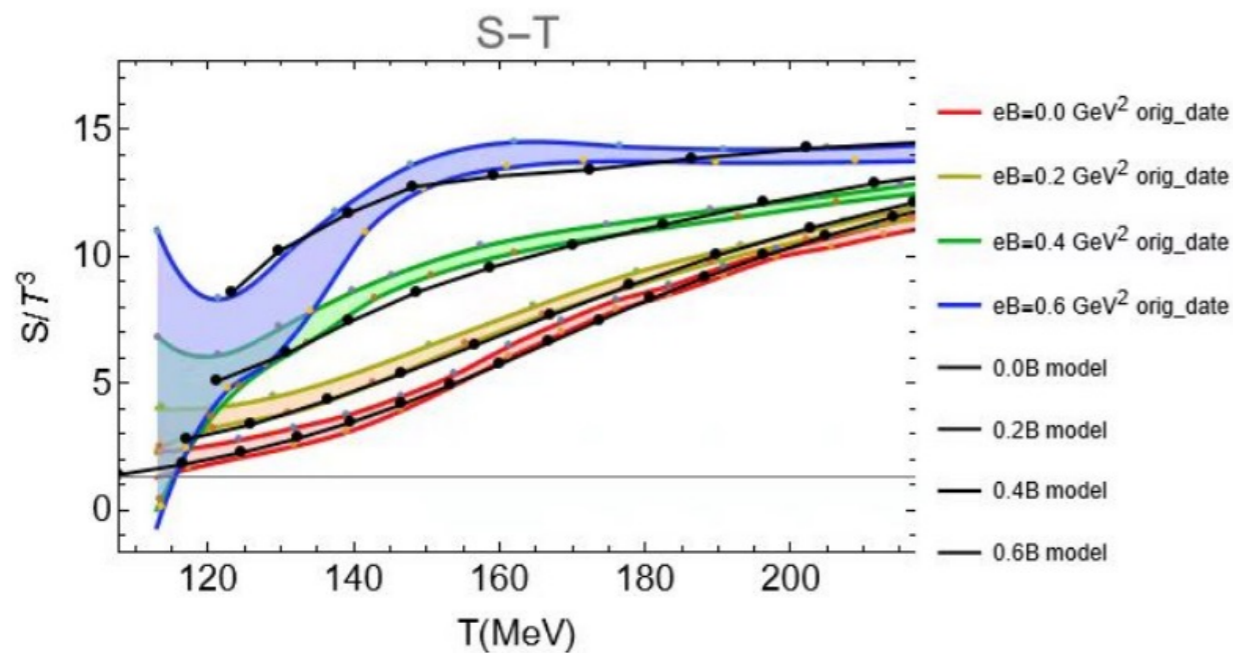
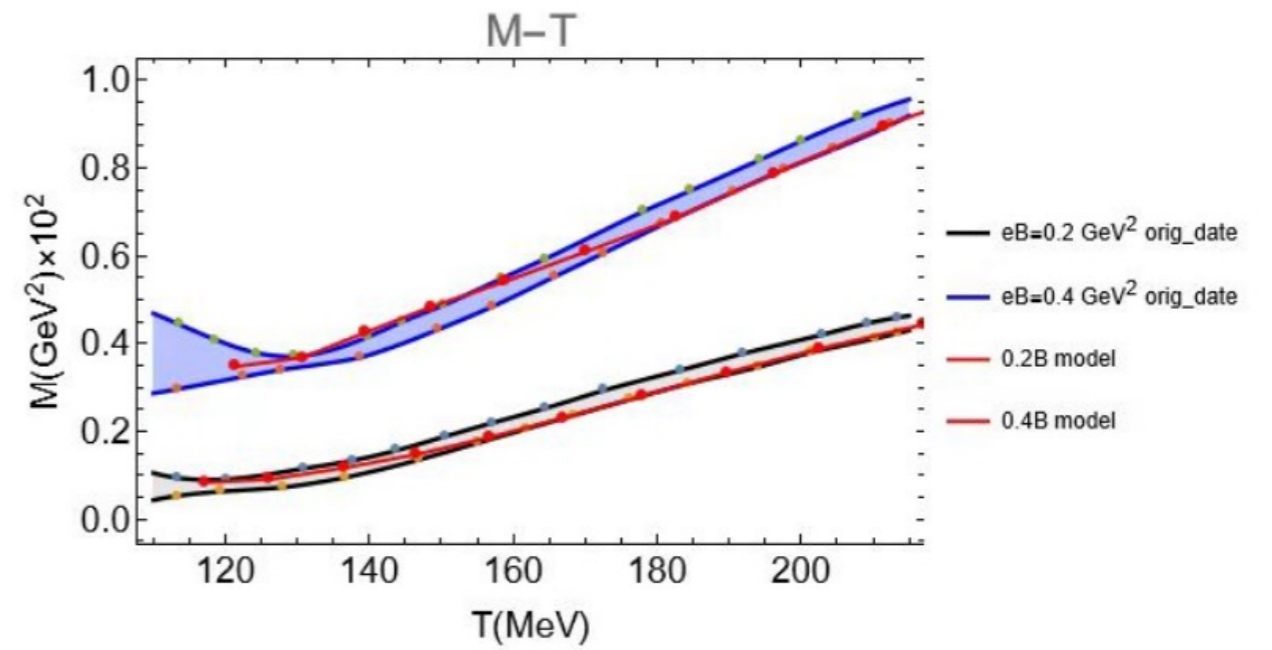
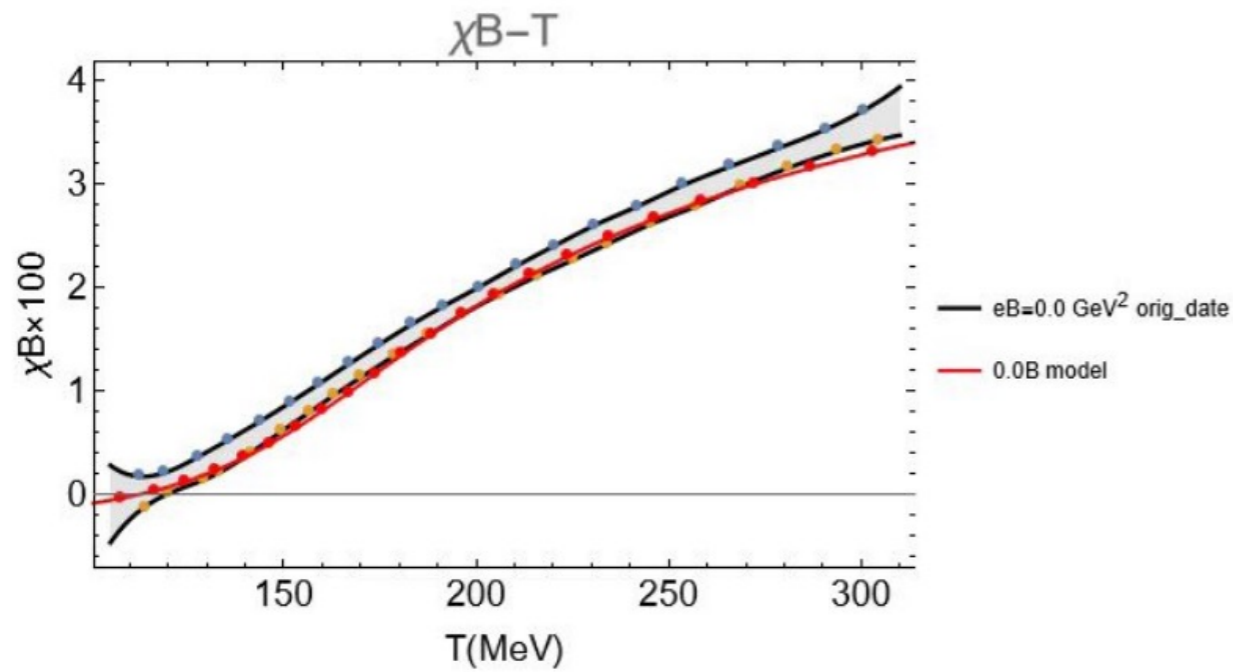
(See talk by Keun-Young Kim)

Target: To find a Z_B -function that matches the thermodynamic quantities from Lattice QCD

Neural Network

$$S = \frac{1}{2\kappa_N^2} \int d^5x \sqrt{-g} \left[\mathcal{R} - \frac{1}{2} \nabla_\mu \phi \nabla^\mu \phi - \frac{Z(\phi)}{4} F_{\mu\nu} F^{\mu\nu} - V(\phi) - \frac{Z_B(\phi)}{4} F_{\mu\nu}^B F^{B\mu\nu} \right]$$



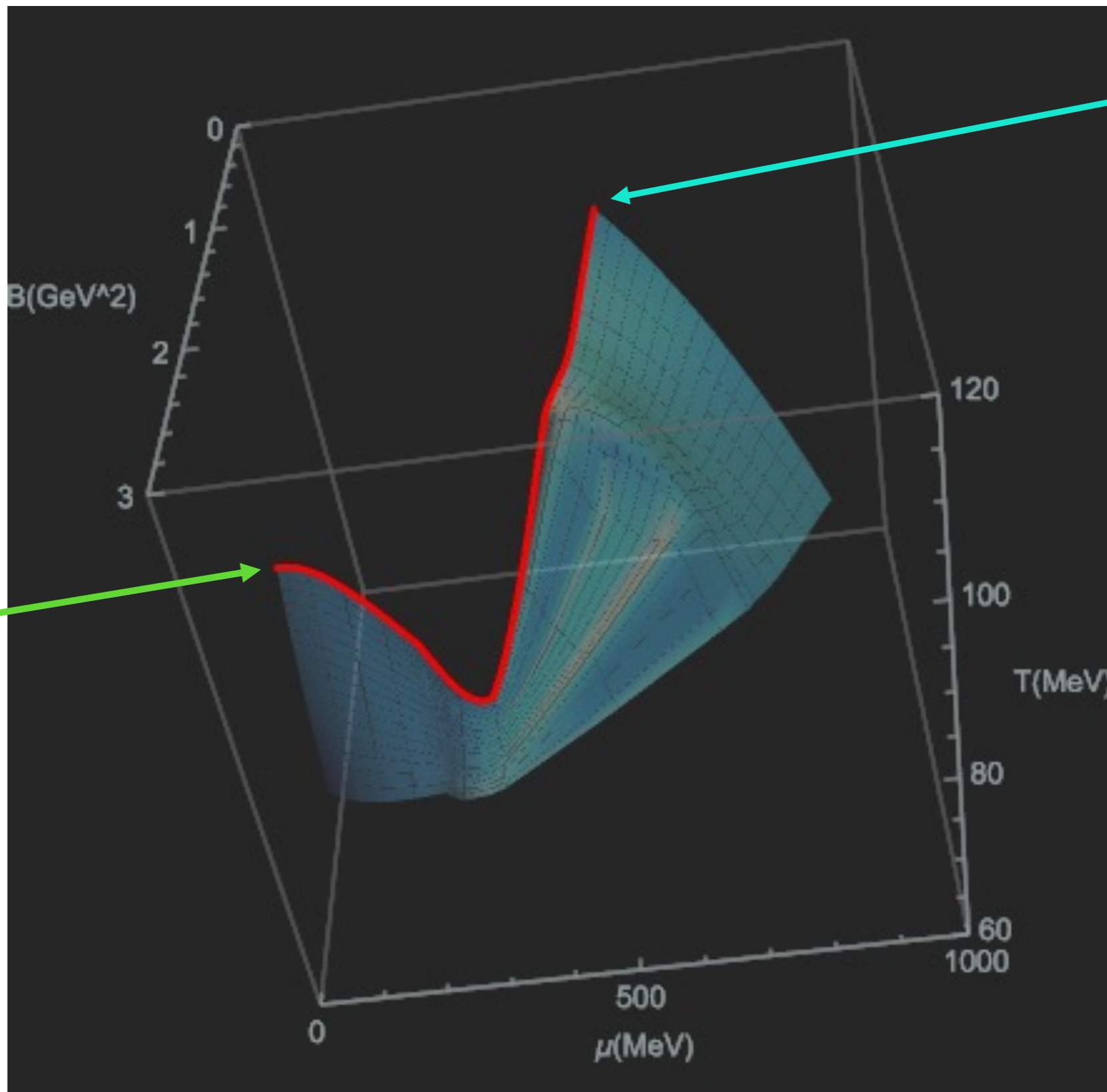


G.S. Bali, et al, The QCD equation of state in background magnetic fields
 [arXiv:1406.0269 [hep-lat]]

$$eB = 1\text{GeV}^2 \leftrightarrow 1.602 \times 10^{19} \text{ Gauss}$$

3D Phase diagram

Rong-Gen Cai, Song He, **Li Li**, Hong-An Zeng, 2406.12772

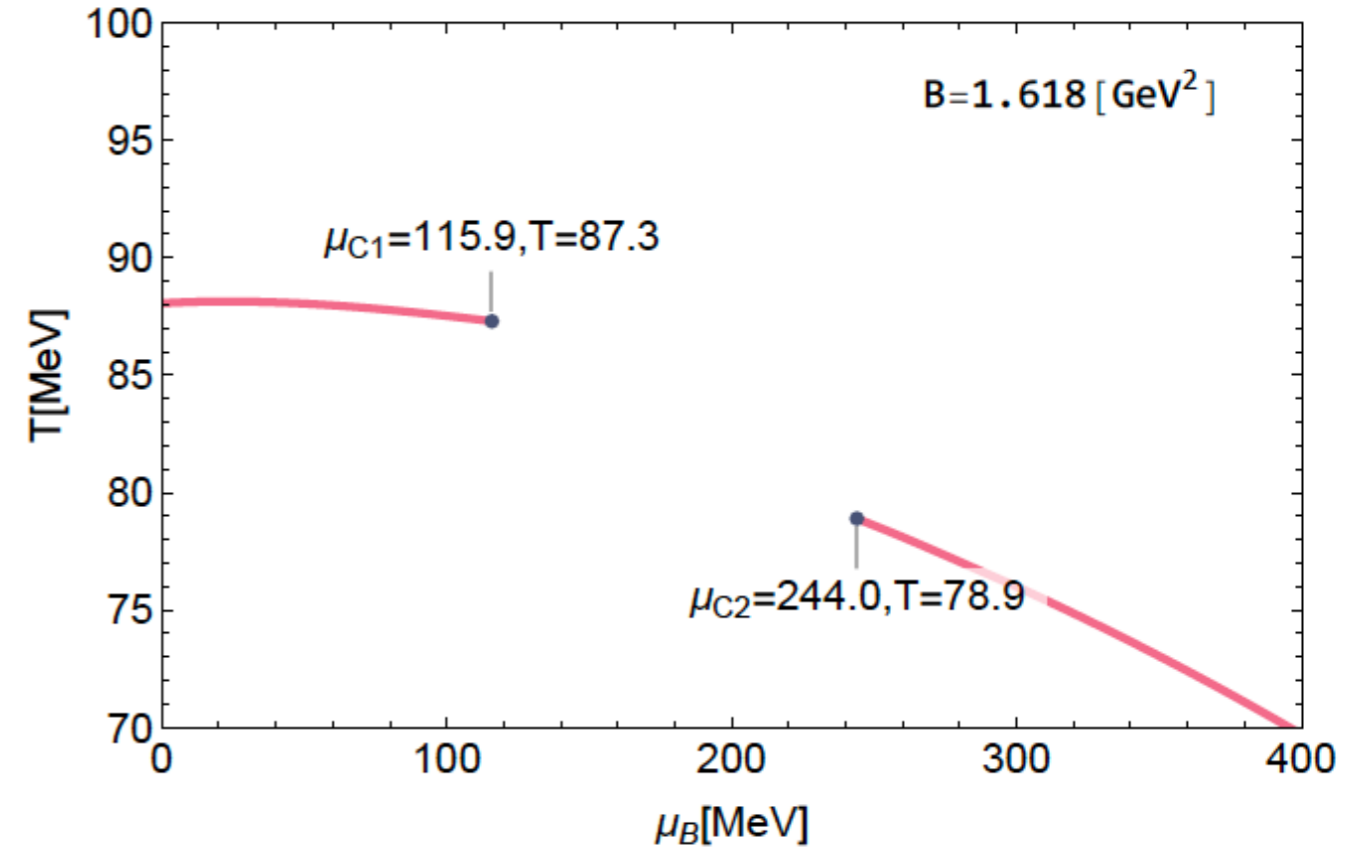
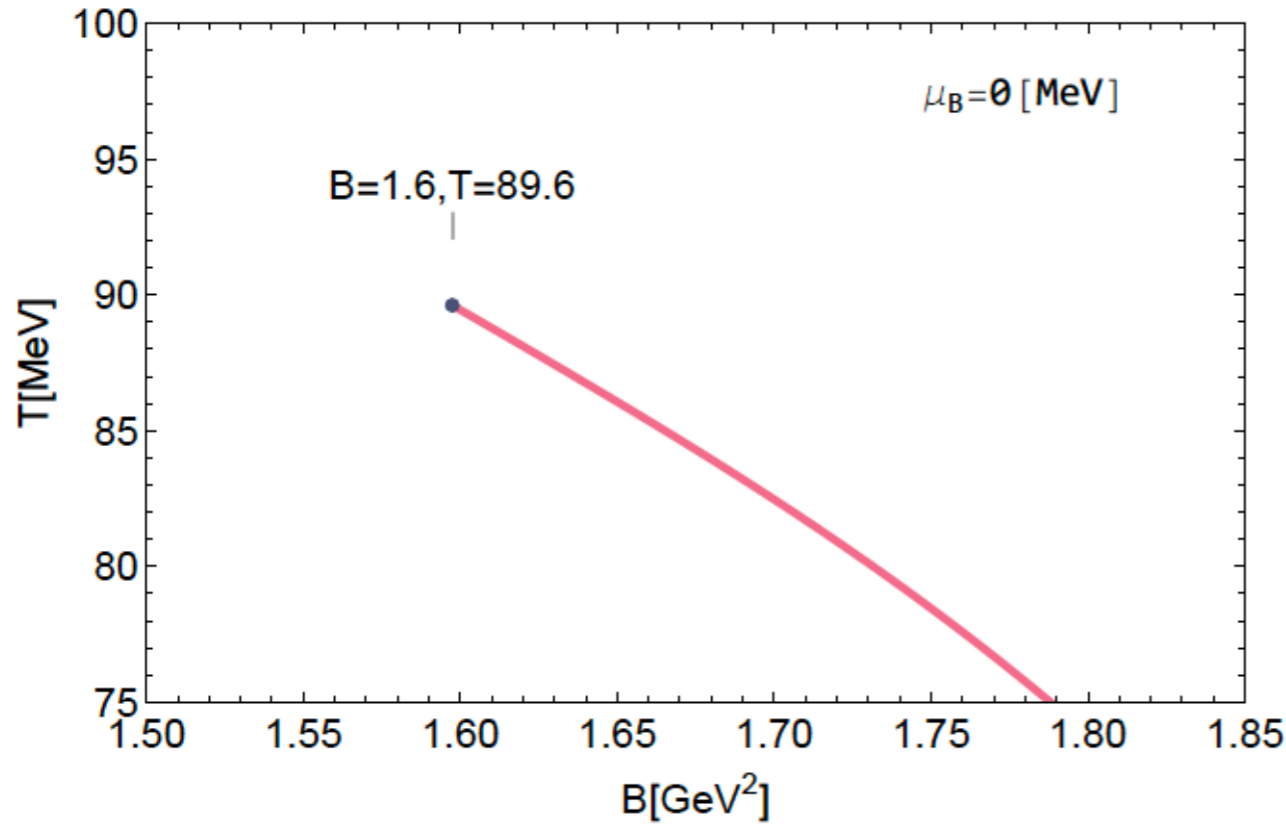


B=0:
 $T_c = 105 \text{ MeV}$,
 $\mu_c = 555 \text{ MeV}$

$\mu=0$:
 $T_c = 89.6 \text{ MeV}$,
 $B_c = 1.6 \text{ GeV}^2$

Rich phase structure

Rong-Gen Cai, Song He, **Li Li**, Hong-An Zeng, 2406.12772



	α	β	γ	δ
Experiment	0.110-0.116	0.316-0.327	1.23-1.25	4.6-4.9
3D Ising	0.110(5)	0.325 ± 0.0015	1.2405 ± 0.0015	4.82(4)
Mean field	0	1/2	1	3
DGR model	0	0.482	0.942	3.035
hQCD(I)	0.0046233	0.532779	0.91629	3.00825
hQCD(II)	0.0233477	0.481381	1.05119487	3.238166
hQCD(III)	0.019778	0.46259	1.03499	3.48613

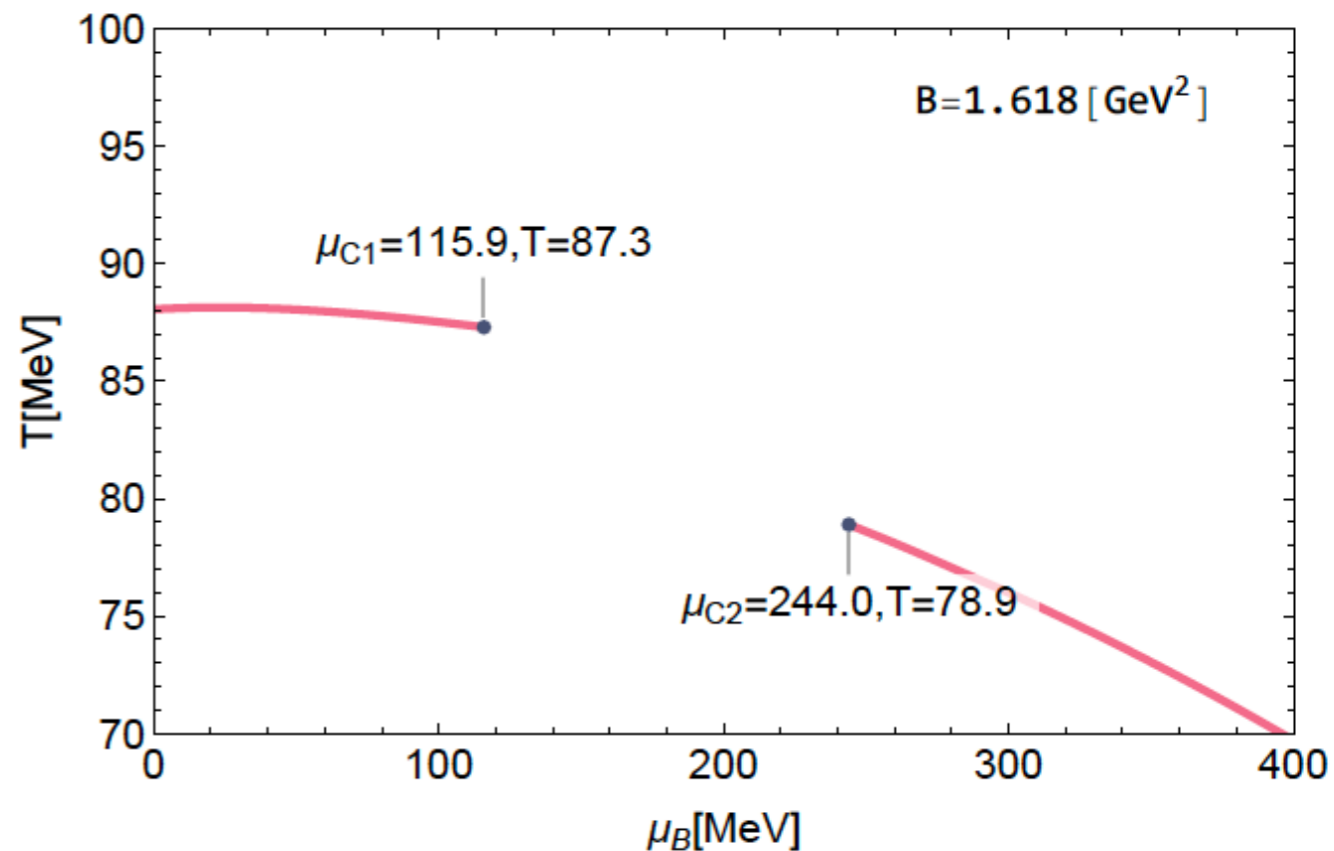
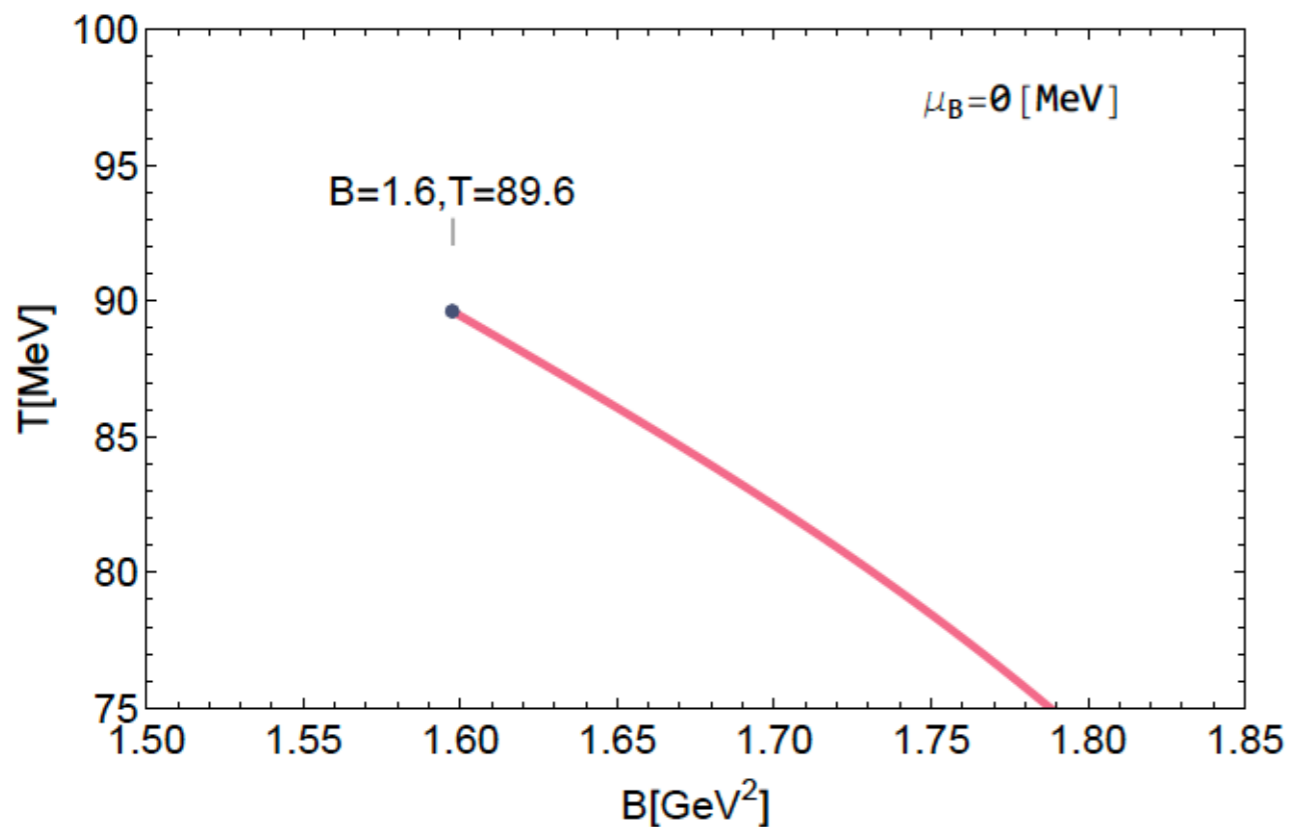
$\mu_B = 554.66 \text{ MeV}, B = 0 \text{ GeV}^2$

$\mu_B = 501.4 \text{ MeV}, B = 0.3 \text{ GeV}^2$

$\mu_B = 0 \text{ MeV}, B = 1.6 \text{ GeV}^2$

Rich phase structure

Rong-Gen Cai, Song He, **Li Li**, Hong-An Zeng, 2406.12772



$$\alpha + 2\beta + \gamma = 2, \quad \alpha + \beta(1 + \delta) = 2$$

	α	β	γ	δ
Experiment	0.110-0.116	0.316-0.327	1.23-1.25	4.6-4.9
3D Ising	0.110(5)	0.325 ± 0.0015	1.2405 ± 0.0015	4.82(4)
Mean field	0	1/2	1	3
DGR model	0	0.482	0.942	3.035
hQCD(I)	0.0046233	0.532779	0.91629	3.00825
hQCD(II)	0.0233477	0.481381	1.05119487	3.238166
hQCD(III)	0.019778	0.46259	1.03499	3.48613

$\mu_B = 554.66 \text{ MeV}, B = 0 \text{ GeV}^2$

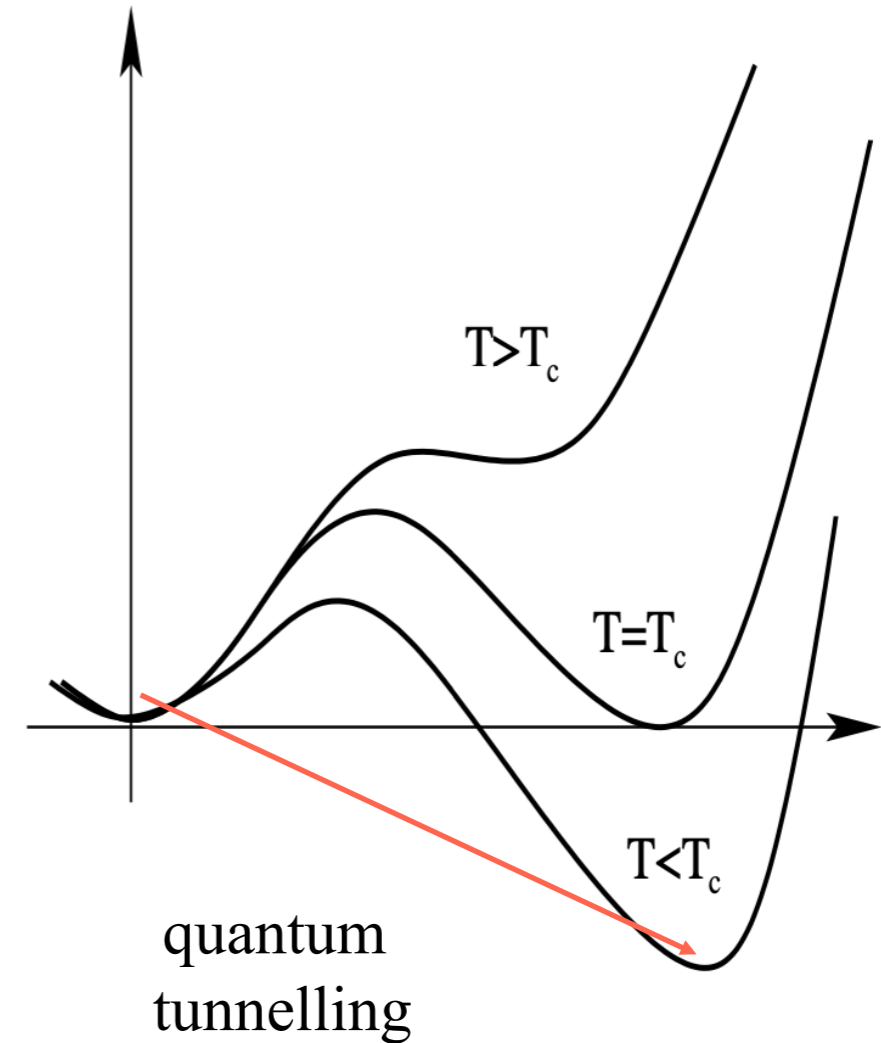
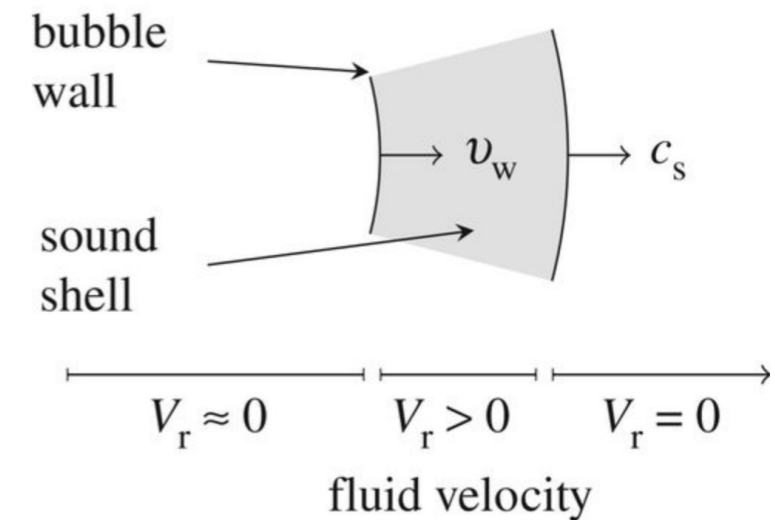
$\mu_B = 501.4 \text{ MeV}, B = 0.3 \text{ GeV}^2$

$\mu_B = 0 \text{ MeV}, B = 1.6 \text{ GeV}^2$

Induced gravitational wave

Strong first order phase transition will result in the production of GWs:

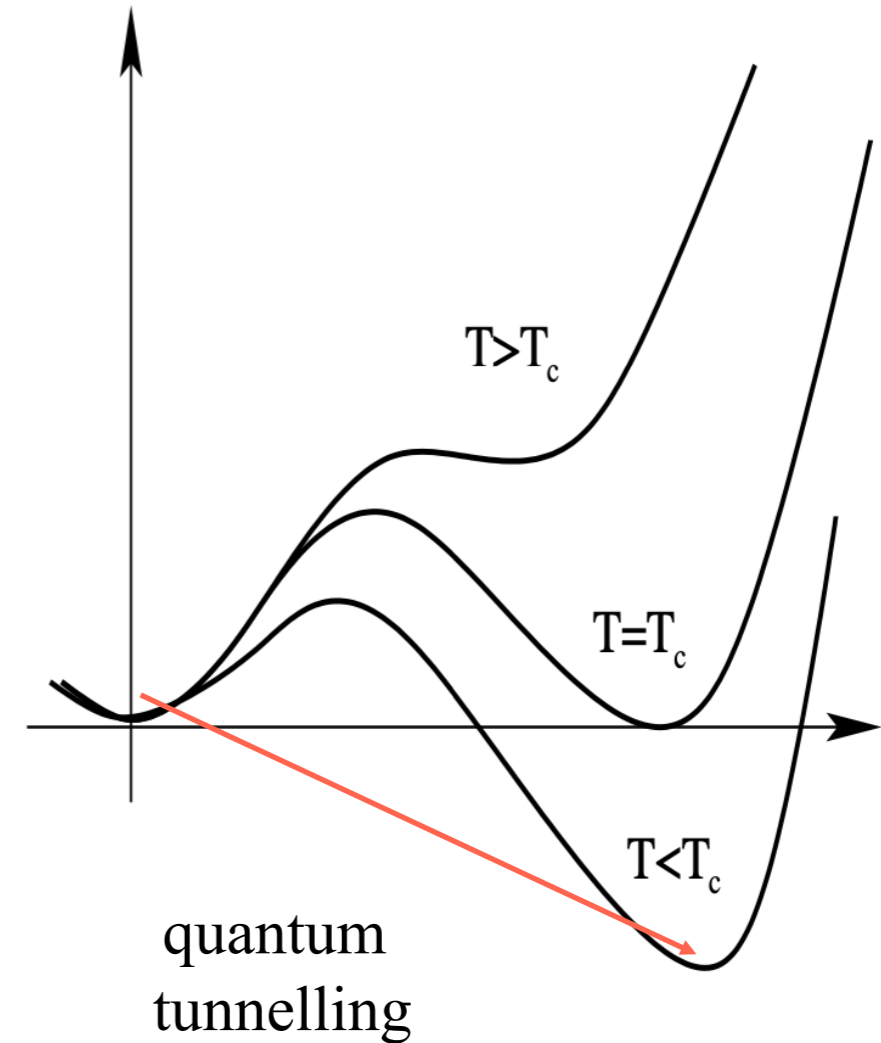
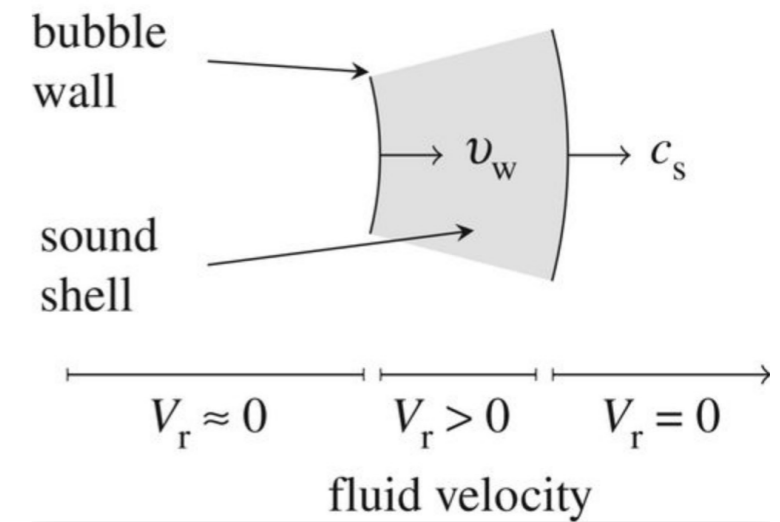
bubble collision + sound wave + MHD turbulence



Induced gravitational wave

Strong first order phase transition will result in the production of GWs:

bubble collision + sound wave + MHD turbulence



Induced gravitational wave

Strong first order phase transition will result in the production of GWs:

bubble collision + sound wave + MHD turbulence

GWs are dominated by **sound waves** with the energy spectrum

$$h^2 \Omega_{GW}(f) = 8.5 \times 10^{-6} \left(\frac{100}{g_n} \right)^{1/3} \left(\frac{\kappa \alpha}{1 + \alpha} \right)^2 \times \left(\frac{H_n}{\beta} \right) v_w S_{SW}(f).$$

α : phase transition strength parameter

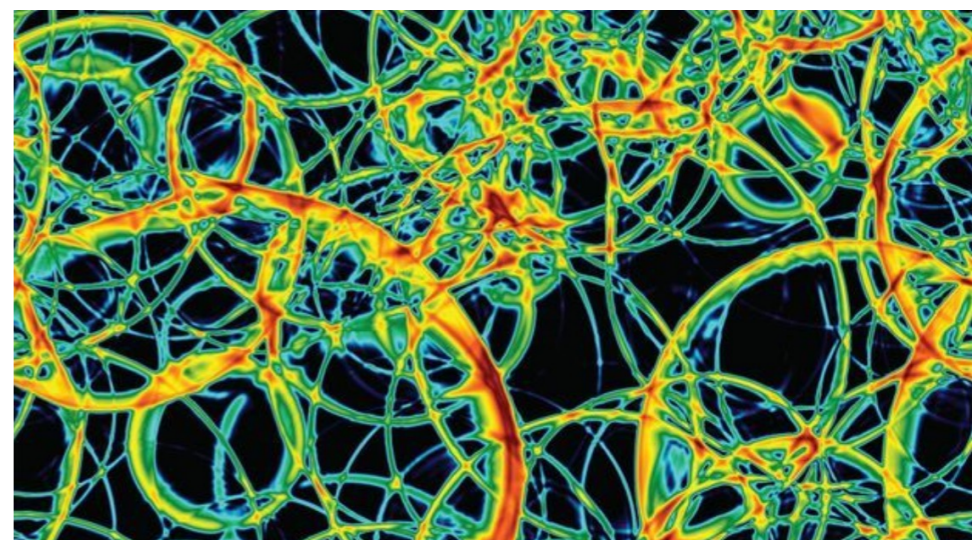
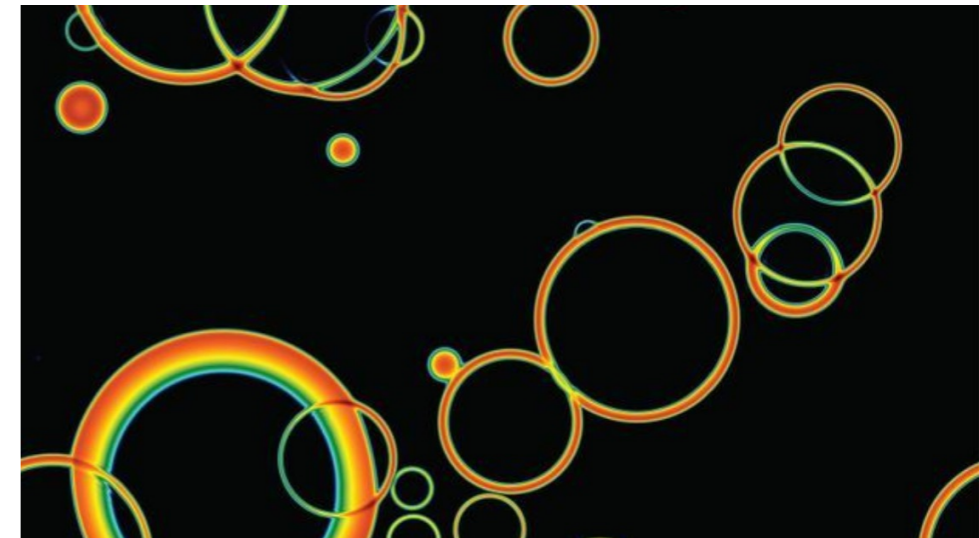
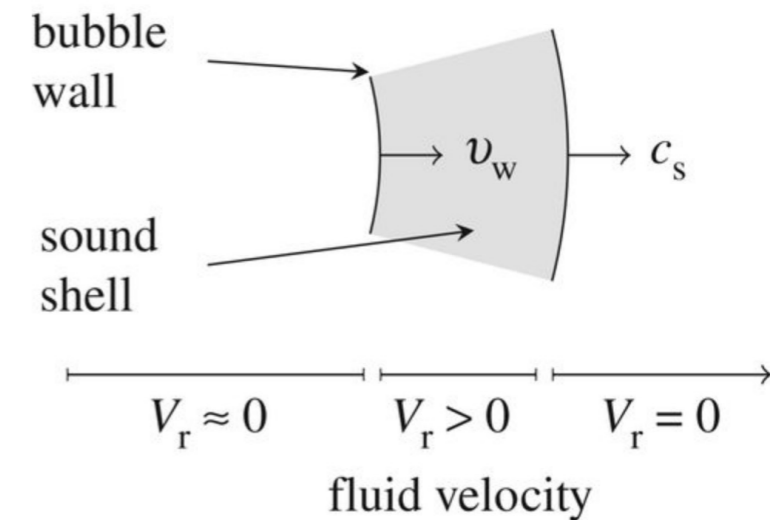
v_w : bubble wall terminal velocity

$\frac{\beta}{H_n}$: the inverse time duration of the phase transition

H_n : Hubble rate at the nucleation temperature T_n

g_n : the number of degrees of freedom

κ : the fraction of bulk kinetic energy relative to the available vacuum energy.



Induced gravitational wave

Spectral shape and peak frequency

$$h^2 \Omega_{GW}(f) = 8.5 \times 10^{-6} \left(\frac{100}{g_n} \right)^{1/3} \left(\frac{\kappa \alpha}{1 + \alpha} \right)^2 \times \left(\frac{H_n}{\beta} \right) v_w S_{SW}(f).$$

$$S_{SW}(f) = \left(\frac{f}{f_{SW}} \right)^3 \left[\frac{7}{4 + 3(f/f_{SW})^2} \right]^{7/2},$$

$$f_{SW} = 1.9 \times 10^{-8} \left(\frac{\beta}{H_n} \right) \left(\frac{T_n}{100 \text{ MeV}} \right) \left(\frac{g_n}{100} \right)^{1/6} \text{ Hz}$$

Parameters:

$$g_n = \frac{45S_+}{2\pi^2 T_n^2} \quad v_w = 0.95$$

$$\kappa = \frac{\alpha}{0.73 + 0.083\sqrt{\alpha} + \alpha}$$

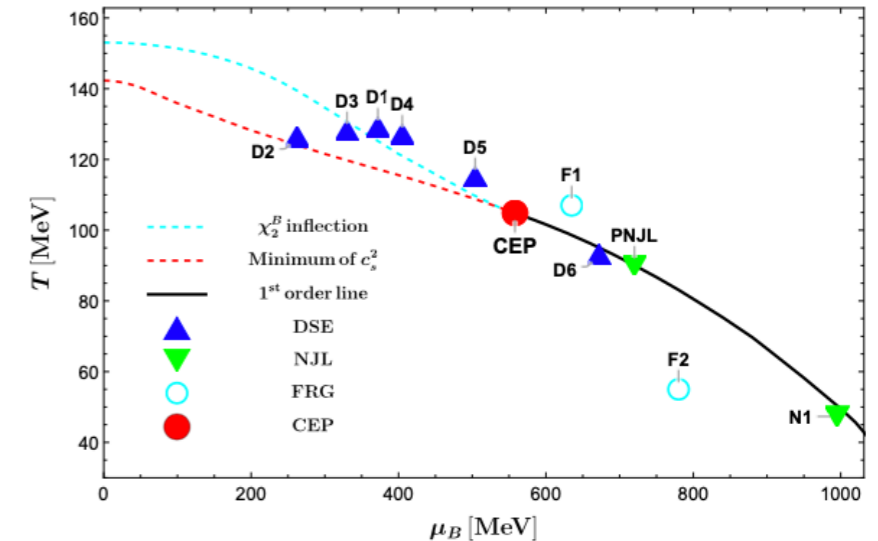
$$\alpha = \frac{4(\theta_+ - \theta_-)}{3w_+}$$

$$\theta = (\epsilon - 3P)/4$$

$$w = \epsilon + P$$

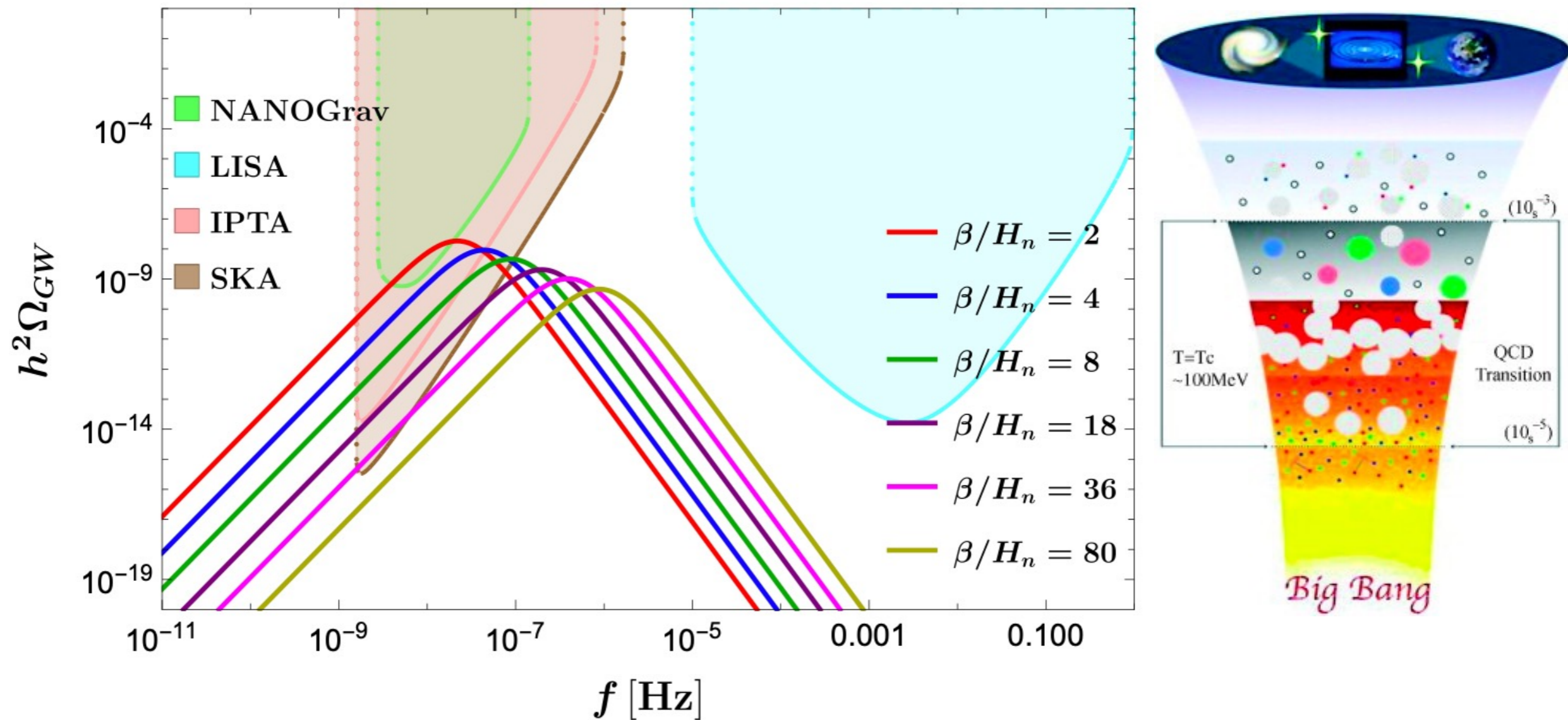
between the false (+) and true (-) vacuums

Most parameters can be fixed.



Induced gravitational wave

Kai Schmitz, JHEP 01 (2021) 097



$(\mu, T, \alpha) = (1000 \text{ MeV}, 49.53 \text{ MeV}, 0.33)$.

The upper curve in each band is for $\beta/H_n = 2$ and the lower curve is for $\beta/H_n = 80$.

The GW energy spectrum is within the projected sensitivity of **IPTA** and **SKA**

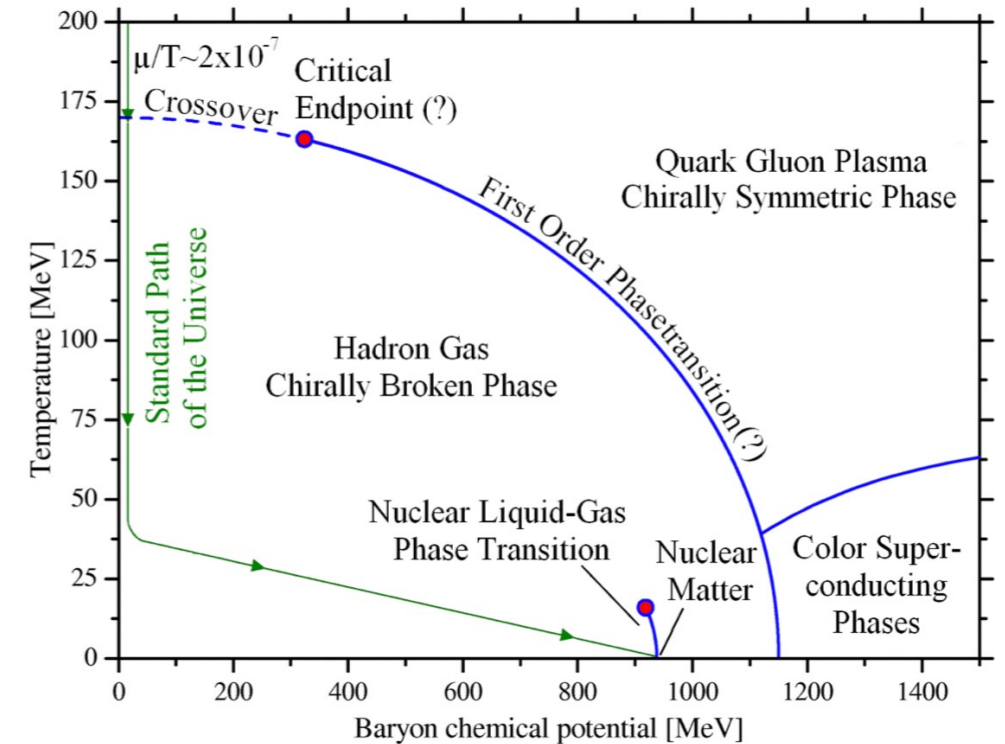
Standard cosmology: from microwave background radiation (CMB) and big bang nucleosynthesis (BBN)

$$\eta_B = \frac{n_B}{s} \sim \frac{n_B}{n_\gamma} \sim \frac{\mu_B}{T} \sim 10^{-9}$$

Baryon number per entropy is conserved and early universe evolves along $\mu/T \sim 10^{-9}$



crossover, no cosmological signals



[Boeckel and Bielich, 2011]

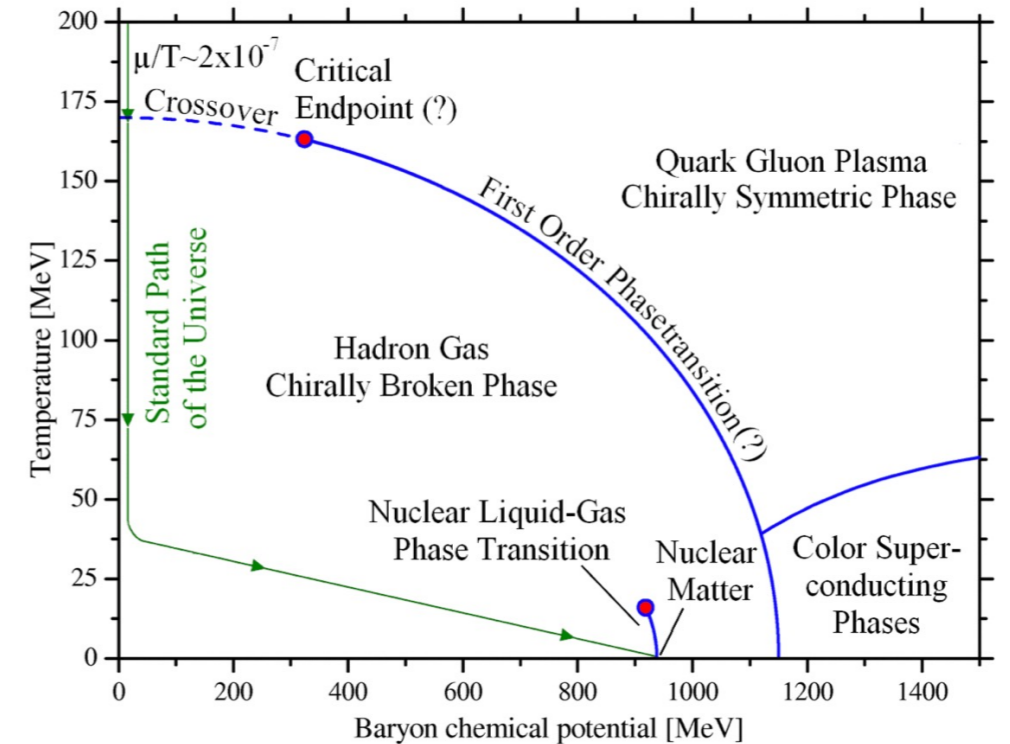
Standard cosmology: from microwave background radiation (CMB) and big bang nucleosynthesis (BBN)

$$\eta_B = \frac{n_B}{s} \sim \frac{n_B}{n_\gamma} \sim \frac{\mu_B}{T} \sim 10^{-9}$$

Baryon number per entropy is conserved and early universe evolves along $\mu/T \sim 10^{-9}$

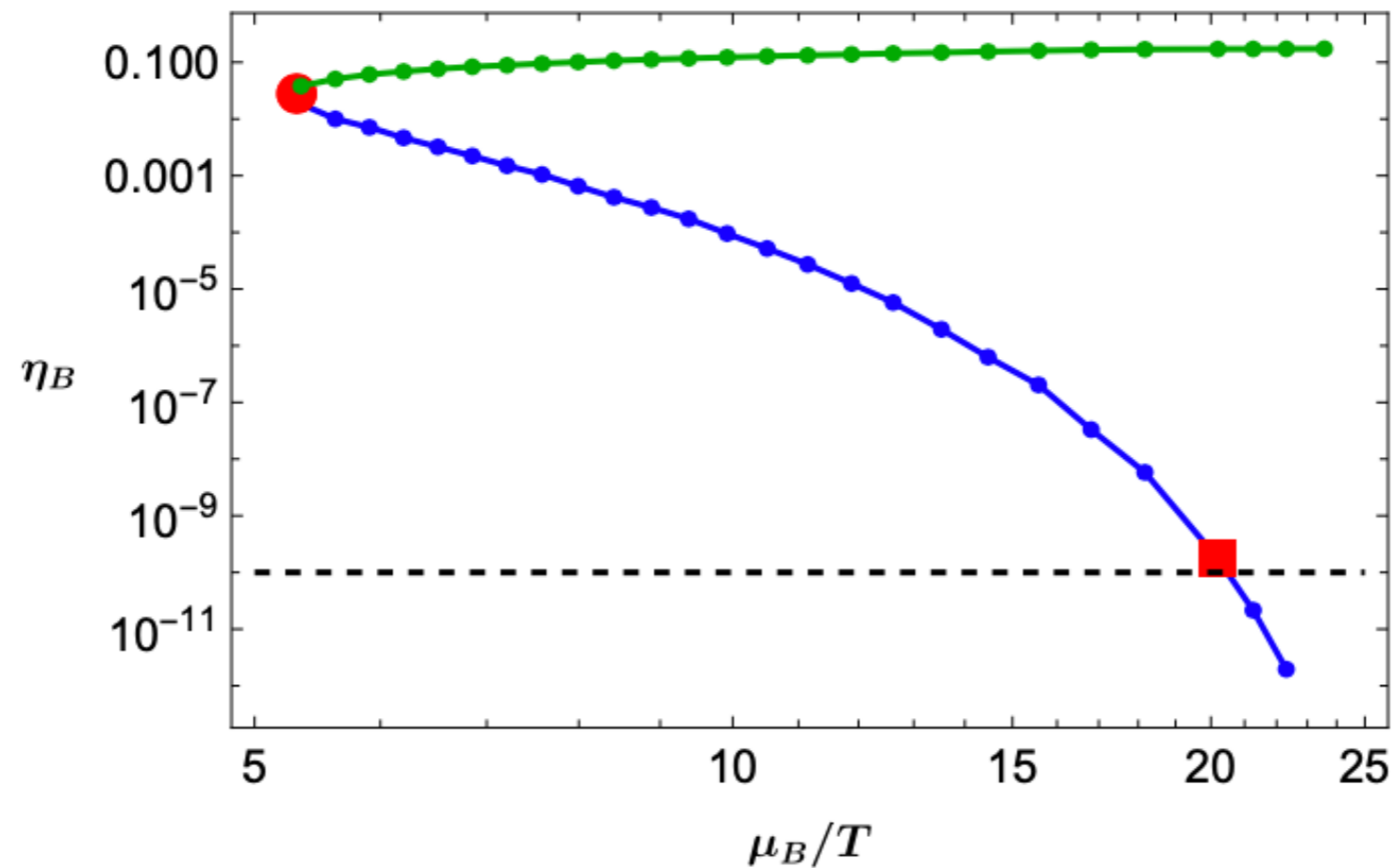


crossover, no cosmological signals



[Boeckel and Bielich, 2011]

Is it possible to have a 1st phase transition without contradiction with present data?



Is it possible to have a 1st phase transition without contradiction with present data?

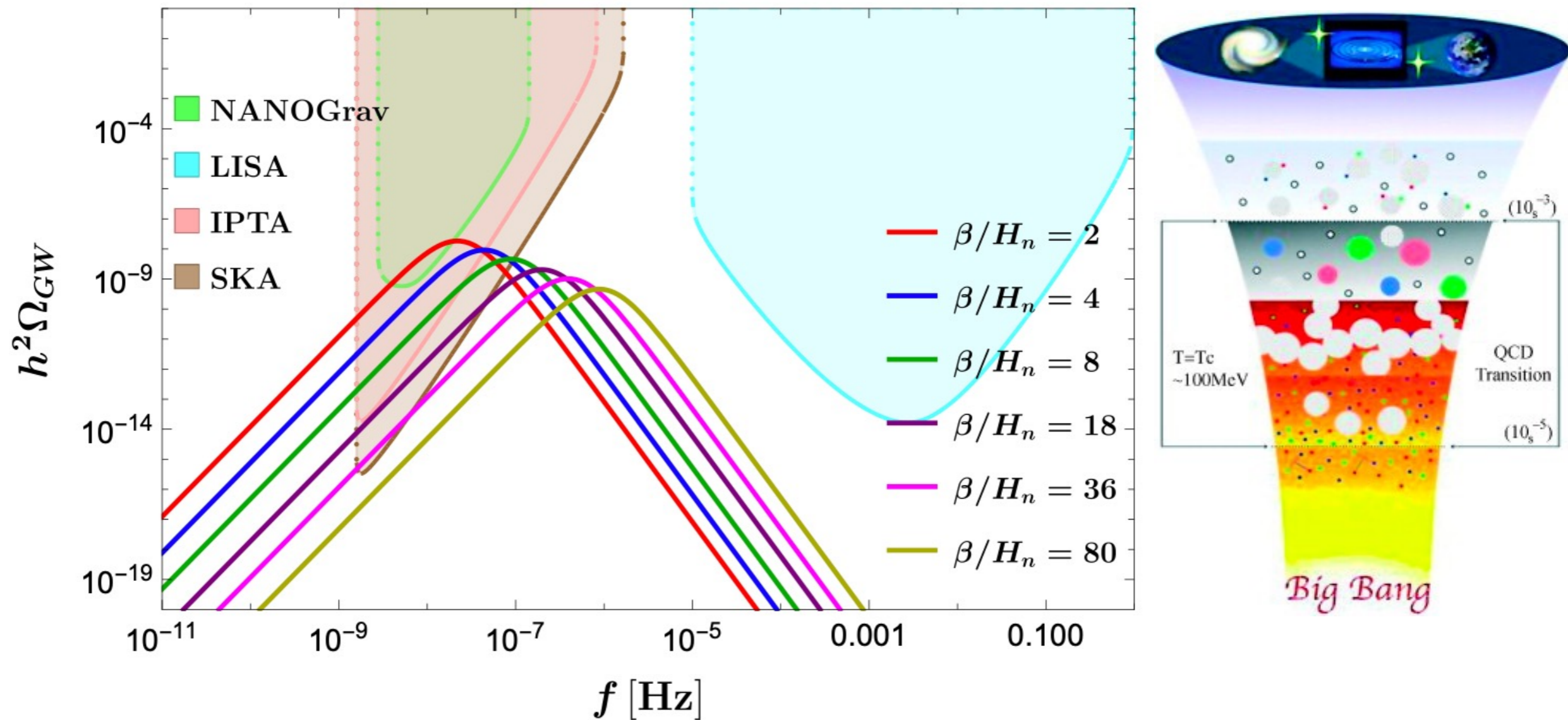
Start with $\eta_B \sim O(0.1)$ generated by Affleck-Dine baryogenesis

[hep-ph/0303065]

The upper limit for the Affleck-Dine baryogenesis: $\eta_B \sim O(1)$
 [Linde, PLB, 1985]

GWs from sound wave

Kai Schmitz, JHEP 01 (2021) 097

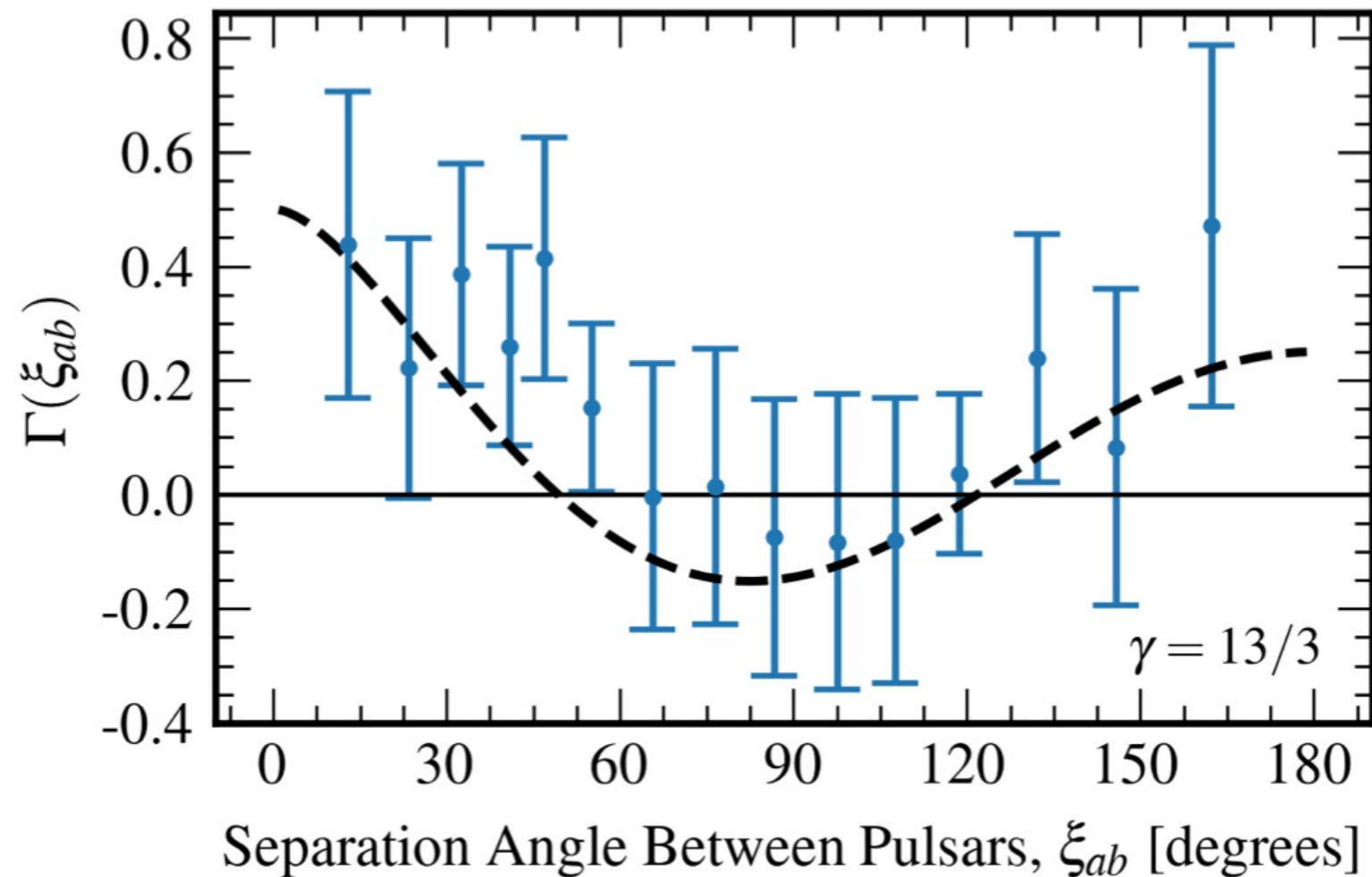


$(\mu, T, \alpha) = (1000 \text{ MeV}, 49.53 \text{ MeV}, 0.33)$.

The upper curve in each band is for $\beta/H_n = 2$ and the lower curve is for $\beta/H_n = 80$.

The GW energy spectrum is within the projected sensitivity of **IPTA** and **SKA**

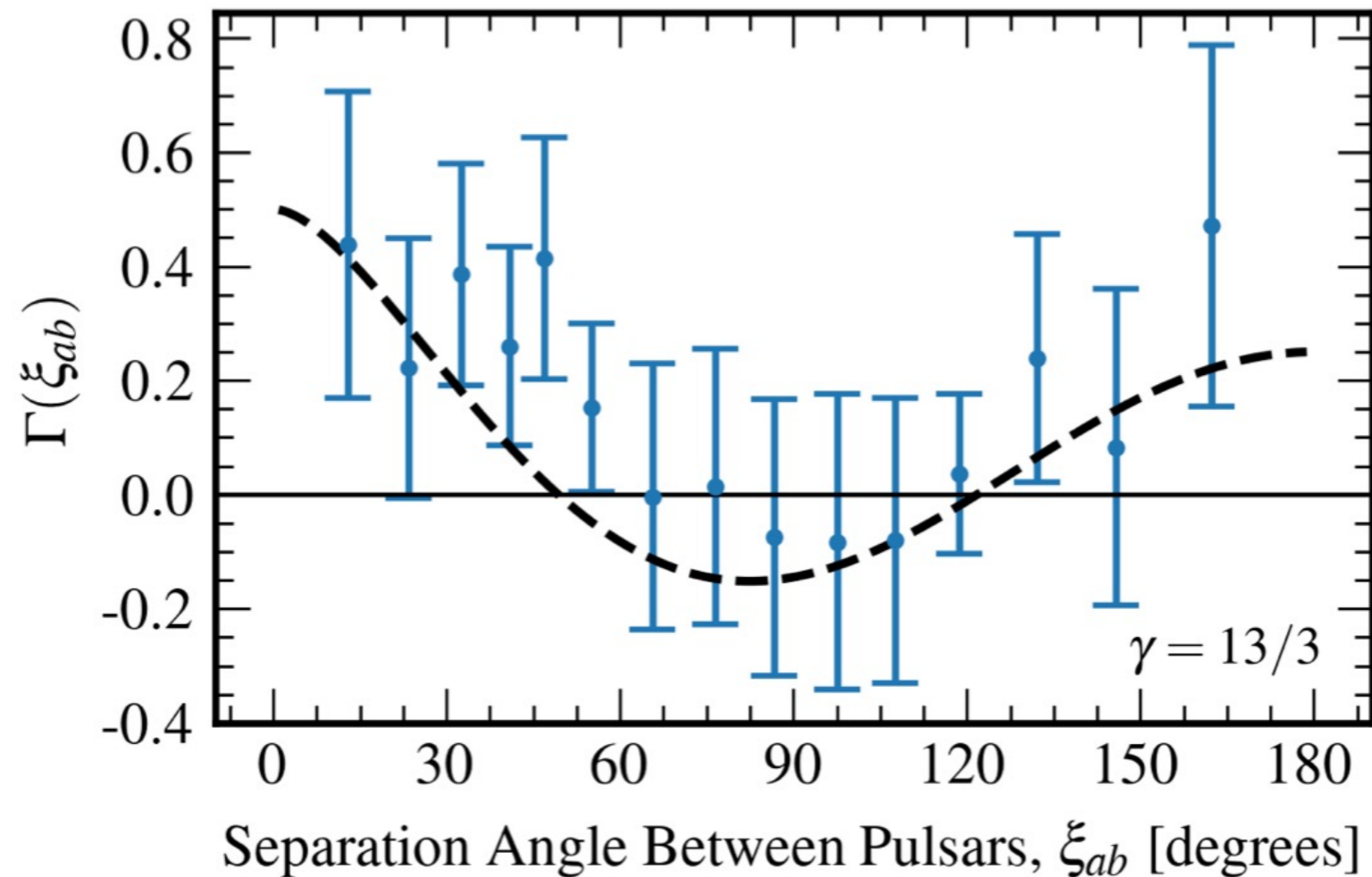
Recently, independent evidence for detecting a GW background around the nano-Hz band has been reported by different **PTA observations**.



NANOGrav 15yr data
[2306.16213]

The parameter space of the FoPT predicted by our QCD model can be constrained by NANOGrav data by assuming that it produces the dominant contribution to the signals.

Recently, independent evidence for detecting a GW background around the nano-Hz band has been reported by different **PTA observations**.



NANOGrav 15yr data
[2306.16213]

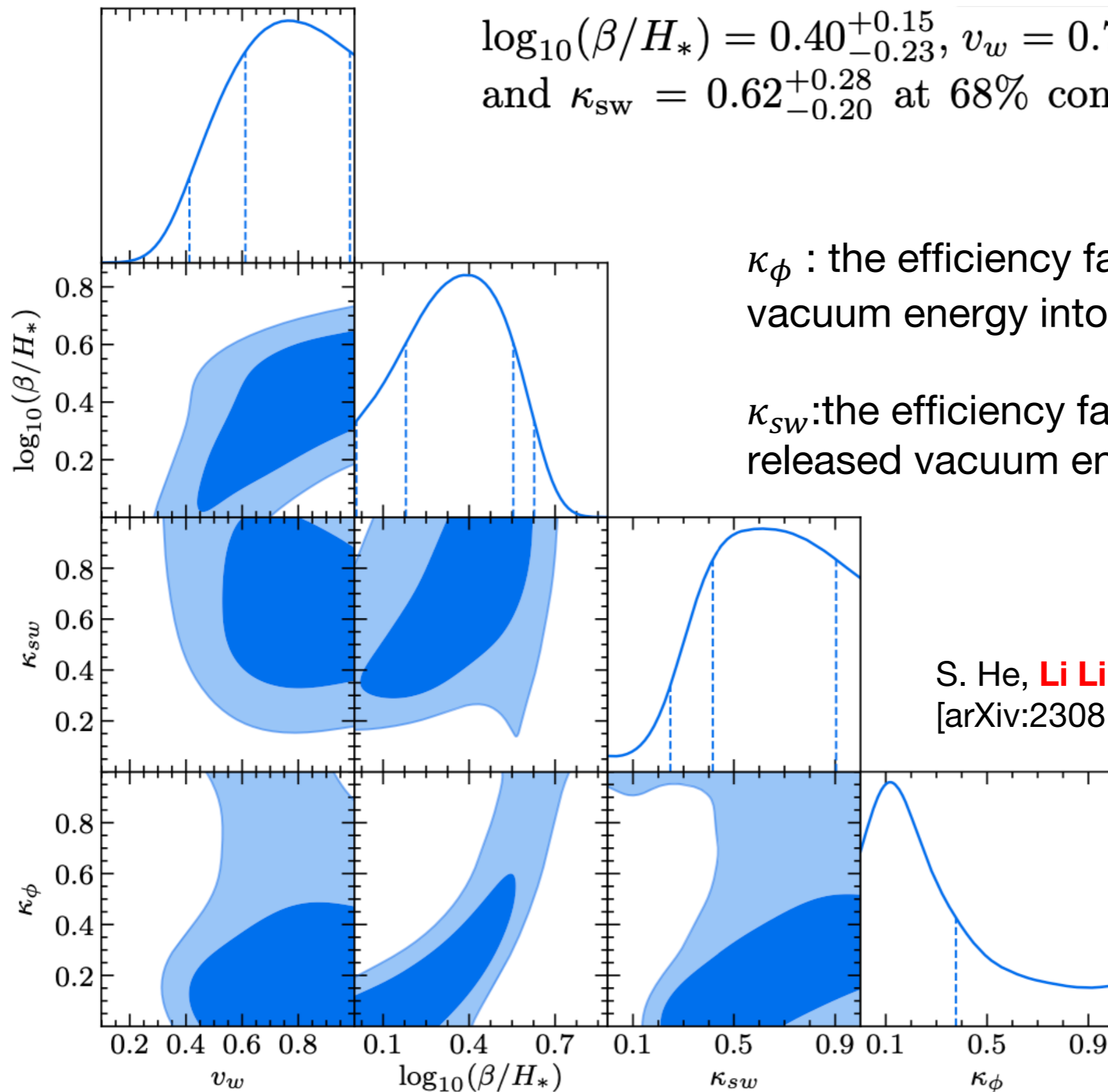
The parameter space of the FoPT predicted by our QCD model can be constrained by NANOGrav data by assuming that it produces the dominant contribution to the signals.

bubble collision + sound wave + MHD turbulence

Posteriors of the four independent model parameters inferred from the NANOGrav 15-year data release

$$\log_{10}(\beta/H_*) = 0.40^{+0.15}_{-0.23}, v_w = 0.76^{+0.22}_{-0.15}, \kappa_\phi = 0.12^{+0.26}_{-0.12},$$

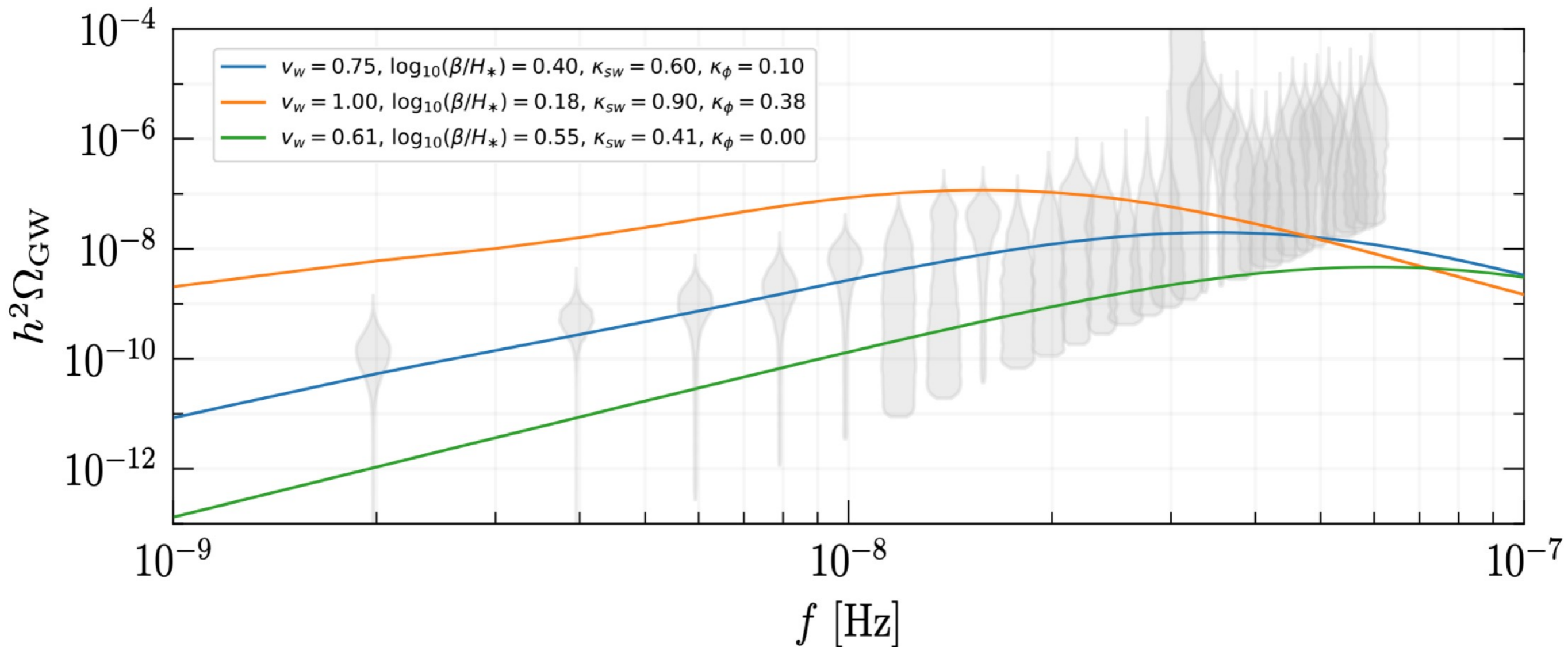
$$\text{and } \kappa_{sw} = 0.62^{+0.28}_{-0.20} \text{ at 68\% confidence level.}$$



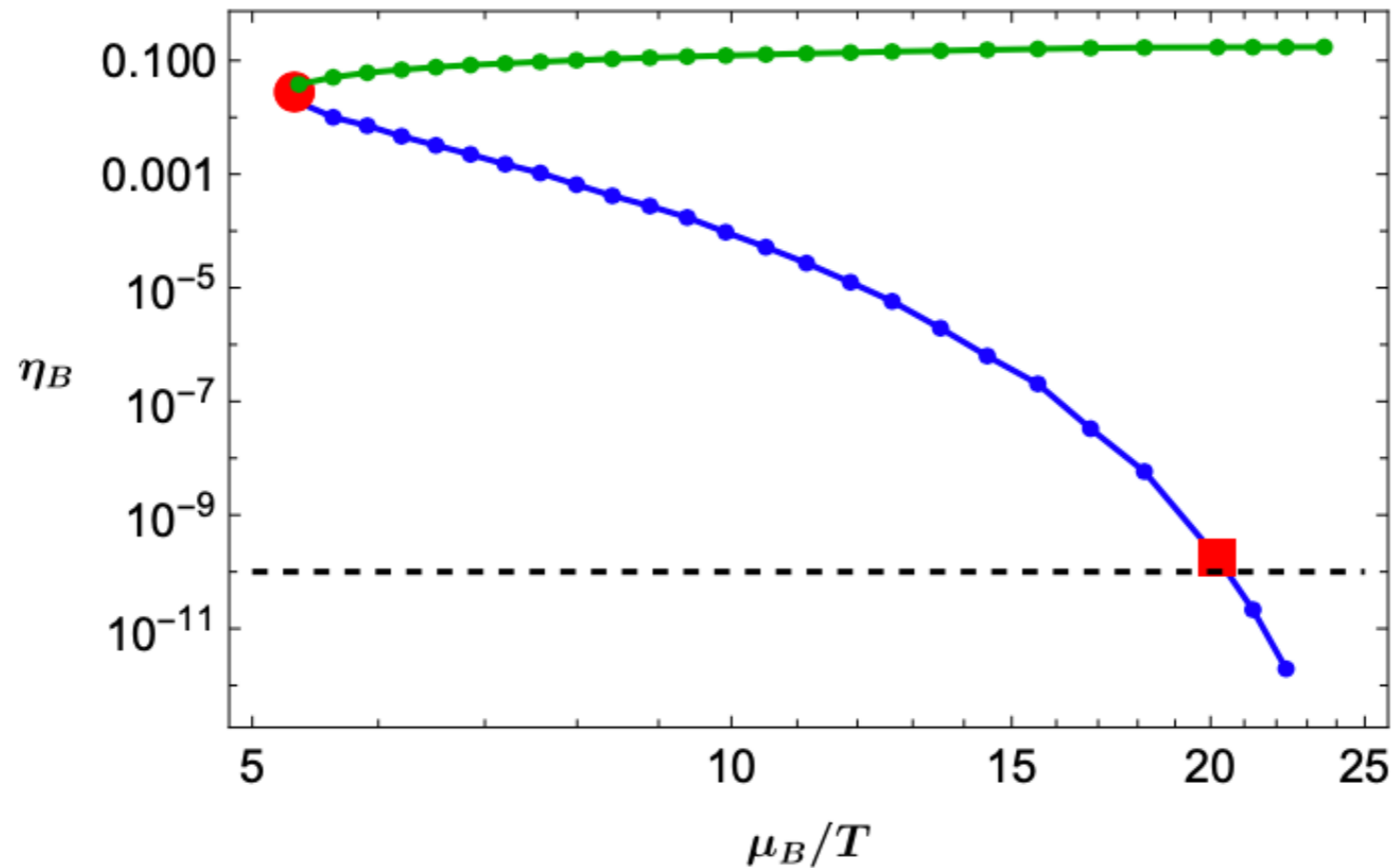
κ_ϕ : the efficiency factor of converting the vacuum energy into the bubble wall motion,

κ_{sw} :the efficiency factor of converting the released vacuum energy into the fluid motions

S. He, **Li Li**, S. Wang and S. J. Wang,
[arXiv:2308.07257 [hep-ph]].



Energy-density spectra with three different sets of values for the four independent model parameters. Violin data points stand for the NANOGrav 15yr observations.



Is it possible to have a 1st phase transition without contradiction with present data?

Little inflation scenario
at cosmological QCD phase transition

A strong mechanism for baryogenesis + A quasistable QCD-medium state that triggers a short inflationary period of inflation diluting the baryon asymmetry to the value observed today.

[Linde, 1985; Kampfer et al., 1986, Borghini et al., 2000]

A little inflation in QCD phase diagram

a few e-folds are enough (standard inflation needs $N \sim 50$)

$$\frac{a_f}{a_i} = \left(\frac{\eta_{Bi}}{\eta_{Bf}} \right)^{1/3} = \left(\frac{\eta_{B+}}{\eta_B^{ob}} \right)^{1/3}$$

Hence $N = \ln\left(\frac{a_f}{a_i}\right) = \ln(10^3) \approx \mathbf{7 \text{ e-folds}}$ is enough

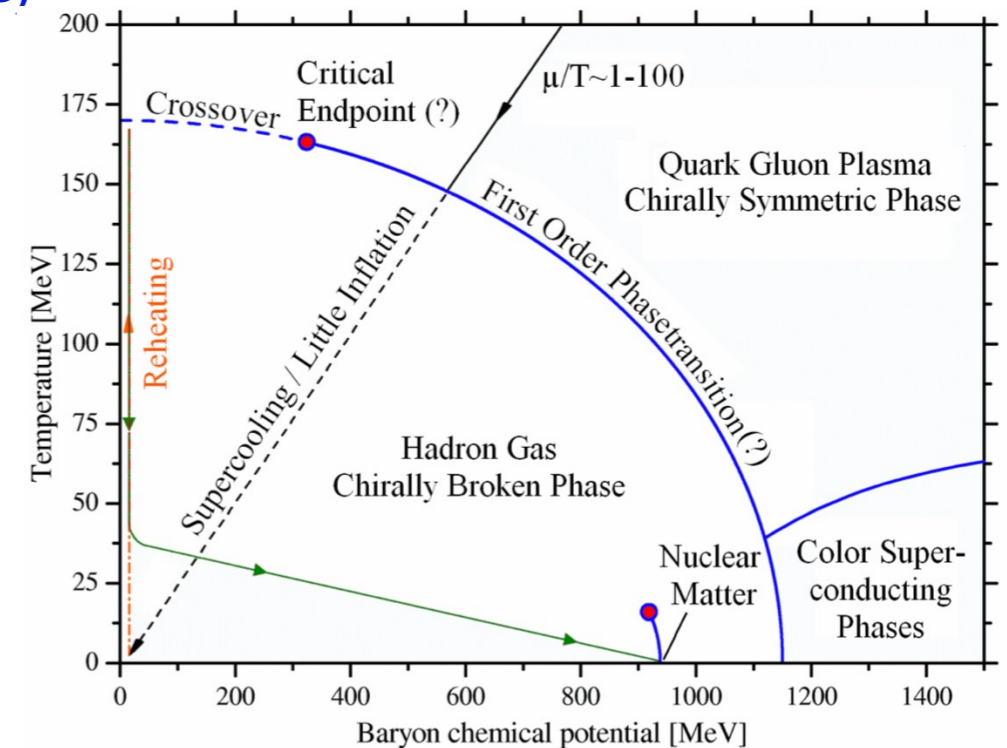
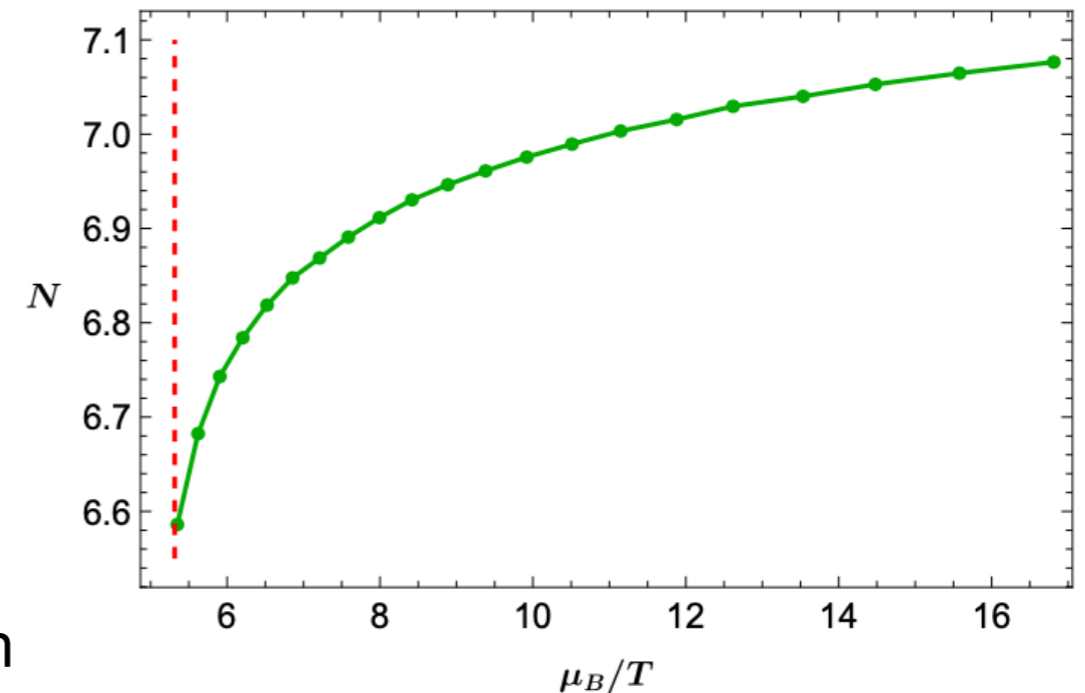
➤ Start with $\mu/T \sim O(1)$ (e.g. Affleck-Dine baryogenesis)

➤ Universe trapped in false vacuum at the 1st transition line

➤ Supercooling and dilution with $\mu/T = \text{const}$

➤ Decay to the true vacuum state → reheating so that $\mu/T \sim 10^{-9}$

➤ Then standard cosmological evolution to BBN



[Boeckel and Bielich, 2011]

Outline

1. Introduction
2. Holographic QCD model
3. Phase diagram and GWs
- 4. Summary and discussion**

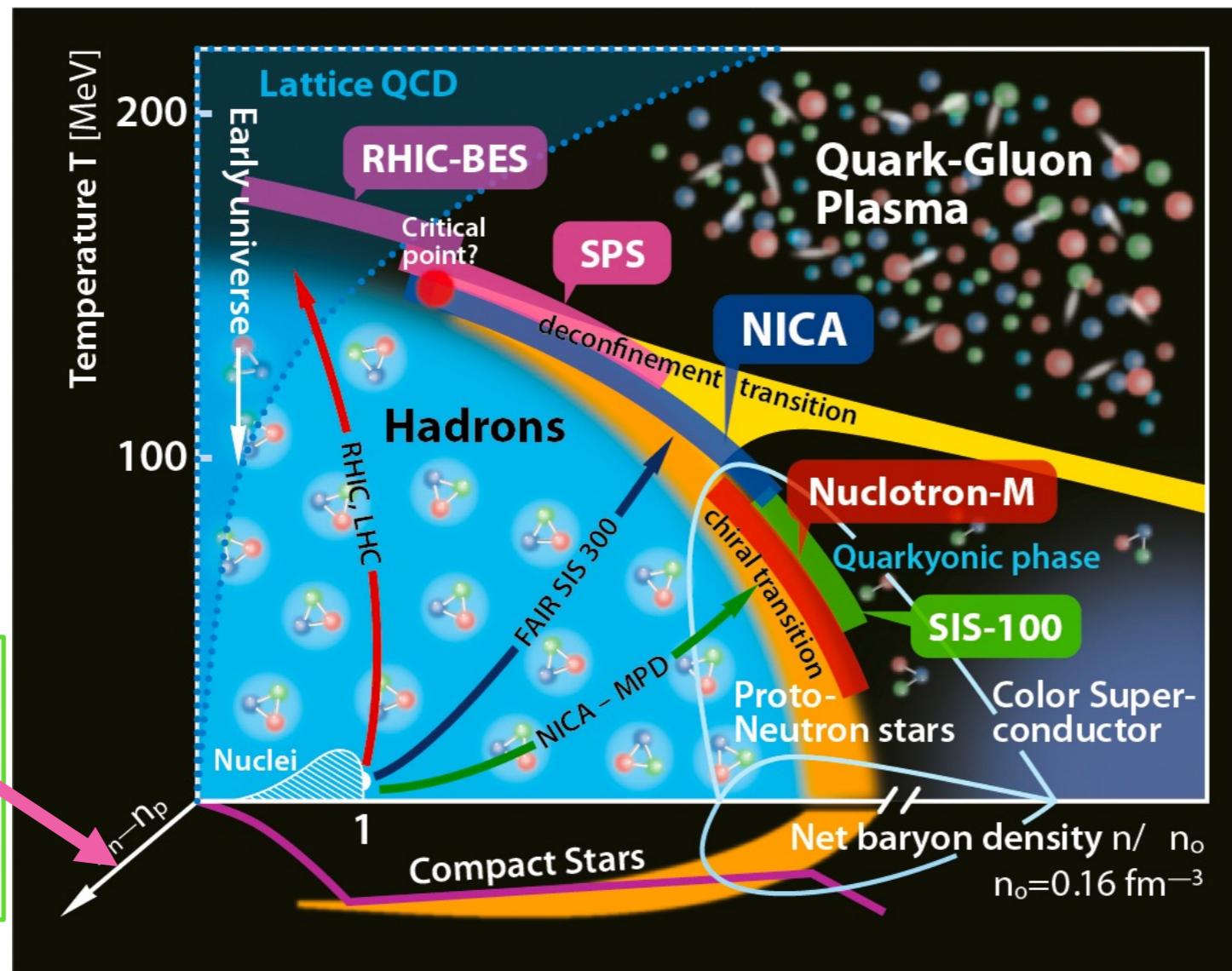
4. Summary

- Build a hQCD model to describe real QCD dynamics.
- Find good quantitative agreement with lattice data at zero/non-zero chemical potential.
- Predict the QCD CEP that agrees qualitatively with effective field results.
- The predicted location of CEP is within the coverage of future (FAIR, JPARC-HI, and NICA) experimental facilities.
- Compute the stochastic GW spectrum

Holography is a useful approach to study real hot and dense QCD matter in non-perturbative regime.

4. Discussion

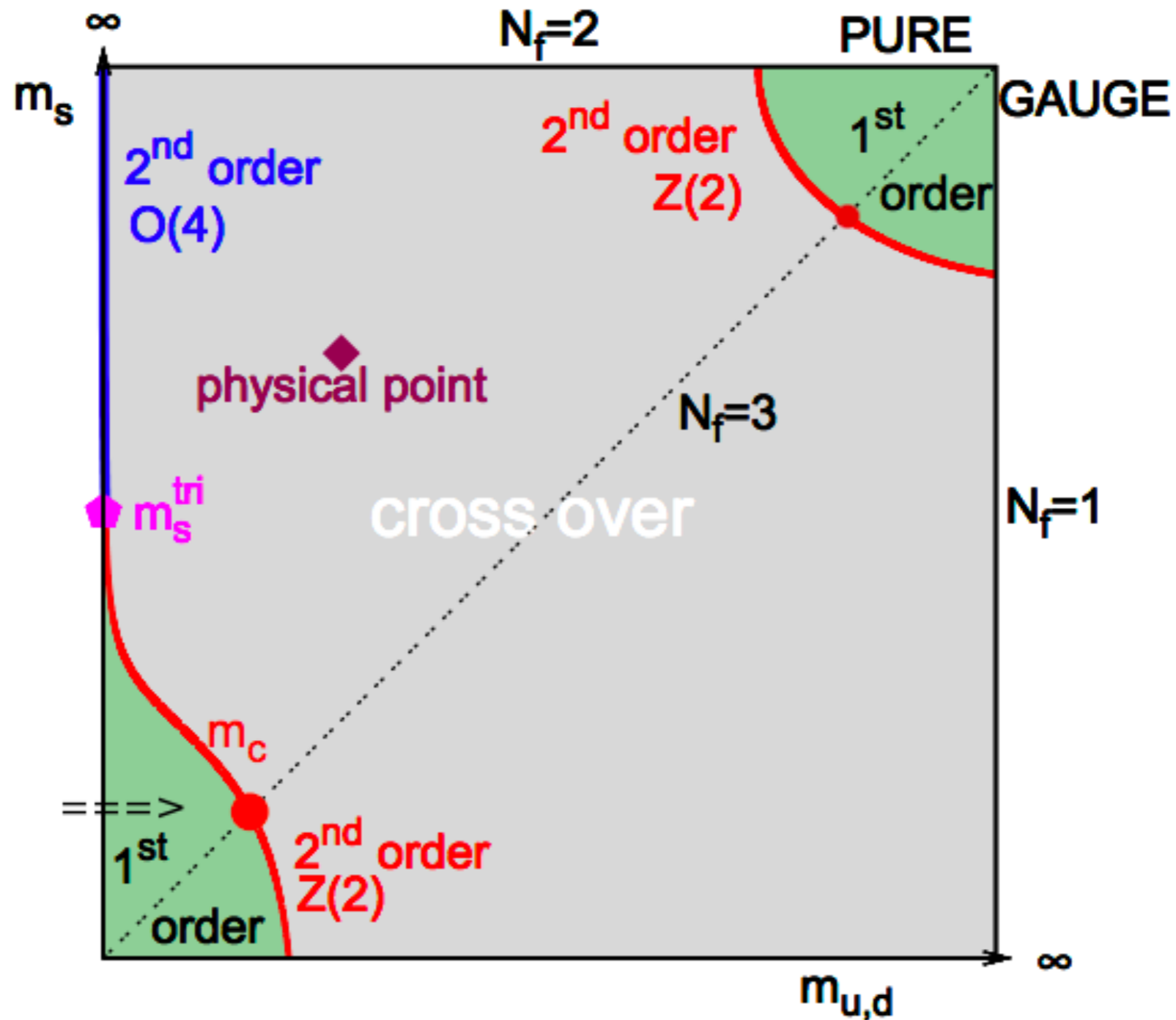
It is desirable to further study the non-perturbative features of QCD dynamics using this holographic model.



GWs:
1st phase transition
bubble collisions
PBH
...

New method is necessary: Machine Learning...

Columbia plot of QCD at $\mu_B = 0$



To build effective models to capture the main feature of QCD matter;

Non-perturbative effects are effectively adopted into the model parameters.

QCD at zero chemical potential

Einstein-Dilaton theory:

$$S = \frac{1}{2\kappa_N^2} \int d^5x \sqrt{-g} \left[\mathcal{R} - \frac{1}{2} \nabla_\mu \phi \nabla^\mu \phi - V(\phi) \right]$$

To match lattice QCD simulation

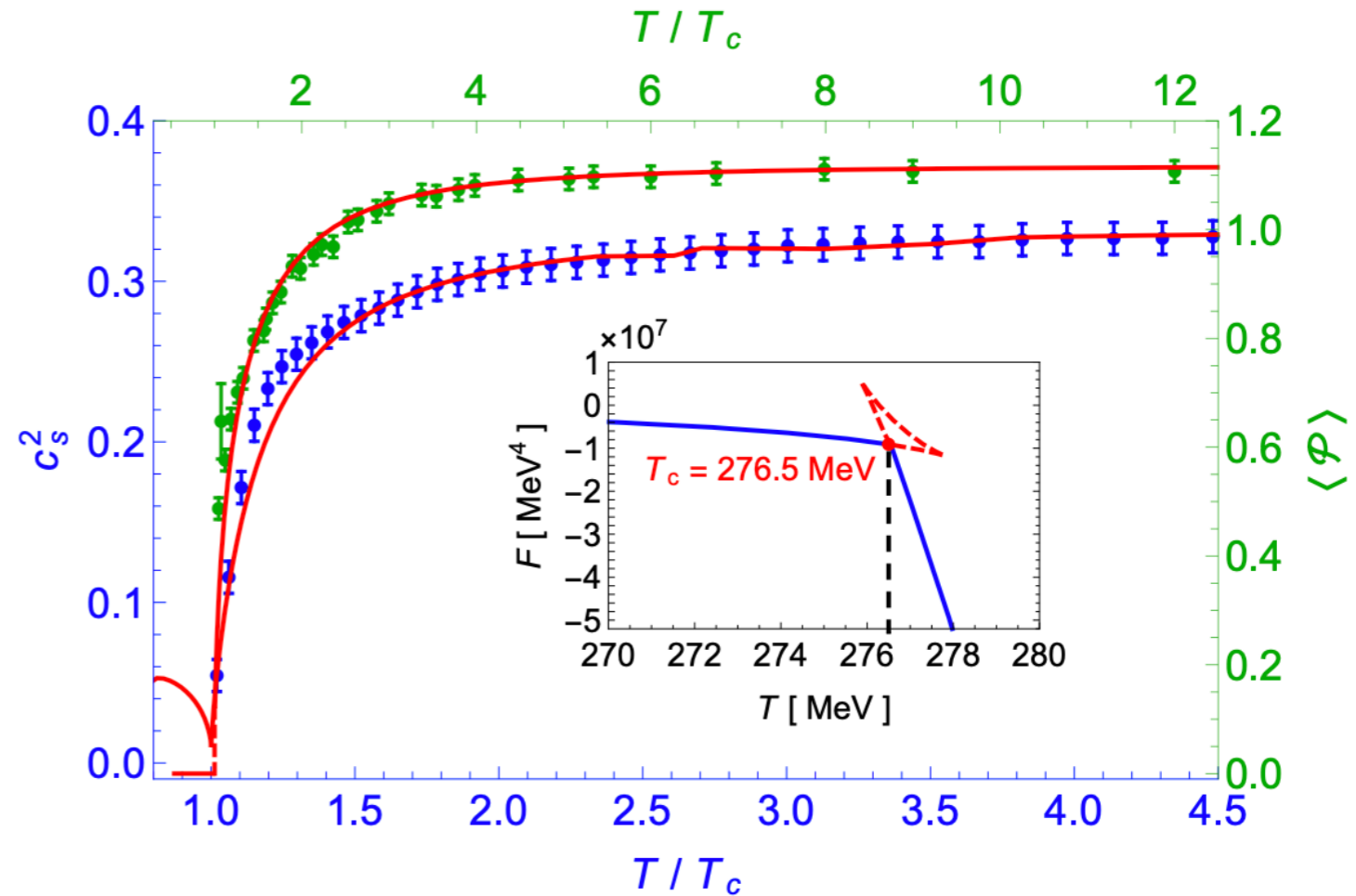
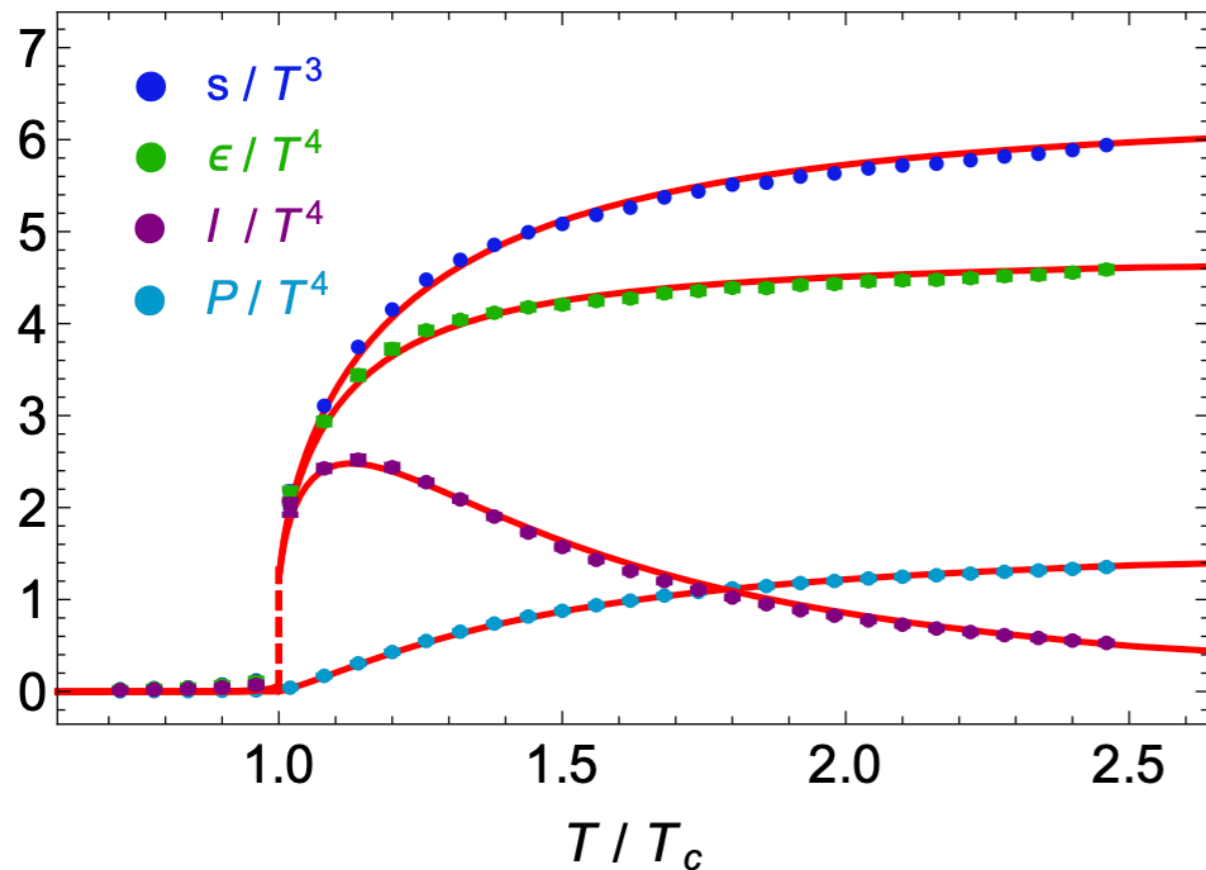
$$V(\phi) = -12 \cosh[c_1 \phi] + \left(6c_1^2 - \frac{3}{2}\right) \phi^2 + c_2 \phi^6$$

Non-perturbative effects are effectively adopted into the model parameters by matching with up-to-date lattice QCD data.

Pure Gluon at zero chemical potential

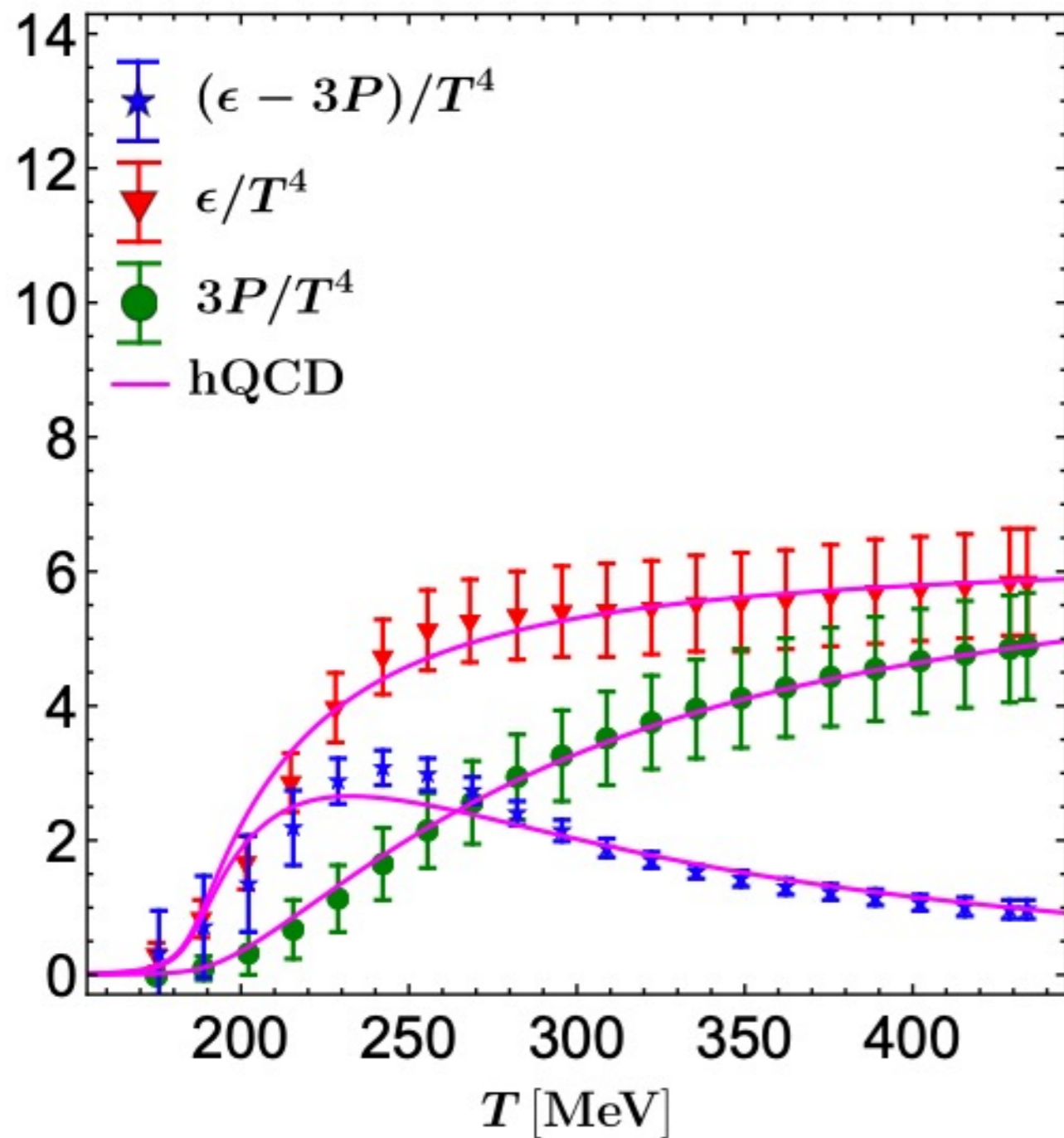
Much simpler than (2+1)-flavor QCD!

$$c_1 = 0.735, c_2 = 0$$



There is a first-order confinement/deconfinement PT at $T_c=276.5$ MeV !

2-flavor QCD at zero chemical potential



$$V(\phi) = -12 \cosh[c_1 \phi] + (6c_1^2 - \frac{3}{2})\phi^2 + c_2 \phi^6$$

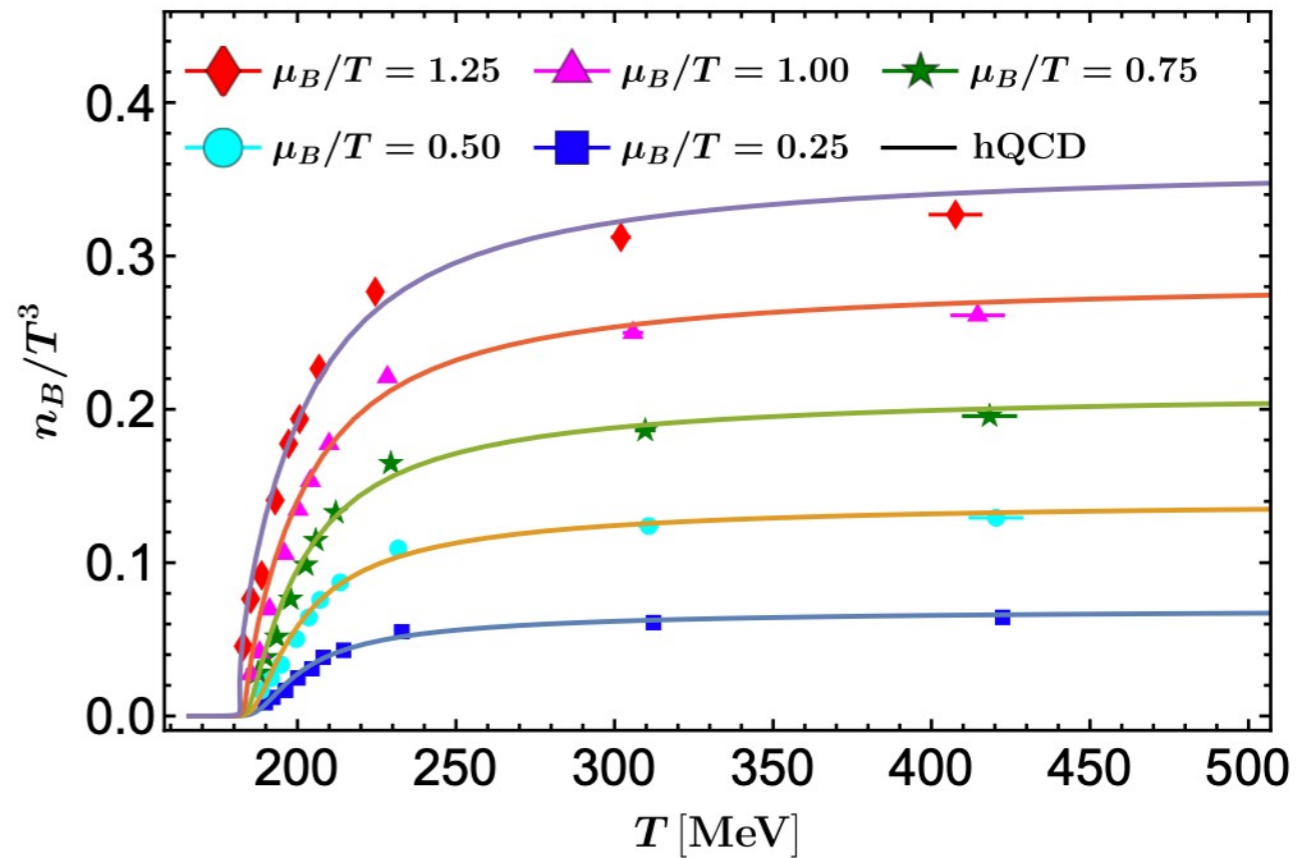
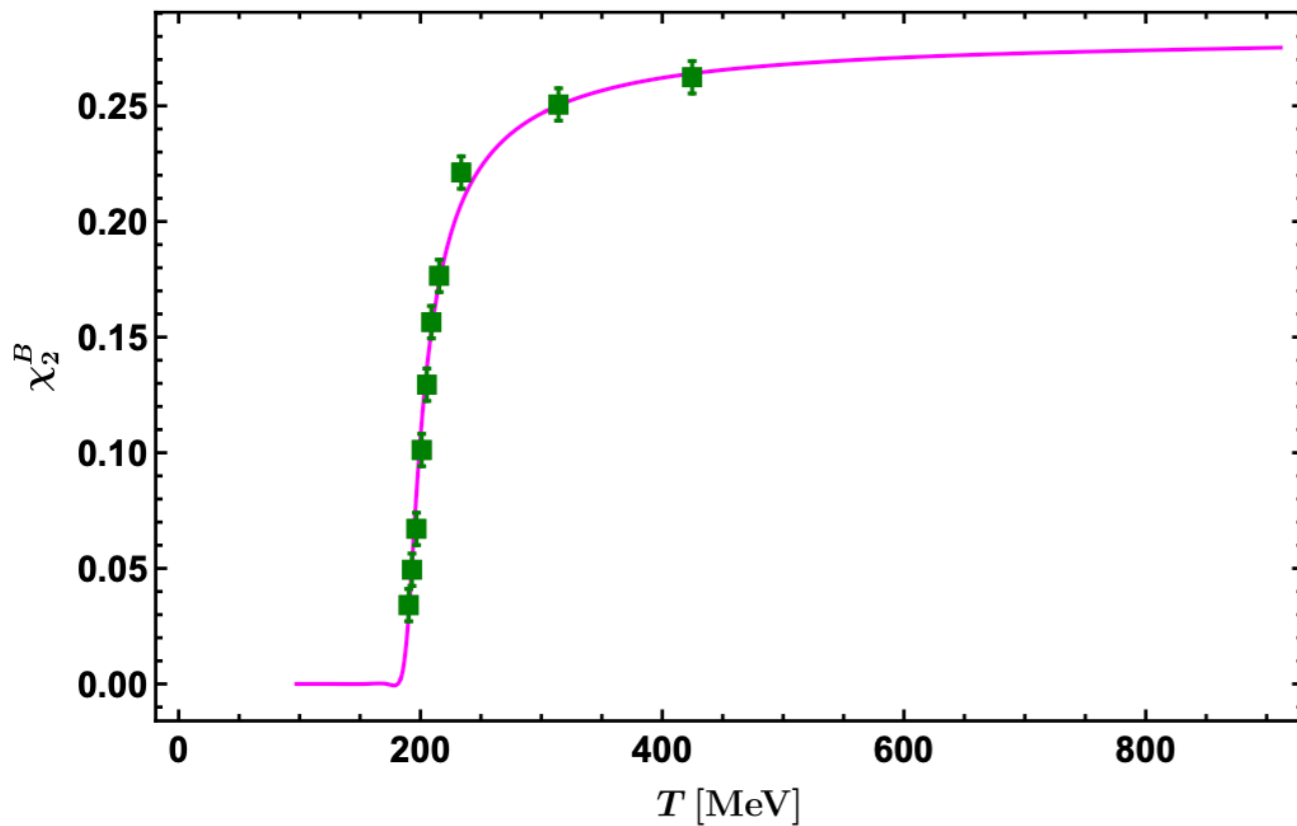
model	c_1	c_2
pure $SU(3)$	0.735	0
2 flavor	0.710	0.0002
2+1 flavor	0.710	0.0037

Yan-Qing Zhao, Song He, Defu Hou, **Li Li**, Zhibin Li,
Phys.Rev.D 109 (2024) 8, 086015

Baryon number density and second-order baryon susceptibility

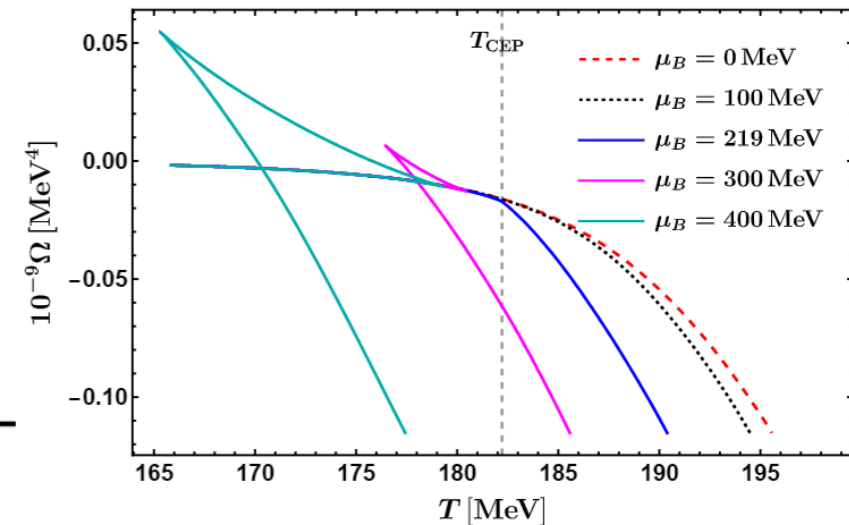
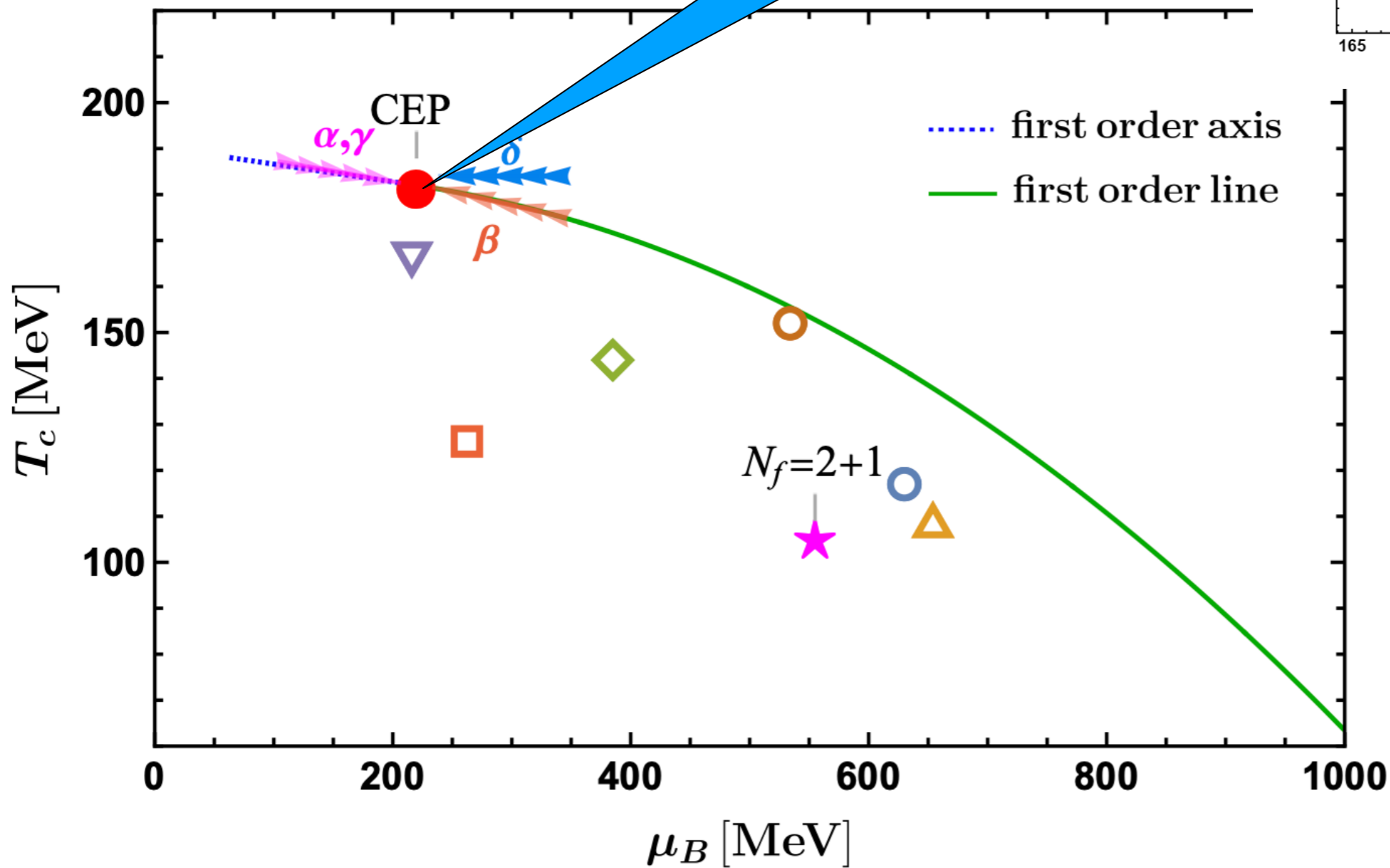
$$Z(\phi) = \frac{1}{1 + c_3} \operatorname{sech}[c_4 \phi^3] + \frac{c_3}{1 + c_3} e^{-c_5 \phi}$$

$$S = \frac{1}{2\kappa_N^2} \int d^5x \sqrt{-g} \left[\mathcal{R} - \frac{1}{2} \nabla_\mu \phi \nabla^\mu \phi - \frac{Z(\phi)}{4} F_{\mu\nu} F^{\mu\nu} - V(\phi) \right],$$



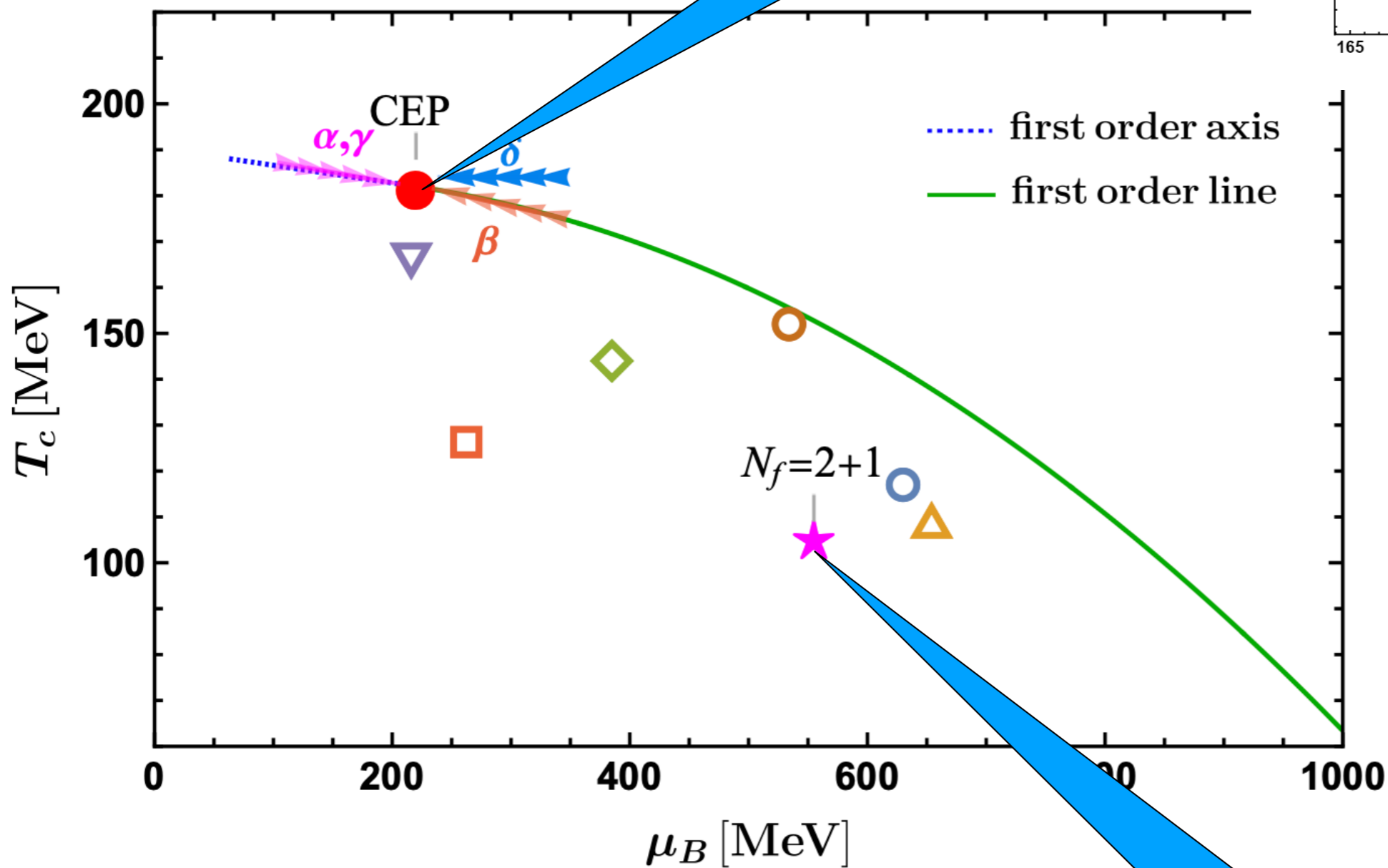
2-flavor QCD phase diagram

$T_c = 182 \text{ MeV}$
 $\mu_c = 219 \text{ MeV}$



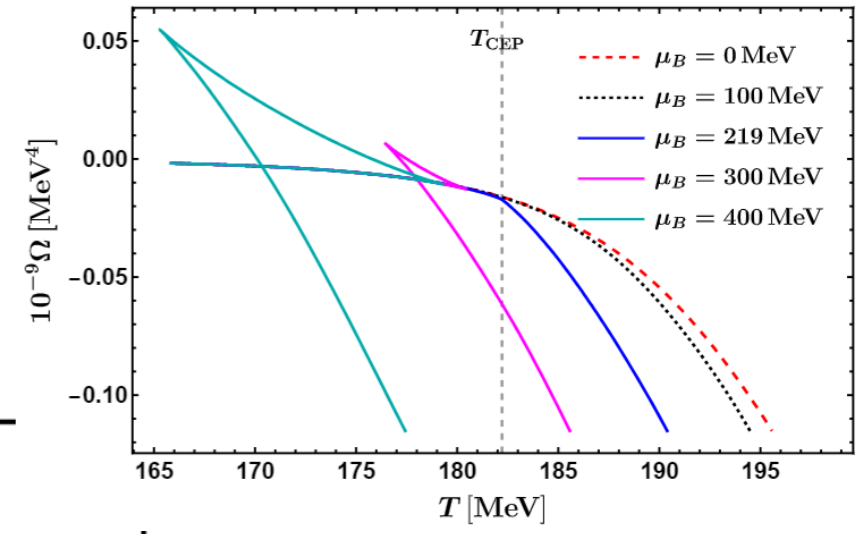
- fRG - 1
- △ DSE and fRG
- ◇ Coalescence model
- DSE
- ▽ PNJL - 1
- PNJL - 2

2-flavor QCD phase diagram



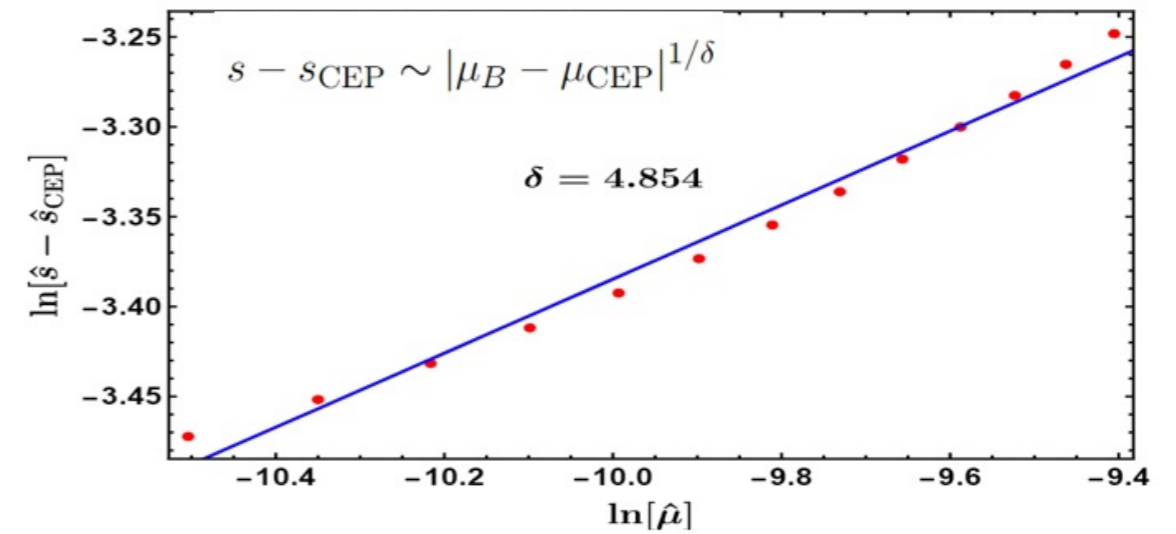
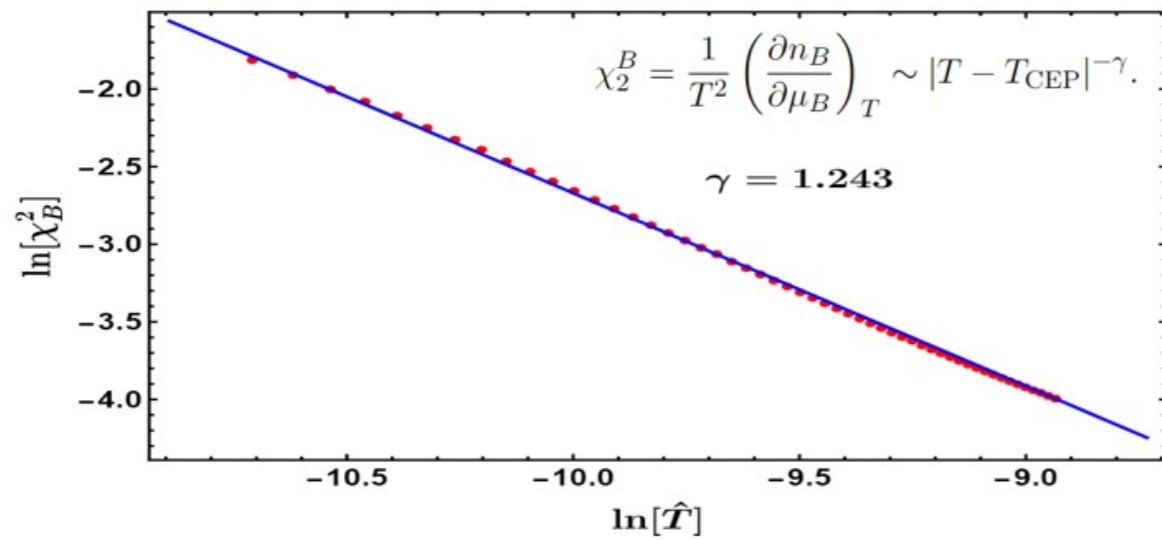
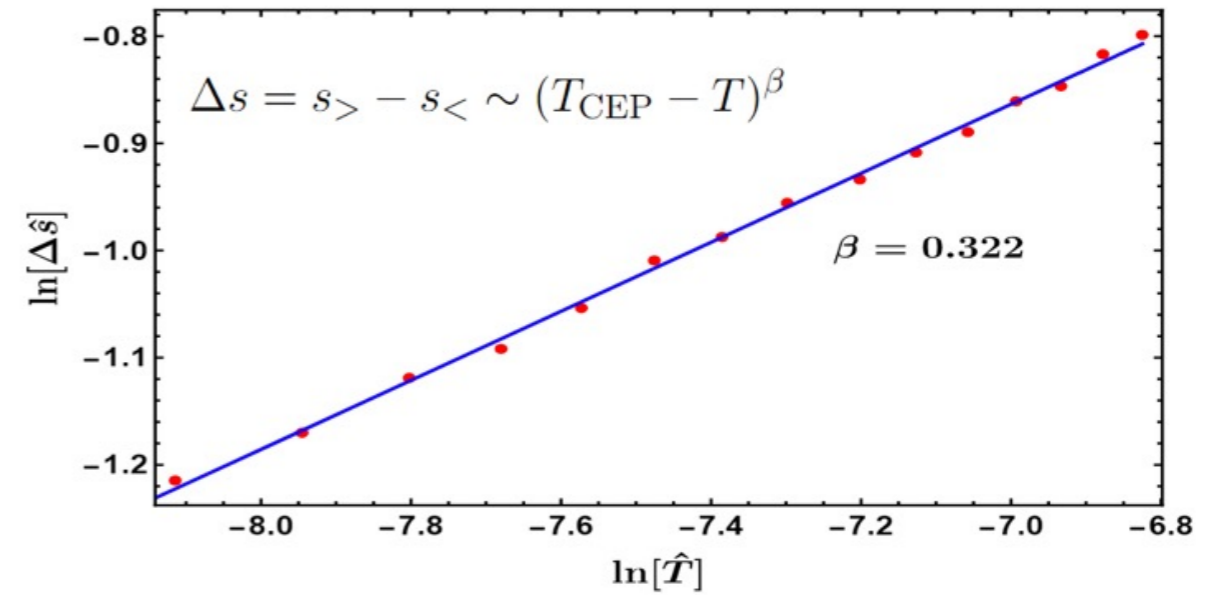
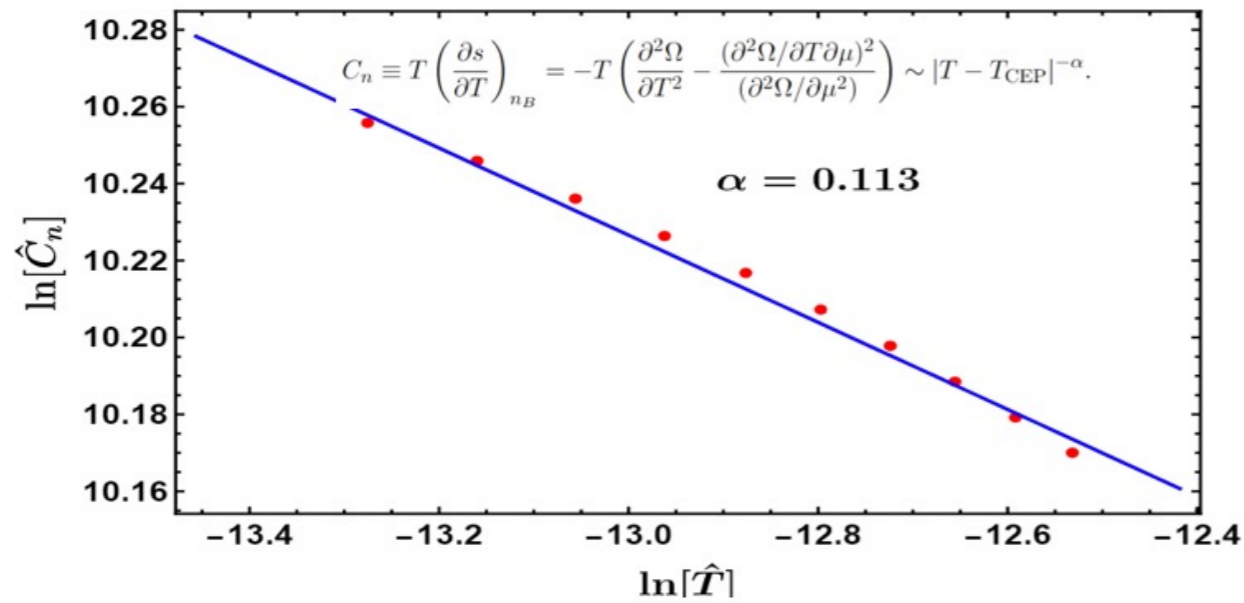
$T_c = 182 \text{ MeV}$
 $\mu_c = 219 \text{ MeV}$

$T_c = 105 \text{ MeV}$
 $\mu_c = 555 \text{ MeV}$



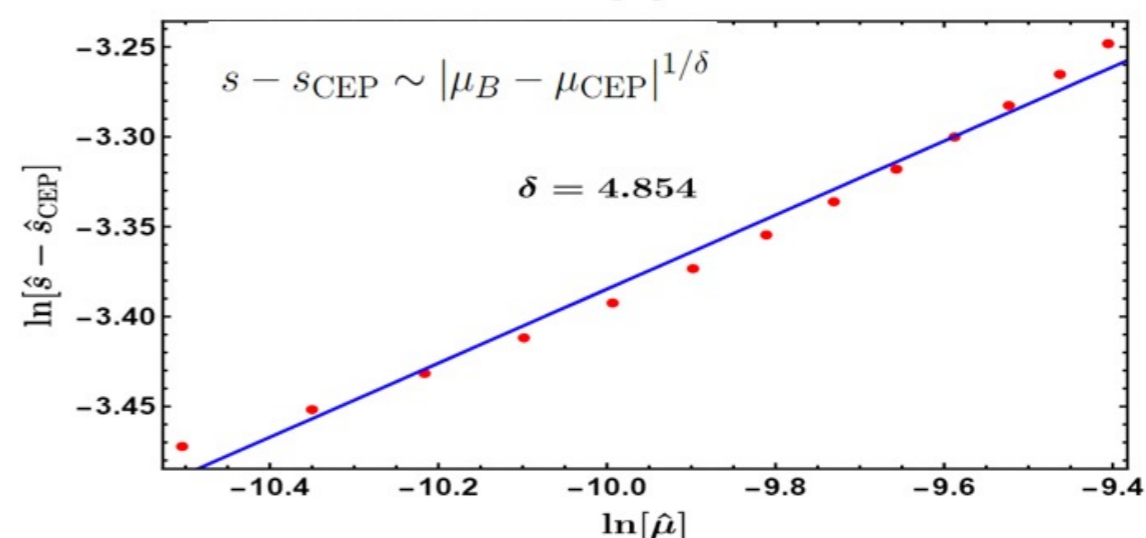
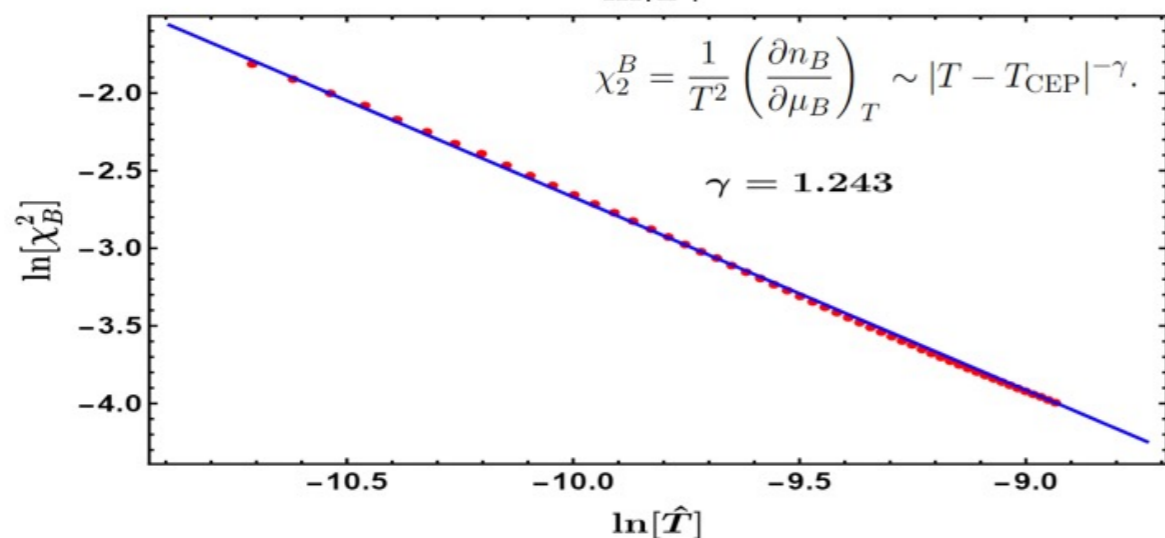
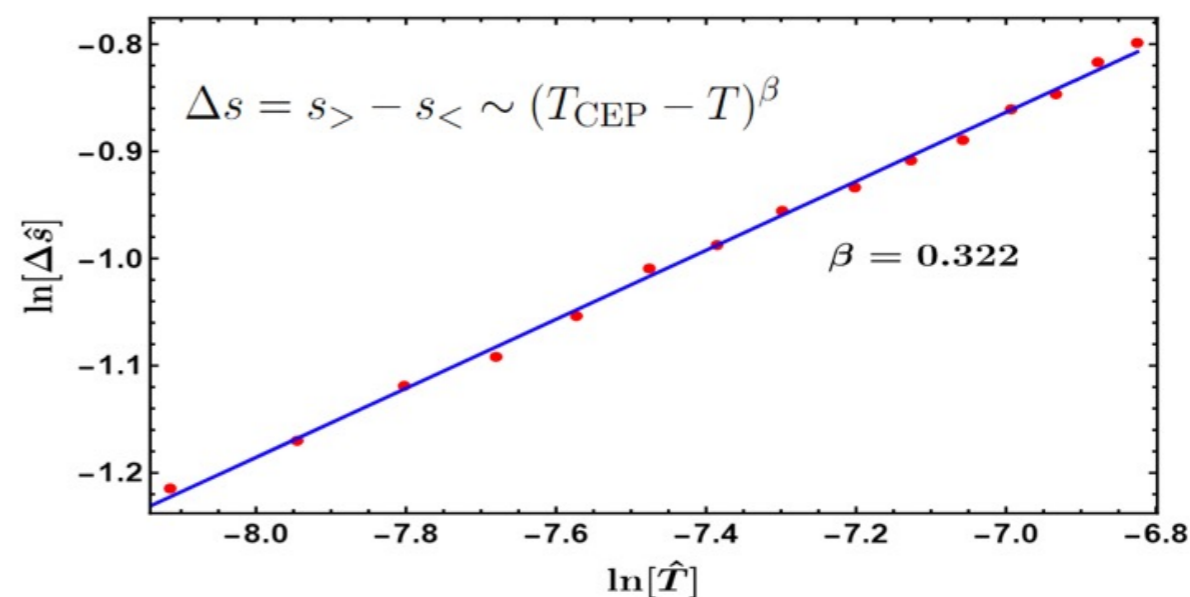
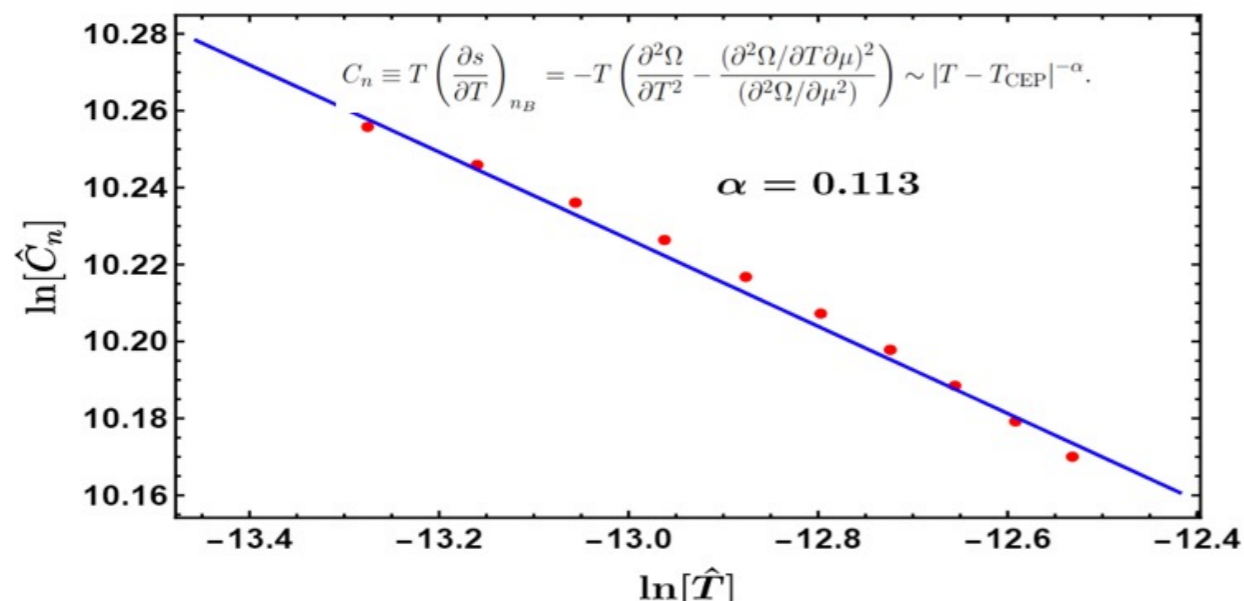
- fRG - 1
- △ DSE and fRG
- ◇ Coalescence model
- DSE
- ▽ PNJL - 1
- PNJL - 2

2-flavor QCD critical exponents



$$\alpha + 2\beta + \gamma = 2, \quad \alpha + \beta(1 + \delta) = 2$$

2-flavor QCD critical exponents



$$\alpha + 2\beta + \gamma = 2, \quad \alpha + \beta(1 + \delta) = 2$$

	Experiment	3D Ising	Mean field	DGR model	Ours
α	0.110-0.116	0.110(5)	0	0	0.113
β	0.316-0.327	0.325 ± 0.0015	1/2	0.482	0.322
γ	1.23-1.25	1.2405 ± 0.0015	1	0.942	1.243
δ	4.6-4.9	4.82(4)	3	3.035	4.854

The image features a white background with decorative rainbow arcs in the corners. The arcs are composed of multiple overlapping bands of color, including purple, blue, and pink, creating a soft, multi-colored effect. One arc is in the top right corner, and another is in the bottom left corner.

Thank you!